UNIVERSITY OF COPENHAGEN

Master Thesis

Sissel Olsen

GEUS

Simulation of flow and transport at field site Estrup

Supervisor: Karsten Høgh Jensen

Co. Supervisors: Sachin Karan and Annette Rosenbom

Date: 18.10.2019

Institutnavn:	Institut for Geovidenskab og Naturforvaltning
Name of department:	Department of Geosciences and Natural Resources Management
Author:	Sissel Olsen
Title:	Simulation of flow and transport at field site Estrup
Supervisor:	Karsten Høgh Jensen (IGN, Department of Geosciences and Natural Resources Management)
Co. Supervisors	Sachin Karan and Annette Rosenbom (GEUS, Geological Survey and Denmark and Greenland)
Submission date:	18th of October 2019
ECTS:	60
Number of Characters:	87628

Abstract

An unsaturated water flow and transport model for the upper 5 m of the Estrup field is build. Estrup field is a part of the Pesticide Leaching Assessment Programme at GEUS (Geological Survey of Denmark and Greenland) who provided the data the model is based on. The model was built in HydroGeoSphere, where parameters as evapotranspiration and drain was accounted for. Later, a new domain was built into the model, a dual domain which was added to represent the macropores present at Estrup field. The model was calibrated using the inverse calibration software PEST where the observed depth to the groundwater table, saturation and drain flow were used to calibrate against. Three models were developed in total (Model A, B and C), but only two of them were calibrated and had solute transport added to the simulation. This resulted in models, which were not able to simulate the depth to the groundwater table, but simulated saturation and drain flow more accurately. In addition, results from the solute transport generally showed a higher concentration of bromide for the model than the measured concentration.

Table of Content

Introduction

The focus area of this report is one of the test field of The Pesticide Leaching Assessment Programme (PLAP), which is located in Estrup, near Vejen in Central Jutland. In Denmark, there is a rising concern about pesticides in the groundwater and surface water. The Danish National Groundwater Monitoring Programme (GRUMO) has revealed presence of pesticides and their degradation product in about 30% of monitored screens. The Pesticide Leaching Assessment Programme (PLAP) in Denmark aims to monitor how pesticides and their degradation products reaches the groundwater under real field condition. PLAP consists of six testing field around Denmark (see Figure 1), and are selected because of their differences (Lindhardt et al., 2001). Earlier assessments of pesticides leaching to the groundwater consists mainly of laboratory and lysimeter studies governed by the EU.

PLAP was initiated in 1998 and monitoring of the fields began in 1999, and currently covers six sites with different soil types in Denmark. The program MACRO (Larsbo, Roulier, Stenemo, Kasteel, & Jarvis, 2005) is used as modelling tool for hydrological simulations of all sites. There is a unique database available from the Estrup site, with data for the past 20 year, including climatic data such as; precipitation rates, temperature and evapotranspiration, and soil properties data such as; soil moisture, groundwater flow and drain flow. Additionally, data for tracer, pesticide and isotope concentrations and compositions are also provided. Besides the large data base of the test field, the fields have been subject to a very detailed geological characterization and the important hydraulic parameters have been measured.

HydroGeoSphere (Therrien, McLaren, Sudicky, & Panday, 2010) have a complex modelling code for simulation flow and transport and will be used as modelling tool in this thesis. HydroGeoSphere allows for consideration to all important flow and transport processes including macropores and fractured flows, which are of relevance for this site. A model of the site in Estrup will be established in HydroGeoSphere and described. The model performance will afterward be evaluated against monitored and measured data provided from the test field in Estrup.

It is the objective of this project to:

- Establish a model for simulation of flow and transport, of the variable-unsaturated zone of the test field in Estrup, in HydroGeoSphere.
- Calibration of the model using the inverse code PEST (Doherty, 2016).
- Further developing the model by adding macropores and fractures.

The Pesticide Leaching Assessment Programme

The Pesticide Leaching Assessment Programme (PLAP) has the aim of monitoring pesticides and their degradation products, and whether they are leaching to the groundwater under actual agricultural field conditions. PLAP consists of six test fields (see Figure 1), which are selected to represent the different soil types and the difference climate in Denmark.

The work of designing the programme started in august 1998, and the selection of the six test fields was in 1999, where the equipment for monitoring was installed the same year. Monitoring was initiated between May 1999 and April 2000 (Lindhardt et al., 2001), and continues today.

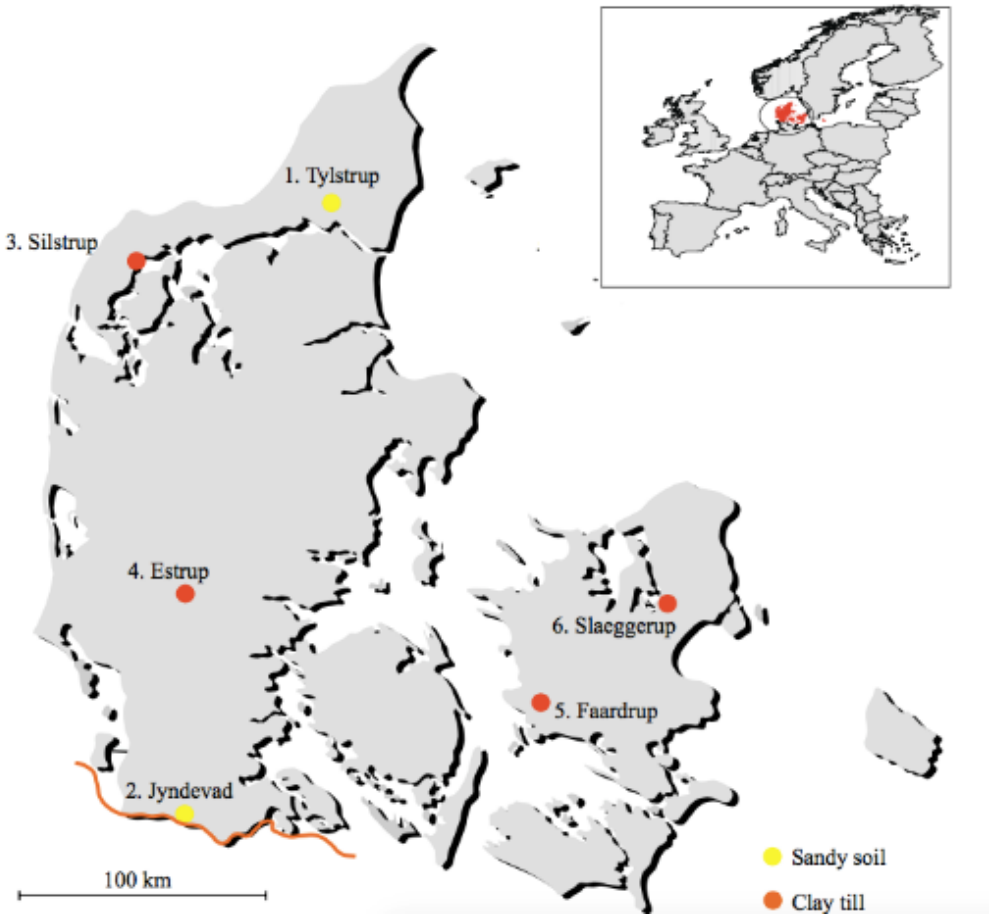

Figure 1: Map of Denmark showing the location of the six PLAP fields, and which soil type they are representing (Lindhardt et al., 2001).

For the selection of the fields, some of the parameters there were considered was soil type, hydrogeology, climate and agricultural practice. However, the selection did not only depend of the mentioned parameters, but also such as site access, i.e. permission from the owner, access to the field all year round, access to electric power and in the case of drained sites, a description of the existing drainage system.

Because of the lack of information and information availability on how to identify the most vulnerable soil types in Denmark, it was decided to select a number of soils type where pesticides are commonly applied on in Denmark. Another very important factor on pesticide leaching is the precipitation. The annual mean precipitation in Denmark during the period 1961–90 was 712 mm/year, varying from 550 mm/year in the Store Bælt region to 900 mm/year in the southern part of Jutland (Danish

meteorological institute, 1997). The groundwater table was also an important factor for deciding, as it should be as near to the surface as possible for a rapid response in the groundwater downstream of the test field. To avoid surface run-off the sites, the selected sites must have a low topographic slope, and the site with structured soils have to be drained and the drain system have to be well known and only cover the test field. To summarize, the field needs to be sufficiently large to adequately cover the variation in soil structure, but the area should not be too large, because it would make it more difficult to intemperate of the results. The field should also previously be used as conventional agricultural practice, the access to the field should be good, and it should be possible to lease the field long term (Lindhardt et al., 2001).

Estrup

Estrup is one of the test fields located in Central Jutland near Vejen. The field is privately owned and is leased by the Danish Institute of Agricultural Science (DIAS). The field has since 1938 been used as a normal field, for agricultural purposes. The field in Estrup have a length and width of 120 m × 96-112 m and covers an area of 1.8 ha including the buffer zone and 1.26 ha otherwise. The buffer zone is 10 m wide along the northern and western margin and 5 m wide along the south because of the local railway tracks, and on the eastern margin is 15 m wide (Lindhardt et al., 2001).

Technical installations

The location of all technical installations was placed based on the drainage system and the groundwater flow pattern of the field. The location for the different technical installations and drainage system is illustrated in Figure 2.

Suction cups

Suction cups are used, because soil water in the unsaturated zone is under tension and therefore cannot flow into a well as groundwater does. The suction cups (S1 and S2, see Figure 2) were installed from two excavation pits, one in the eastern side and one in the northern side. The suction cups installed at a depth of 1 m are located at a horizontal distance of 2 m from the edge of the test field, while the suction cups installed at a depth of 2 m are located at a horizontal distance of 2.5 meters from the edge of the field. At each depth were there installed four suction cups. Because of the collapse of the

profile, it became necessary to move the boarder of the test field 0.5-1 m to the south (Lindhardt et al., 2001).

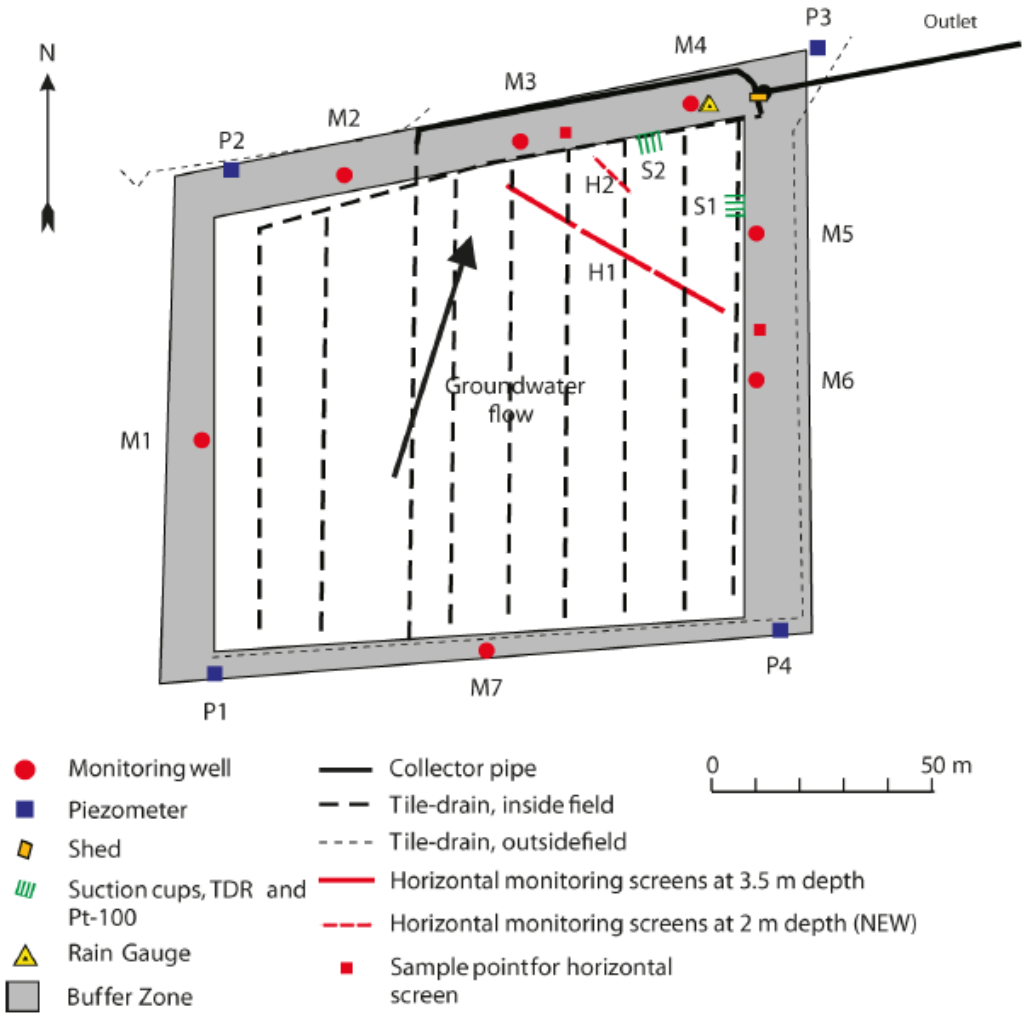

Figure 2: Map of the test field in Estrup, and the location of the technical installations are placed on the field (Rosenbom et al., 2017).

TDR

Soil moisture is measured by a CR10X-controlled Time Domain Reflectometry (TDR)-system. The soil water content is measured in two profiles like the TDR, at the depth of 0.25, 0.4, 0.6, 0.9, 1.1, 1.9 and 2.1 m b.g.s. (below ground surface). At each depth there are three replicate probes. The soil moisture level is measured, and the measurement stored for every hour. The accuracy of the soil water measurements is around 1 vol.% (Lindhardt et al., 2001).

Soil temperature

Pt-100 sensors are installed to measure soil temperature, it is measured in two profiles in five different depth at 0.1, 0.25, 0.6, 1.0 and 2.0, and there is one sensor at each depth. The accuracy of the measurements is 0.1°C (Lindhardt et al., 2001).

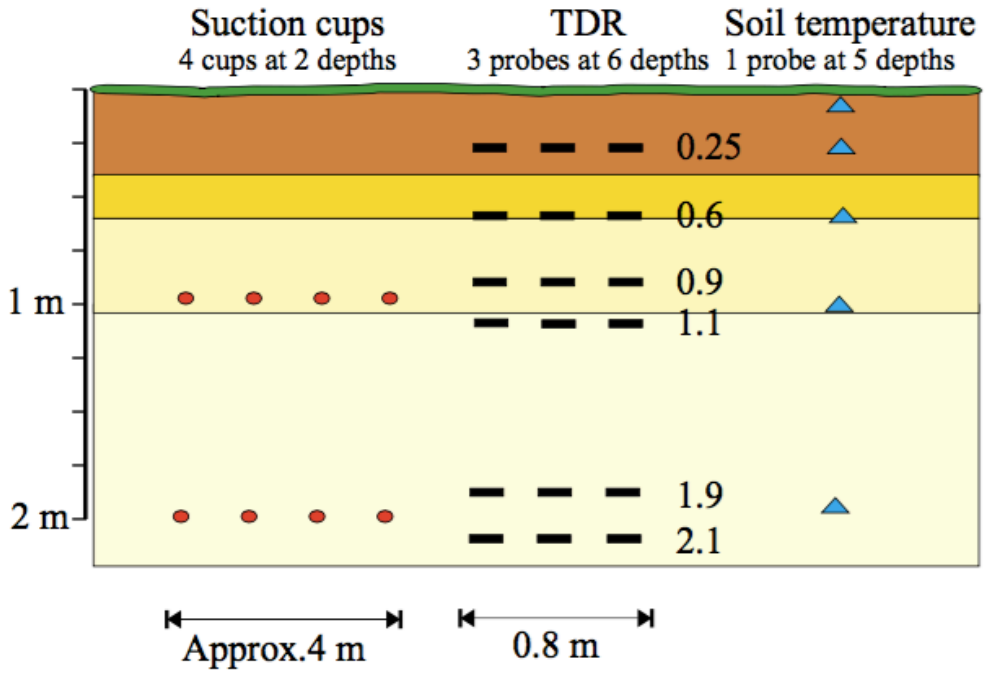

Figure 3: Profile showing the location and depth of the suction cups, TDR and soil temperature measurements (Lindhardt et al., 2001).

Piezometer

Four multiple-level piezometers are installed (P1-4, see Figure 2), where each of them have three separate piezometer screens. The lower screen in each well is located in about 11.5 to 12 m b.g.s. and the top screen is located such that the water table is permanently above the screen. Every time samples are collected, the water level is measured manually as well. Furthermore, the water level is measured in the piezometer closest to the shed (P3) on-line every hour by two druck transducers, one in the upper screen and one in the lower screen. In the piezometer in the opposite corner of the shed (P1), the water level is measured every hour using a D-diver, which is a transducer and data logger. The two wells P1 and P3 were drilled in August 1999 in order to survey the geology and the groundwater head. The other two wells (P2 and P4) were drilled in November 1999. P2 was drilled to 23 m b.gs. in order to monitor the regional groundwater flow (Lindhardt et al., 2001).

Vertical monitoring well

Seven vertical monitoring wells in the site were also installed at the site (M1-M7, see Figure 2). The monitoring wells were installed in November 1999. Each of the monitoring wells have four screens, which have a length of 100 cm. The screens are placed such that they are covering the upper four meters below the groundwater table. The monitoring wells are placed such that there is one well upstream of the field and the other three is downstream of the test field (Lindhardt et al., 2001).

Horizontal monitoring well

The horizontal wells were installed to monitor the water flow which transport pesticides, as can be difficult in clayey soils because of the effect of vertical preferential flow and the sand lenses which can lead to lateral flow. The horizontal well in Estrup (H1) consist of three 18 m screen sections and four 1 m bentonite seals, the well is placed 3.5 m b.g.s. in the northern corner of the test field, see Figure 2. The well was installed in November 1999. Sampling from the horizontal well screens is conducted by a peristaltic pump on the surface (Lindhardt et al., 2001). The monitoring system was extended in September 2011, where three horizontal screens (H2) 2 m b.g.s. was installed in the North-Eastern part of the field (Rosenbom et al., 2017).

Drain water

In Estrup, the drainage system was already installed and described in the criterion for selecting the field. The only information on the drainage system for the field was a hand-drawn sketch, made in 1965. The sketch only contained the distance between the drain pipes and therefore lacked information on the dimensions, depth or gradient of the drainpipes. According to the map, there are eight parallel drains running northwards. These pipes join the main pipe, that runs eastwards parallel to the ditch, and make up the field boundary to the north (Lindhardt et al., 2001).

The measuring chamber was located northeast of the test field. From here the water was led 95 m downstream to the east via a pipe ending in the ditch. The reason for the redirecting pipe is the fact that a more direct outlet further upstream would have necessitated an inconveniently deep ditch (Lindhardt et al., 2001). To cut off water entering the test field from the upstream side, a new drain was installed along the southern and eastern boundaries, which led to the ditch northeast of the measurement chamber (Lindhardt et al., 2001).

Under the construction work for the cut-off drains, small drainpipes were discovered. The spacing between the small pipes was 13 m, which was the same as the distance stated on the map. It seems that the small drainpipes are part of the same drainage system, and all the eight drainpipes inside the test field properly are the same diameter. Because of the narrow size of the drains, indicate that these drains have not been used after 1932. So, the year 1965 seems likely to be the year the map was made, properly in connection with maintenance of the drainage system (Lindhardt et al., 2001).

Precipitation

For measuring precipitation, a tipping bucket rain gauge was used. Sampling was conducted every minute, and data for precipitation stored every hour. The rain gauge accuracy is 0.1 mm (Lindhardt et al., 2001).

Geology

The Estrup site is located west of the Main Stationary Line of the Weichselian glaciation and placed on a hill island. Therefore, the clay till that dominates the site is Saalian, and this till is probably the Little Belt till. This also means that the area has been exposed to both weathering and erosion and other geomorphological processes for approximately 140,000 years (it has both been exposed for interglacial and glacial climate under this time span). Although clay tills are the dominating lithology present, glaciofluvial sand bodies are present locally as well see Figure 4.

A geological-pedological clay till model has been made for the test field in Estrup, see Figure 4. The model consists four units. The topsoil (Unit 1) from 0-0.4 m b.g.s. consists of a dark greyish brown clay and clayey sand (sandy loam). The next unit (Unit 2) range from 0.4-1.0 to 4.0 m b.g.s. is a yellow brown clay till which is noncalcareous oxidized. Root channels are present to a depth of two meters, and these occur together with randomly orientated small desiccation fractures. From two to four meters depth, the fractures are randomly oriented, but systems of small vertical fractures and horizontal-subhorizontal fractures also occur. The saturated hydraulic conductivity is $10^{-7} - 10^{-5}\ m/s$. Other sediment bodies present at the site are in contact with Unit 2 and may influence the upper part of the hydraulic system of the Estrup site. Unit 3, from 4 to approximate 12 m b.g.s, consists of oxidized light yellow to brown sandy clay till. There are large vertical fractures and horizontal fractures present, which form a three-dimensional pattern. The saturated hydraulic conductivity in this unit range from $10^{-9} - 10^{-7}\ m/s$. Unit 4, which is the unit there are below 12 m, consist of alternating

reduced calcareous grey clay till and sandy till beds with occasional sand veins (Lindhardt et al., 2001).

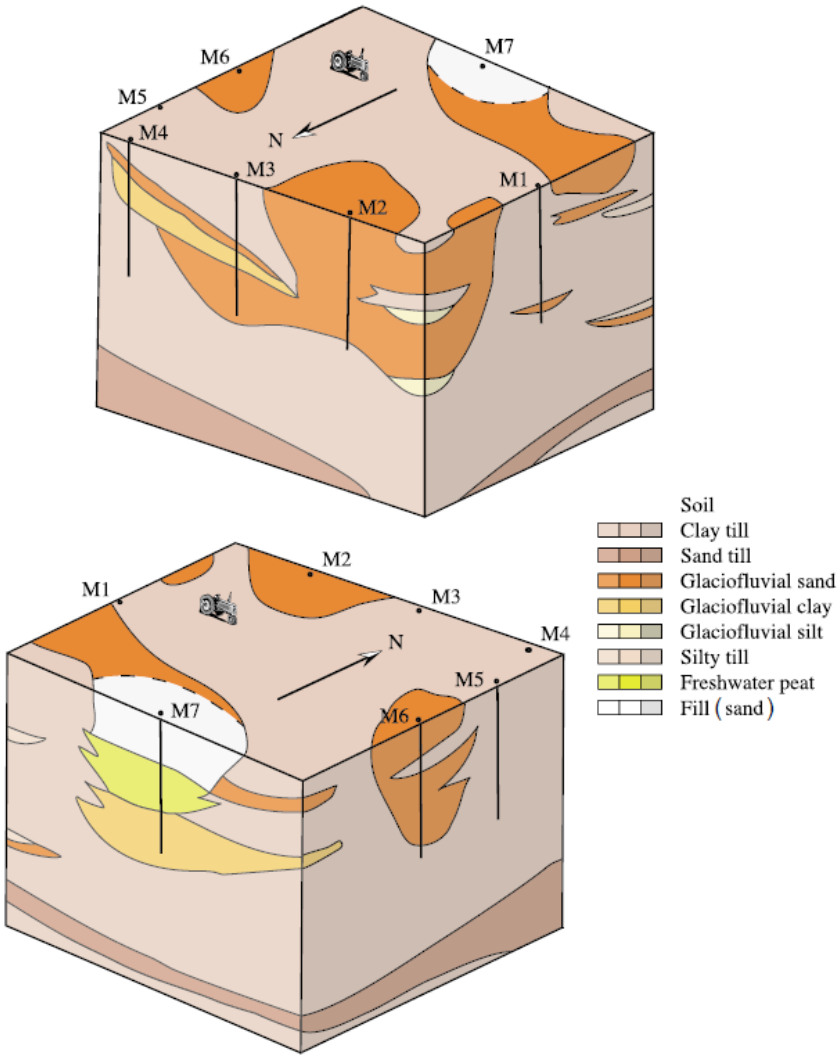

Figure 4: A geological model of the test field Estrup (Lindhardt et al., 2001).

Pedological field work was performed in November 1999, three soil profiles were excavated, in the northern, eastern and western margin of the field. Four soil cores were collected to a depth of 1 m b.g.s. in the buffer zone and 30 soil samples were taken from the topsoil inside the test field in a depth of 0-25 cm b.g.s.

When the monitoring wells and the piezometers were installed, cores were taken to get a better picture of the geology underneath the test field. The cores revealed a more varied geology, consisting of clay

till, glaciofluvial sand and clay, post-glacial peat and fill material (sand) from the construction of the railway. (Lindhardt et al., 2001).

MACRO model

Macro is used as the modelling tool for simulation of all the test fields in PLAP. In the Estrup field, the model simulates the soil profile to a depth at 5 m b.g.s., so the groundwater table always would be in the profile. The model was subsequently calibrated for the monitoring period May 1999 to June 2004 and "validated" for the monitoring period July 2004-June 2016. For the simulation the time series of the observed groundwater table, measures drainage and soil water content is used (Rosenbom et al., 2017).

Theory

Unsaturated water flow

The unsaturated zone sometimes also called the vadose zone, is the zone between the land surface and the groundwater table. As opposed to in the saturated zone where the pores are fully filed with water, the pores in the unsaturated zone is only partially filled, and the remaining part of the pore space is occupied by the gas phase. The unsaturated zone is primarily partially saturated, although there may exist some regions, that are saturated e.g. the capillary fringe, just above the groundwater table, or behind the infiltration front, during or after a high-intensity rainfall event. The way water typically enters the unsaturated zone is by precipitation and irrigation, see Figure 5 where the unsaturated zone is illustrated (Jiří Šimůnek & van Genuchten, 2017).

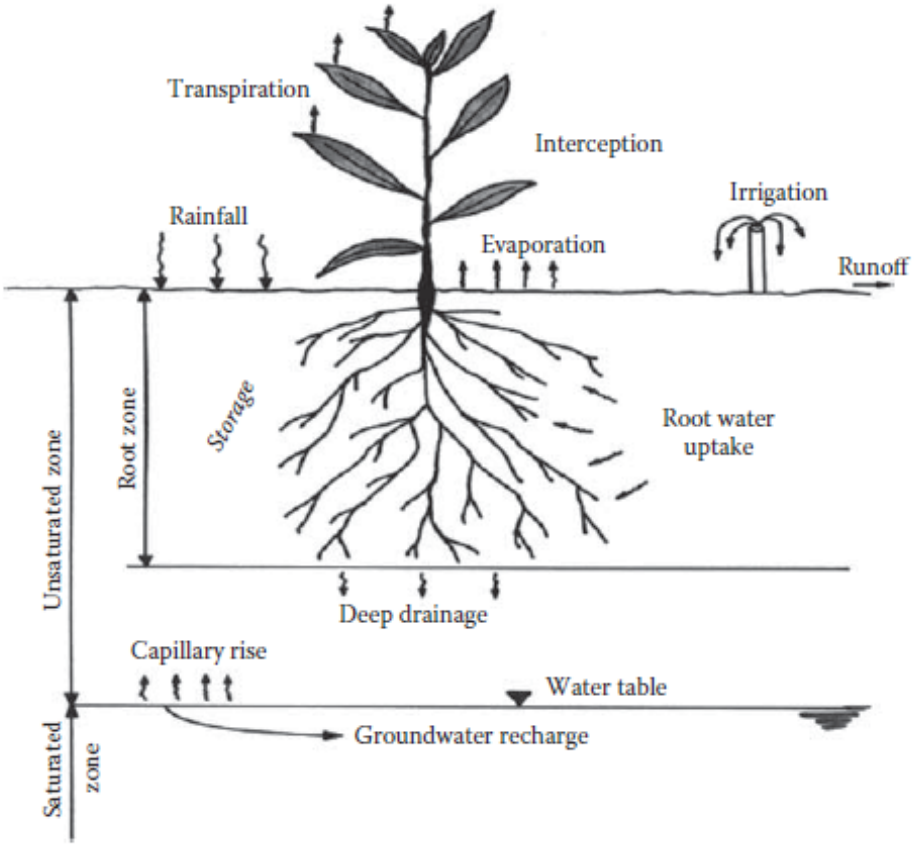

Figure 5: profile of the unsaturated zone and showing the processes there influences the unsaturated zone (Jiří Šimůnek & van Genuchten, 2017).

A fraction of the precipitation or irrigation may also be intercepted on the leaves of the vegetation. If the rainfall or irrigation is greater than the capacity of the soil, the water will be removed by either surface run-off, or accumulate on the soil surface until it evaporates or infiltrate. Some of the water that has infiltrated will evaporate from the soil, and some will be taken up by the roots of the vegetation, where it will return to the atmosphere through transpiration. The process of transpiration and evaporation is often referred as evapotranspiration. The water remaining after the process of evapotranspiration will eventually percolate to the deeper part of the unsaturated zone and eventually reach the saturated zone (Jiří Šimůnek & van Genuchten, 2017).

Water flow in the variably saturated porous media, is usually formulated by the mass balance equation:

$$\frac{\partial \theta}{\partial t} = -\frac{\partial q_i}{\partial x_i} - S \tag{1}$$

Where θ is the volumetric water content, t is time, x_i is the spartial coordinate, q_i is the volumetric flux density and S is the general sink/source term. The mass balance generally states, that the change in the water content in a given volume is due to a spatial change in the water flux (Jiří Šimůnek & van Genuchten, 2017).

Uniform flow in soils are described using the Darcy-Buckingham equation. By extending the exiting equation (Darcy's equation) for water flow in the saturated zone so it could describe flow in the unsaturated zone (Hendriks, 2010).

$$q_i = -K(h)\left(K_{ij}^A \frac{\partial h}{\partial x_i} + K_{iz}^A\right) \tag{2}$$

Where, K is the unsaturated hydraulic conductivity and K_{ij}^A are components of a dimensionless anisotropy tensor K^A (which reduces to the unit matrix when the medium is isotropic).
The Darcy-Buckingham equation is similar to Darcy's equation, except the fact that the proportionality constant (the unsaturated hydraulic conductivity) in the Darcy–Buckingham equation (equation

2) is a nonlinear function of the pressure head. In Darcy's equation K is a constant equal to the saturated hydraulic conductivity K_s. Richard's partial differential equation is derived by combining the mass balance and the Darcy-Buckingham equation, leading to the general form of Richards equation.

$$\frac{\partial \theta(h)}{\partial t} = \frac{\partial}{\partial x_i}\left[K(h)\left(K_{ij}^{A}\frac{\partial h}{\partial x_i} + K_{iz}^{A}\right)\right] - S(h) \quad (3)$$

Richards equation is the governing equation for variable saturated flow in the unsaturated zone (Jiří Šimůnek & van Genuchten, 2017).

Solute transport

Solute transport is the movement of dissolved substances in the groundwater. There are several different physical and chemical processes governing solute transport. Advection is a physical process of solute transport, where the movement of solute is caused by the water flow. As the water is moving, it tends to disperse, as a result of the water velocity not being even in or between the soil pores. Diffusion is a chemical process of solute transport, and is when the molecules randomly move, a process causing the solute to move from a place with higher concentration to a place with lower concentration (Fitts, 2002).

In a 3D groundwater flow model, the x, y and z directions should be defined to allow fluxes in all three dimensions. The three-dimensional advection-dispersion equation for a nonreactive solute is described as:

$$\frac{\partial}{\partial x}\left(D_x\frac{\partial C}{\partial x}\right) - \frac{\partial}{\partial x}(v_x C) + \frac{\partial}{\partial y}\left(D_y\frac{\partial C}{\partial y}\right) - \frac{\partial}{\partial y}(v_y C) + \frac{\partial}{\partial z}\left(D_z\frac{\partial C}{\partial z}\right) - \frac{\partial}{\partial z}(v_z C) = \frac{\partial C}{\partial t} \quad (4)$$

Where D is the macro dispersion coefficient which consist of both the mechanical dispersion and molecular diffusion, in the x, y and z direction, C is the concentration and v is the linear velocity (Fitts, 2002).

Soil water retention

In the unsaturated zone the smaller pores of a medium hold on to the water more strongly than the bigger pores. For this water to be extracted it requires application of a higher matric potential. The volume of water held in the soil at different matric potentials depend on the pore size distribution. The soil water retention is expressed by the volumetric water content (θ) and the matric potential (ψ), which is the pressure head with a negative sign, and can by illustrated by a θ vs. ψ curve, see Figure 6 (Nimmo, 2009). pF is defined as: $pF = \log(-\psi)$ (Hendriks, 2010).To avoid strongly negative numbers for the matric potential, pF is used in Figure 6.

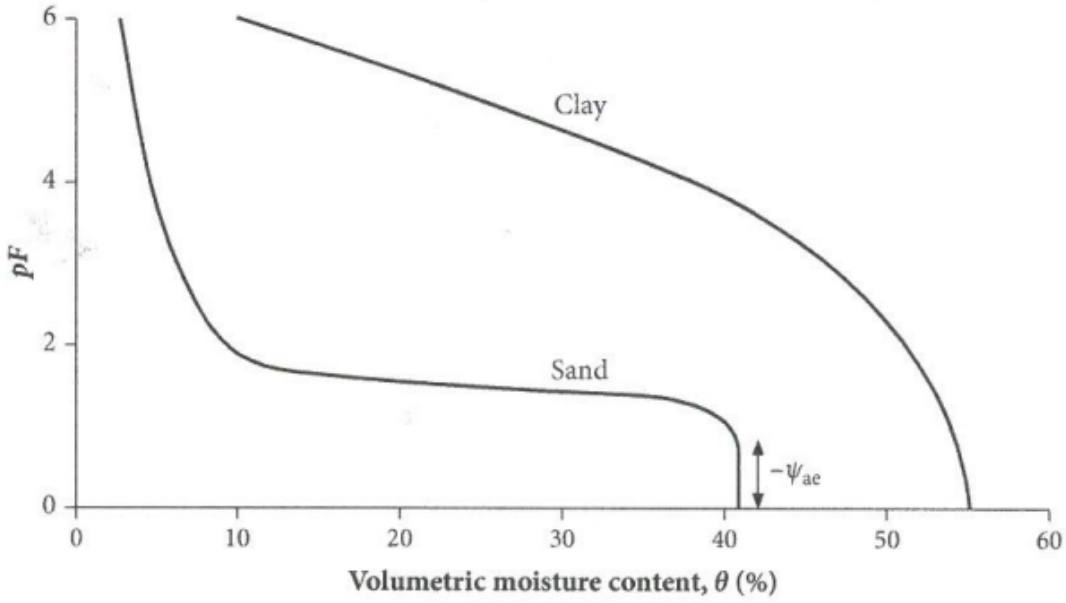

Figure 6: graph showing the soil water retention for two soil types (sand and clay), where the volumetric soil content is illustrated on the x-axis and the matric potential expressed be pF on the y-axis (Hendriks, 2010).

As shown in Figure 6, when pF is cloce to zero (ψ is less negative) then the air-water interface are broadly curved, the pores are almost filled with water and θ is high. Vice versa, if ψ is more strongly negative, the interface becomes more tightly curved, they no longer spans the larger pores and the pores are less filled with water (Nimmo, 2009).

The two water retention curves are illustrated in Figure 6 for two different soil types, sand and clay, the shape for the two soil types are different, and this is due to differences in the nature of water binding forces, because clay has a higher porosity and a larger variety of pore sizes the well sorted

sand (Hendriks, 2010). The water retention curve can in general be represented by measured data, but it is often more convenient to express the water retention curve as an empirical formula. There are several formulas representing the retention curve, but one of the most used is the one from van Genuchten:

$$\theta = (\theta_{max} - \theta_{min}) \left[\frac{1}{1 + \left(\frac{\psi}{\psi_c}\right)^{v}} \right]^{\mu} + \theta_{min} \qquad (5)$$

Where ψ_c, v, μ and θ_{min} are empirical fitted parameters. Fundamentally, θ_{min} should be equal zero but a finite value is used to improve the fit in the higher θ portion of the curve (Nimmo, 2009).

HydroGeoSphere

HydroGeoSphere (HGS) is a fully 3D integrated surface-subsurface flow simulator. HydroGeoSphere uses a modified form of Richards' equation, so it describes the three-dimensional transient subsurface flow in a variable-saturated porous medium:

$$-\nabla \cdot (w_m q) + \sum \Gamma_{ex} \pm Q = w_m \frac{\partial}{\partial t} (\theta_s S_w) \qquad (6)$$

Where w_m is the volumetric fraction of the total porosity occupied by the porous medium. The volume fraction is always equal to 1, except when a second porous continuum is used in the simulation, which for example is the case when dual continuum is used to represent fractures or macropores in the model. θ_s is the saturated water content, which is assumed equal to the porosity. Γ_{ex} is the volumetric exchange rate between the subsurface domain and all other types of domains present in the model. Q is a volumetric fluid flux per unit volume representing a source (when it is positive) or a sink (when it is negative) term to the porous medium system. Thus, it represents the fluid exchange with the outside of the simulation domain. In addition, the fluid flux q is given by:

$$q = -K \cdot k_r \nabla(\psi + z) \qquad (7)$$

Where $k_r = k_r(S_w)$ represents the relative permeability of the medium with respect to the degree of

water saturation S_w, ψ is the pressure head and z is the elevation head. The hydraulic conductivity tensor K is given by:

$$K = \frac{\rho g}{\mu} k \tag{8}$$

Where g is the gravitational acceleration, μ is the viscosity of water, k is the permeability and ρ is the density of water. Moreover, the water saturation is related to the water content (θ) as below:

$$S_w = \frac{\theta}{\theta_s} \tag{9}$$

Van Genuchten proposed an equation for the relation of pressure-saturation:

$$\begin{aligned} S_w &= S_{wr} + (1 - S_{wr})\left(1 + |\alpha\psi|^{\beta}\right)^{-v} && \text{for } \psi < 0 \\ S_w &= 1 && \text{for } \psi \geq 0 \end{aligned} \tag{10}$$

With the relative permeability given by:

$$k_r = S_e^{(lp)} \left[1 - \left(1 - S_e^{\frac{1}{v}}\right)^{v}\right]^2 \tag{11}$$

Where:

$$\left(v = 1 - \tfrac{1}{\beta}\right), \qquad \beta > 1 \tag{12}$$

Where S_{wr} is the residual water saturation, α is the inverse of the air-entry pressure head, β is the pore-size distribution and S_e is the effective saturation, which is given by: $S_e = (S_w - S_{wr})/(1 - S_{wr})$. α and β are usually obtained from a fit of the equation above (equation 11 and 12). For the relative permeability model, Mualem (1976) has estimated that the pore connectivity parameters lp is equal to 0.5 for most soils (Therrien et al., 2010).

Evapotranspiration

Evapotranspiration is modelled as a combination of both plant transpiration and evaporation, which affect both surface and subsurface flow domains. The rate of transpiration (T_p) is estimated using the following relationship (Therrien et al., 2010):

$$T_p = f_1(LAI) f_2(\theta) RDF\left[E_p - E_{can}\right] \tag{13}$$

Where $f_1(LAI)$ is the function of leaf area index, $f_2(\theta)$ is the function of nodal water content and RDF is the time varying root distribution function. The function of leaf area index is expressed as:

$$f_1(LAI) = max\{0, min[1, (C_2 + C_1 LAI)]\} \tag{14}$$

The root depth function is expressed as:

$$RDF = \frac{\int_{z_1'}^{z_2'} r_F(z')dz'}{\int_0^{L_r} r_F(z')dz'} \tag{15}$$

Where L_r is the effective root length, z' is the depth coordinate from the soil surface and $r_F(z')$ is the root extraction function, which typically varies logarithmically with depth. The moisture content dependence term $f_2(\theta)$ is expressed as:

$$f_2(\theta) = \begin{cases} 0 & for\ 0 \le \theta \le \theta_{wp} \\ f_3 & for\ \theta_{wp} \le \theta \le \theta_{fc} \\ 1 & for\ \theta_{fc} \le \theta \le \theta_o \\ f_4 & for\ \theta_o \le \theta \le \theta_{an} \\ 0 & for\ \theta_{an} \le \theta \end{cases} \tag{16}$$

Where:

$$f_3 = 1 - \left[\frac{\theta_{fc} - \theta}{\theta_{fc} - \theta_{wp}}\right]^{C_3} \tag{17}$$

$$f_4 = \left[\frac{\theta_{an} - \theta}{\theta_{an} - \theta_o}\right]^{C_3} \quad (18)$$

Where C_1, C_2 and C_3 are dimensionless fitting parameters, θ_{fc} is the moisture content at field capacity, θ_{wp} is the moisture content at the wilting point, θ_o is the moisture content at the oxic limit and θ_{an} is moisture content at the anoxic limit (Therrien et al., 2010).

Potential evapotranspiration can be used as a command in HydroGeoSphere, which sets the input type to be a special specified flux boundary condition and converts the evaporative fluxes to nodal volumetric fluxes (Therrien et al., 2010).

Drain

Drain flux is assigned to one or several nodes in the model as a boundary condition. The drain flux only allows water to flow out of the system, depending on the differences in head of the drain node and the specified drain head value. The following equation describes the drain flow for a given drain node i (Therrien et al., 2010):

$$\begin{aligned} Q_i &= C_{DR}(h_i - h_{DR}) \qquad && h_i > h_{DR} \\ Q_i &= 0 && h_i \leq h_{DR} \end{aligned} \quad (19)$$

Where C_{DR} is an equivalent conductance for the drain node and h_{DR} is the drain hydraulic head. Therefore, the drain only becomes active, when the hydraulic head for the node become bigger than the drain hydraulic head (Therrien et al., 2010).

Solute transport

Solute transport in HydroGeoSphere for porous medium in a variable saturated matrix is described by following equation for three-dimensional flow:

$$-\nabla \cdot w_m(qC - \theta_S S_w D \nabla C) + [w_m \theta_S S_w R \lambda C]_{par} + \sum \Omega_{ex} \pm Q_c = w_m \left[\frac{\partial(\theta_S S_w R C)}{\partial t} + \theta_S S_w R \lambda C\right] \quad (20)$$

Where C is the solute concentration, λ is the first order decay constant (the subscript designates parent

species for the case of a decay chain), w_m is the volumetric fraction of the total porosity, S_w is the subsurface water saturation, θ_S is the subsurface saturated water constant, q is the fluid flux and Q_c is either a source (positive) or a sink (negative) in the porous medium system. It is assumed in the solute transport flow equation (equation 20) that the fluid is incompressible. Ω_{ex} represents the mass exchange rate of solutes per unit volume between the subsurface domain and all other types of domains supported by the model. The retardation factor R is given by:

$$R = 1 + \frac{\rho_b}{\theta_S S_w} K' \tag{21}$$

where ρ_b is the bulk density of the porous medium and K' is the equilibrium distribution coefficient describing a linear Freundlich adsorption isotherm. The hydrodynamic dispersion tensor D is given by:

$$\theta_S S_w D = (\alpha_l - \alpha_t)\frac{qq}{|q|} + \alpha_t |q| I + \theta_S S_w \tau D_{free} I \tag{22}$$

Where α_l and α_t are the longitudinal and transverse dispersivity, $|q|$ is the magnitude of the Darcy flux, τ is the tortuosity, D_{free} is the free-solution diffusion coefficient and I is the identity tensor. The product τD_{free} representing the effective diffusion coefficient for the matrix. In the unsaturated zone, the tortuosity is allowed to vary with the water saturation, according to the Millington-Quirk relationship there is given by (Therrien et al., 2010):

$$\tau = \frac{(\theta_S S_w)^{7/3}}{\theta_S^2} \tag{23}$$

Dual domain

HydroGeoSphere is able to simulate variable-saturated flow in a dual continuum. The first continuum, which is the porous medium, is linked to the other continuum by a fluid exchange term. The dual continuum could be for example facture or macropores present in the porous matrix. In the same way as flow in the porous medium, the three dimensional variably-saturated flow in the dual continuum is described by a modified Richard's equation (equation 6). The equation is the same as previously

described, where the notation d is used to represent the dual continuum, and the modified Richards equation is given by (Therrien et al., 2010):

$$-\nabla \cdot (w_d q_d) - \Gamma_d \pm Q_d = w_d \frac{\partial}{\partial t}(\theta_{sd} S_{wd}) \tag{24}$$

The fluid flux is given the same way as previous for porous media flow (equation 6), and the same for the hydraulic conductivity K. They are used as an exchange term when simultaneous flow in the subsurface porous medium and a second continuum are modelled. The exchange term can be defined as:

$$\Gamma_d = \alpha_{wd} K_a k_{ra} (\psi_d - \psi) \tag{25}$$

Where K_a is the hydraulic conductivity of the interface between the two domains and k_{ra} is the realative permability. α_{wd} is given by:

$$\alpha_{wd} = \frac{\beta_d}{a}\left[\frac{\gamma_w}{a}\right] \tag{26}$$

Where, β_d/a is the macropores surface area per unit total volume of the medium, β_d is a geometrical shape factor, a is the fracture-matrix skin thickness over which the flow exchange will occur and γ_w is an empirical coefficient (Therrien et al., 2010).

Calibration and inverse calibration

Inverse calibration is a method where a mathematical algorithm is used to optimize the selected parameters. Inverse Calibration or automatic parameter optimization can be illustrated as in Figure 7. The simulation model consists of a numerical model code, composed of a model setup and a model forcing. The model setup or the conceptual model is the flow elements, boundary condition, etc. The model forcing is e.g. precipitation, pumping, discharge, etc. Another important point is the parameterisation and the selection of the parameters to be calibrated. Outside the model, the overserved data is needed in the objective function and the optimization algorithm.

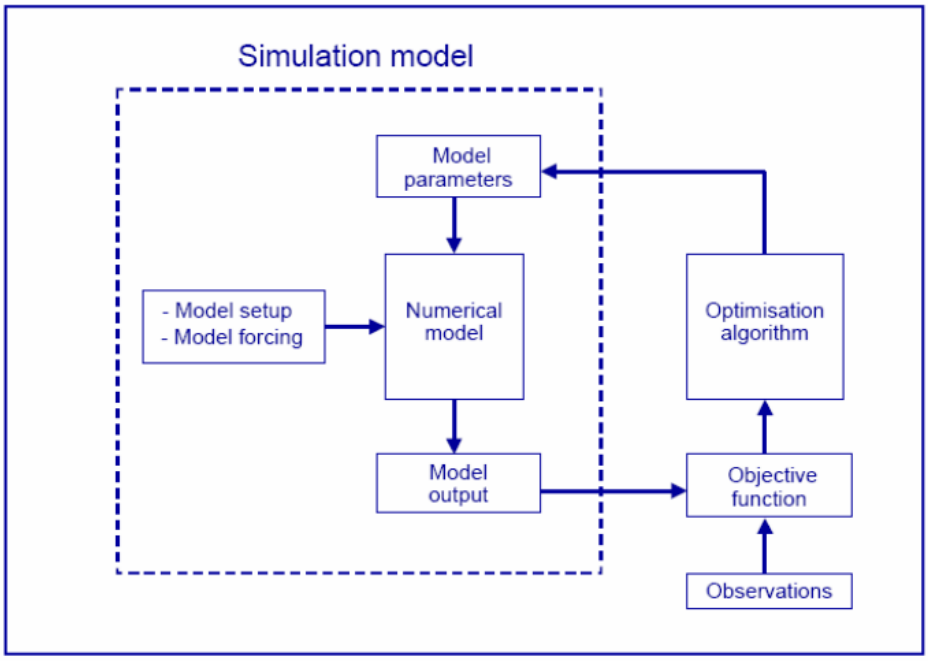

Figure 7: illustration of inverse parameter optimization and the different steps involved (Sonnenborg & Henriksen, 2005).

For the inverse solution, the invers modelling tool PEST is used PEST stands for Parameter ESTimation, and was originally developed to expedite the process of model calibration, wherein values for model parameters are back calculated by matching model outputs to measurements of system state (Doherty, 2016).

The expression (equation 27) describes the deviation between the observed data and the simulated data is called the objective function, which is expressed by G. G is expressed as the weighted sum of the squared residuals (Sonnenborg & Henriksen, 2005).

$$G(\underline{b}) = \sum_{i=1}^{n} w_i r_i^2 \qquad (27)$$

b the vector of the calibration parameters and w_i is the weighting of the parameters. Weighting of the residuals can be handled in many different ways. One subjective way is to assign the observation with a more accurate reproduction a higher weighting coefficient, than an observation where the accuracy not is necessarily as good, which therefore is assigned a lower weighting coefficient. Another way is to estimate the uncertainty of the residuals, which theoretically would be in favour to assign a small weight to the residuals with a great uncertainty and vice versa, a higher weight to the residuals with

a lower uncertainty. It is often used to assign the residual a weight, which is inversely proportional to the variance of the error of the residuals, so w_i is expressed as:

$$w_i = \frac{1}{\sigma_1^2} \tag{28}$$

It is both possible and often also more appropriate to calibrate against more than one parameter. If the selected residuals are weighted with the uncertainty on the observation, the weighted residuals will be dimensionless and therefore there will not be any difficulties calculating the weighted sum of the squared residuals (G). But there will often be more measurements of one of the observation types than the others, and this could lead to a tendency, where the one type with the most observations will dominate the results in the optimization function. If the model is chosen to optimize against two parameters, they could be expressed as single objective functions by G_1 and G_2, then G would be:

$$G = v_1 G_1 + v_2 G_2 \tag{29}$$

Where, $0 \leq v_i \leq 1$ and $\sum v_i = 1$ (Sonnenborg & Henriksen, 2005).
Another method is weighting v_i by the number of observations available for the different datatypes. Then v_i is expressed by:

$$v_i = 1 - \frac{N_i}{N} \tag{30}$$

Where N_i is the number of observations for data type i and N is the total number of observations. The weighting approach assumes that the used residuals have the same dimension (Sonnenborg & Henriksen, 2005).

An efficient way to assess how well the simulated data fits the observed data is a visual comparison of the simulated and observed data. In addition, a calculation of summary statistic like RMSE (Root Mean Squared Error), which is the average squared error, can help evaluate how well the data fits. RMSE is defined as:

$$RMSE = \sqrt{\frac{1}{n}\sum_{i=1}^{n} r_i^2} \tag{31}$$

Where, n is the number of observation and r is the residuals for a given datatype (Sonnenborg & Henriksen, 2005).

To supplement the RMSE calculations a R^2 value can be calculated. This value expresses how much of the total variation in the observed data can be explained by the model. R^2 is expressed by:

$$R^2 = \frac{\Sigma\left(\psi_{obs} - \overline{\psi}_{obs}\right)^2 - \Sigma\left(\psi_{obs} - \overline{\psi}_{sim}\right)^2}{\Sigma\left(\psi_{obs} - \overline{\psi}_{obs}\right)^2} \tag{32}$$

Where $\overline{\psi}_{obs}$ and $\overline{\psi}_{sim}$ are respectively the observed value for the observed and simulated data (Sonnenborg & Henriksen, 2005).

A method to see the model ability to simulate the average flow is by the function Fbal (in %), which is given by:

$$Fbal = 100\frac{\overline{Q_o} - \overline{Q_s}}{\overline{Q_o}} \tag{33}$$

Where Q_o and Q_s respectively is the average flow for the simulated and observed data (Sonnenborg & Henriksen, 2005).

A correlation matrix is another useful tool to evaluate whether the selected parameters are correlated. In a correlation matrix, 1 is a perfect correlation, diagonally the matrix will always have the correlation value 1, because it shows the correlation between the same parameter. If the correlation between two parameters is 1 or close to 1, it is doubtful if the calibration is able to give a unique value for the correlated parameter. A guidance is if the correlation coefficient is above 0.95 it should be neglected from the calibration because of problems with the uniqueness (Sonnenborg & Henriksen, 2005).

Methods

Model development

The model is a column representing the field in Estrup. The column is designed so it is 500 cm long (z direction) and 10x10 cm wide (x and z direction). The model is 500 cm in depth to ensure the groundwater table always is in the model domain. The discretization of the column is 1 in both the x and y direction and 500 in the z direction. The column is divided into four different zones with different properties. Zone 1 is from the surface and 27 cm deep, zone 2 goes from 27 cm to 55 cm, zone 3 from 55 cm to 105 cm and the last and the deepest zone 4 goes from 105 cm to 500 cm, see Figure 8. The depth of the different zones is earlier defined from the pedological soil profiles in the MACRO model. Pressure head are used as input, where the model first was run with an initial head of -100 cm. Around day 350, the pressure head settled at a value of about 0 cm, and this head value was then used as the initial head condition instead. The initial head condition is shown in Figure 8, where it is illustrated in hydraulic head.

The model simulates over a period of three years from 2005-2007 and have output times for every second day, a total amount of 1095 days and 549 output times. This period is chosen based on breakthrough curves on bromide concentration (see Appendix 1, Figure 35-38). These concentrations are measured from the suction cups, the drain and vertical and horizontal wells. There are implemented observation points in the model in the depth of where the suction cups, drain, horizontal well and TDR probes are installed. In addition, one observation points is placed in the depth of the filter for the piezometer where the groundwater is measured. Three observation wells are made as well, these are placed in the depth of the screens for the vertical wells. The fourth screen is located too deep, would therefore exceed the model domain, and is therefore not used in the simulation.

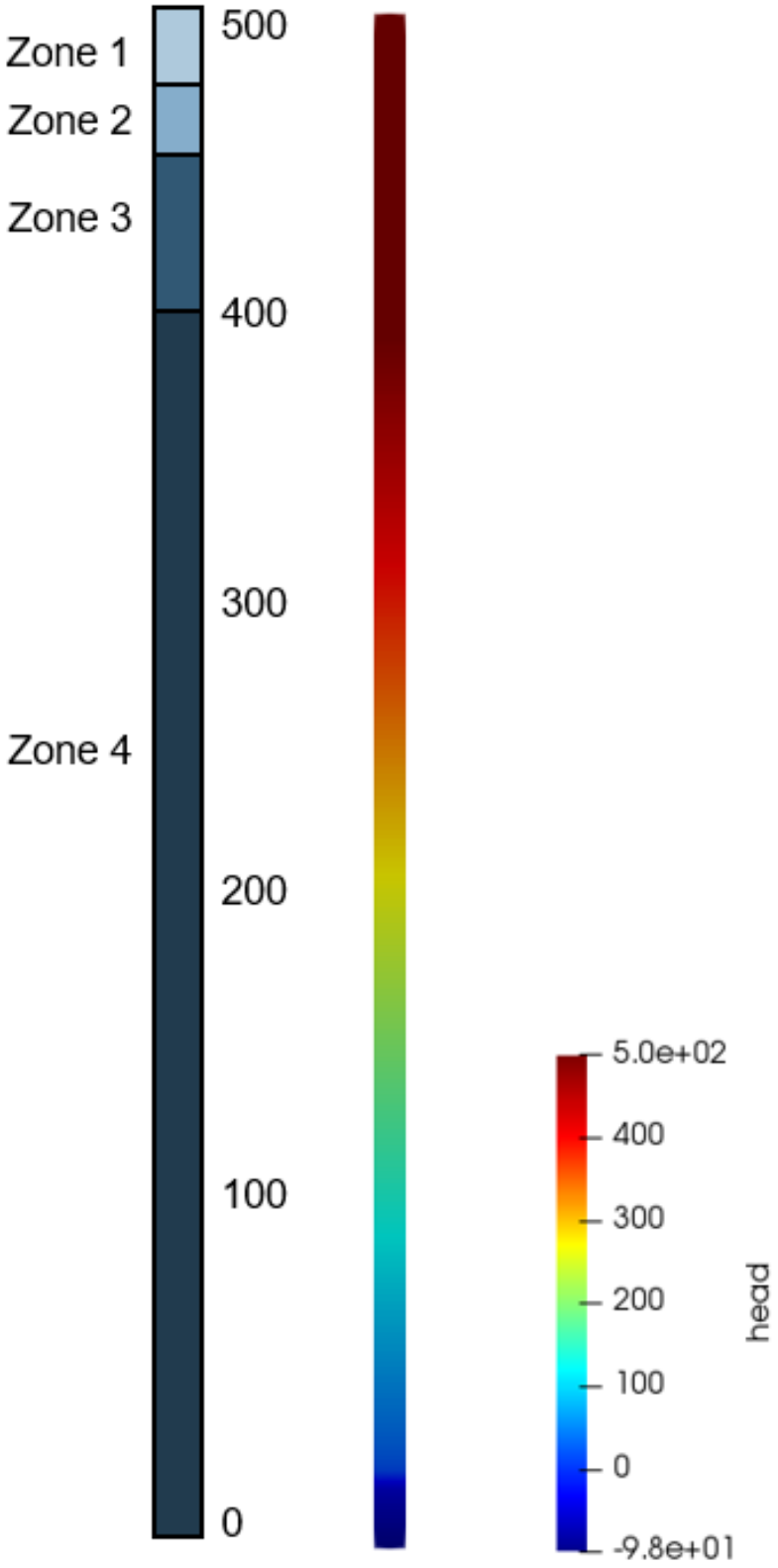

Figure 8: Conceptual figure of the model column showing the four zones, where the surface is in 500 cm and the lower boundary is 5 m b.g.s (0 cm) and the initial head condition for the model.

Drain is included in the model at a depth of 1.1 m b.g.s., 110 cm below the top of the model. The drain is only activated when the head in the drain node become higher that the selected drain head. The drain head is set to 0, so when the pressure head rises above 0, in the selected node the model will remove the water from the model. A value for drain conductance is set as well, an initial value was set to 10, but this value will later be calibrated.

The boundary condition in the model in the top is precipitation and evapotranspiration. Precipitation is imported as a daily value in cm/day. The potential evapotranspiration is imported in the same way as precipitation with a daily value. In addition, a property file (*etprops*) (Appendix 2) is made for different evapotranspiration properties, see Table 1. The transpiration fitting parameters are from Kristensen & Jensen (1975). A Table is also defined for leaf area index values in the *etprops*, these values are extracted from the MACRO model.

ET Materials	Value
Evaporation depth (cm)	100
Root depth (cm)	70
Wilting point	0.2
Field capacity	0.32
Oxic limit	0.76
Anoxic limit	0.9
transpiration fitting parameters	
c1	0.34
c1	0.15
c3	1

Table 1: Table of the material properties for evapotranspiration. These values are represented in the model in the etprops file.

Because of limitations in HydroGeoSphere, it was not possible to include potential evapotranspiration without a surface domain. Therefore, a surface domain was built into the model and an *oprops* (Appendix 2) file was made with the parameter properties for overland flow. In the properties file, four parameters are determined, the x and y friction, which is the Manning roughness coefficients in the x

and y direction, obstruction storage height and the coupling length, which is used in the exchange term for the surface and subsurface domain.

The hydraulic properties for the different zones are extracted from the MACRO model and a material properties file (*mprops*) (Appendix 2) is made where the different zones are represented by the values presented in Table 2. The values for the van Genuchten fitting parameters α and β are from Carsel and Parrish (1988) based on the hydraulic conductivity value for the zone. The reason why the van Genuchten fitting parameters which was extracted from MACRO not was used, were because the model could not run with these parameter values. A model was also establish in HYDRUS (J. Šimůnek, Šejna, Saito, Sakai, & Th., 2009) to test the parameters and how much they should be changed to run the model.

Material Properties	Zone 1	Zone 2	Zone 3	Zone 4
K isotropic (cm/day)	571	24	28	0.05
Specific storage (cm^{-1})	1E-07	1E-07	1E-07	1E-07
Porosity	0.41	0.36	0.34	0.4
Tortuosity	1	1	1	1
Bulk density (kg/cm^{-3})	0.00151	0.00168	0.00173	0.00164
Unsaturated van Genuchten functions				
Residual saturation	0.01	0.01	0.01	0.01
α (cm^{-1})	0.145	0.036	0.059	0.01
β	2.68	1.56	1.48	1.2

Table 2: Table of the material properties for the soil in the four different zones. These values are represented in the model in the mprops file.

Transport of bromide is implemented in the model as well. Bromide is added on the field in form of potassium (KBr). On the 11th of November 2005 (day 312 in the model) 30 kg/ha potassium was added and spread out on the field, to calculate this to a concentration it was decided that it was spread with 1 mm water. The concentration for bromide is converted to be $1.98 \cdot 10^{-6}\ kg/cm^3$ and added to the field in total on day 312. One issue appeared when the model should run with solute transport, because output only was set to every second day, it would not calculate the bromide concentration in the different observation points, when day 313 was used as the end day for applying bromide. Therefore, the input was halved and added over a two day period instead, such that the end day was day

314. In the *mprops* file the dispersivity is defined to be 50 cm. The dispersivity is an unknown factor, but a rule of thumb is 10% of the flow length. The dispersivity can also be estimated from the plot in Gelhar, Welty, & Rehfeldt (1992).

The model was extended to a dual continuum model because of the soil type present at the Estrup field is mainly clay and contains fracture and macropores. Therefore, is a second continuum added to represent the macropores which are present. Dual continuum was applied to the whole model, and a *dprops* (Appendix 2) file was made with properties for the fracture in the dual continuum. The values in the *dprops* file is shown in Table 3. The α and β in the unsaturated van Genuchten function are from Rosenbom et al. (2009). Some of the parameters did not get tested due to lack of time but values are taken from the verification example Gerke (Therrien et al., 2010).

Dual continuum properties	Value
K isotropic (cm/day)	1000
Specific storage (cm^{-1})	1.00E-07
Porosity	0.95
Volume fraction dual medium	0.05
First-order fluid exchange coefficient	0.3
Interface k	0.01
Longitudinal dispersivity (cm)	10
Transverse dispersivity (cm)	0.01
Vertical transverse dispersivity (cm)	0
tortuosity	1
Bulk density (kg/cm^{-3})	0.002
First-order mass exchange	0.15
Unsaturated van Genuchten functions	
Residual saturation	0.01
α (cm^{-1})	0.1
β	2

Table 3: Table of the material properties for dual domain. These values are represented in the model in the dprops file.

Inverse calibration

The inverse calibration of the model was executed with the use of the inverse calibration software PEST (Doherty, 2016). The parameters chosen to be calibrated is the hydraulic conductivity (k1-4), the van Genuchten parameters alpha (a1-4) and beta (b1-4) for all the four zones, and the drain conductance. In total 13 parameters are chosen to be optimized. The observation data used for the optimization is the observed data for the depth to the groundwater table (gwt), saturation (wsat) and drainage (drain). The saturation is calculated from the observed water content (equation 9). However, when the saturation was calculated for other depths than 25 cm b.g.s. many of the values exceed 1, which is not possible. This is due to a quite large uncertainty on the TDR data, when the soil is close to or fully saturated. Therefore, only observed saturation data for the depth of 25 cm b.g.s. was used to optimize against. The initial values used in the inverse calibration is the illustrated in Table 2. When performing the inverse calibration, the weight for the individual observation groups are 1 and the total weight of the objective function is 3. In this thesis, parameters where the correlation value exceed 0.9 are excluded. The uncertainty limits for the different groups are recommended by K. H. Jensen, and for the depth to groundwater table the accepted uncertainties should be less than 50 cm, for saturation it is 0.1 and for the drain the accepted uncertainty is 10% differences from the average observed data.

Different scenarios are established in this thesis to determine if changes to the model setup has any impact on model performance. The First model setup (Model A) is the simplest setup, as it is only simulating water transport. Model B is an attempt to determine if the drain was moved 10 cm up, and thereby located in zone 3, would have an impact on model performance, especially for simulating drain flow. Model C is the model with a dual continuum. For each calibration, a model with the calibrated parameter values will be executed with added solute transport. In addition, a calibration for Model A and B where solute transport is included will be executed as well. See model descriptions in Table 4.

Model name	Description
Model A	Model with only flow condition. • Without dual domain
Model B	Model similar to model A, but the drain is moved to 400 cm (1 m b.g.s.) so it is located in zone 3, to see of it has any impact on the calibration.
Model C	Incorporation of dual domain for macropores, in Model A

Table 4: Description of the different scenario set up together with their name.

Results

Calibration results Model A

The following section present the results of the calibration of the more simple Estrup field model (Model A), where only water flow is taking into account.

A sensitivity analysis for the model is made, see Figure 9. The most sensitive parameters are the hydraulic conductivity for zone 3 and 4 (k3 and k4) and the van Genuchten parameter α for zone 3 (a3). The parameters, which are not quite as sensitive, are the van Genuchten parameter β (b4) for the deepest layer (zone 4) and the conductance for the drain, see Figure 9.

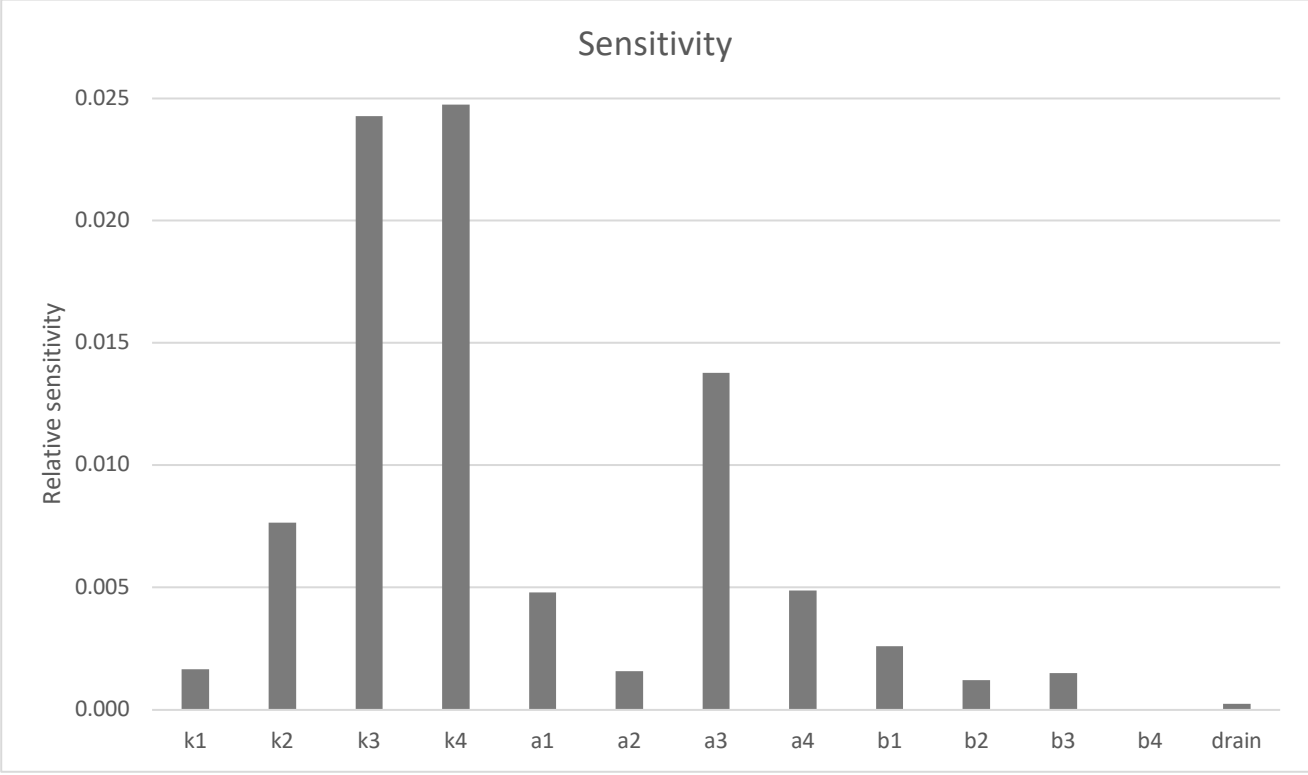

Figure 9: Graph of the parameter sensitivity for Model A.

From the sensitivity analysis the correlation matrix was made as well (Table 5). In Table 5 the correlation is shown between the different parameters, and the parameter which are correlated are illustrated by the green colour. This means, that k2 is correlated with a4, and a3 is correlated with b2. The

correlation of the parameters means, that optimization of these parameters is difficult, and they are therefore not included in the optimization.

Correlation matrix													
	k1	**k2**	**k3**	**k4**	**a1**	**a2**	**a3**	**a4**	**b1**	**b2**	**b3**	**b4**	**Drain**
k1	1	0.11	0.01	0.01	0.06	0.31	0.17	0.14	0.10	0.10	0.03	0.01	0.05
k2	0.11	1	0.07	0.07	0.46	0.07	0.18	0.98	0.32	0.10	0.17	0.32	0.75
k3	0.01	0.07	1	0.84	0.01	0.01	0.02	0.06	0.02	0.01	0.02	0.02	0.07
k4	0.01	0.07	0.84	1	0.02	0.00	0.02	0.06	0.00	0.01	0.02	0.02	0.08
a1	0.06	0.46	0.01	0.02	1	0.35	0.07	0.44	0.34	0.12	0.33	0.02	0.44
a2	0.31	0.07	0.01	0.00	0.35	1	0.23	0.01	0.22	0.07	0.20	0.09	0.21
a3	0.17	0.18	0.02	0.02	0.07	0.23	1	0.23	0.16	0.94	0.76	0.15	0.27
a4	0.14	0.98	0.06	0.06	0.44	0.01	0.23	1	0.25	0.17	0.24	0.28	0.74
b1	0.10	0.32	0.02	0.00	0.34	0.22	0.16	0.25	1	0.02	0.07	0.19	0.18
b2	0.10	0.10	0.01	0.01	0.12	0.07	0.94	0.17	0.02	1	0.72	0.01	0.08
b3	0.03	0.17	0.02	0.02	0.33	0.20	0.76	0.24	0.07	0.72	1	0.36	0.35
b4	0.01	0.32	0.02	0.02	0.02	0.09	0.15	0.28	0.19	0.01	0.36	1	0.28
Drain	0.05	0.75	0.07	0.08	0.44	0.21	0.27	0.74	0.18	0.08	0.35	0.28	1

Table 5: Table of the correlation matrix, with all the parameters there are in the optimization, the green colour illustrates the parameters which are too correlated and is excluded in the calibration.

The calibration of the model resulted in an objective function of 2.03. The estimated value from the inverse solution is presented in Table 6 together with 95% confidence interval. For all the calibrated values, a narrow 95% confidence interval is presented, which generally indicate a low uncertainty for the estimated parameter values.

Parameter	Parameter value	95 % confidence interval	
		Lower bound	Upper Bound
K1 (cm/day)	836.5	787.1	889.1
K3 (cm/day)	23.34	13.65	39.92
K4 (cm/day)	0.033	0.031	0.036
A1 (cm^{-1})	0.090	0.083	0.097
A2 (cm^{-1})	0.032	0.019	0.056
b1	1.599	1.585	1.612
b3	1.472	1.348	1.608
b4	1.370	1.040	1.805
Drain (cm^2/day)	1.019	0.632	1.642

Table 6: Table showing the results of the parameter values from the calibration of Model A, and their 95% confidence interval indication how good the value is.

A comparison of the observed and simulated data is made for the three groups of observation data included in the inverse calibration. Several statistics are calculated for the different groups (Table 7). The RMSE for the groundwater table is calculated with and without the values that reach the limit of the model domain (500 cm). The RMSE value is 149.1 cm, when calculated with the values of 500 cm, and 38.8 when taking them out of the calculation. The RMSE for the saturation is 0.29 and for the drain an Fbal value is calculated, which states that the simulated average value deviates 12.77% from the observed average value for the data set. A R^2 value is calculated to supplement the RMSE value, these values are 0.2 for the depth to the groundwater table and 0.65 for the saturation. For the depth to the groundwater table it means that 20% of the simulated data can explain the variation in the observed data. For the saturation 65% of the observed data can be explained by the simulation.

	Gwt (cm)	wsat	Drain (cm^3/day)
RMSE	149.1 or 38.8	0.29	
Fbal (%)			12.77

Table 7: Table with RMSE values for the depth to groundwater table and saturation and Fbal value for drain, for the results of Model A.

The simulated depth to the groundwater table and the observed depth is illustrated in Figure 10. In Figure 10 the graphs illustrate the dynamic of the groundwater table in the fall and winter periods, where the groundwater table is closer to the surface, even though it is rare that the model fits the observed data entirely. In the summer periods where the groundwater table decrees, the graph for observed values in Figure 10 decrease, and the model simulates a decrease in the groundwater table as well, but this decrease in the simulated data is more rapid and reach the lower limit of the model. The decrease in the simulated data reaches 500 cm, which is the model domain, so the depth could be even greater than 500 cm in the model.

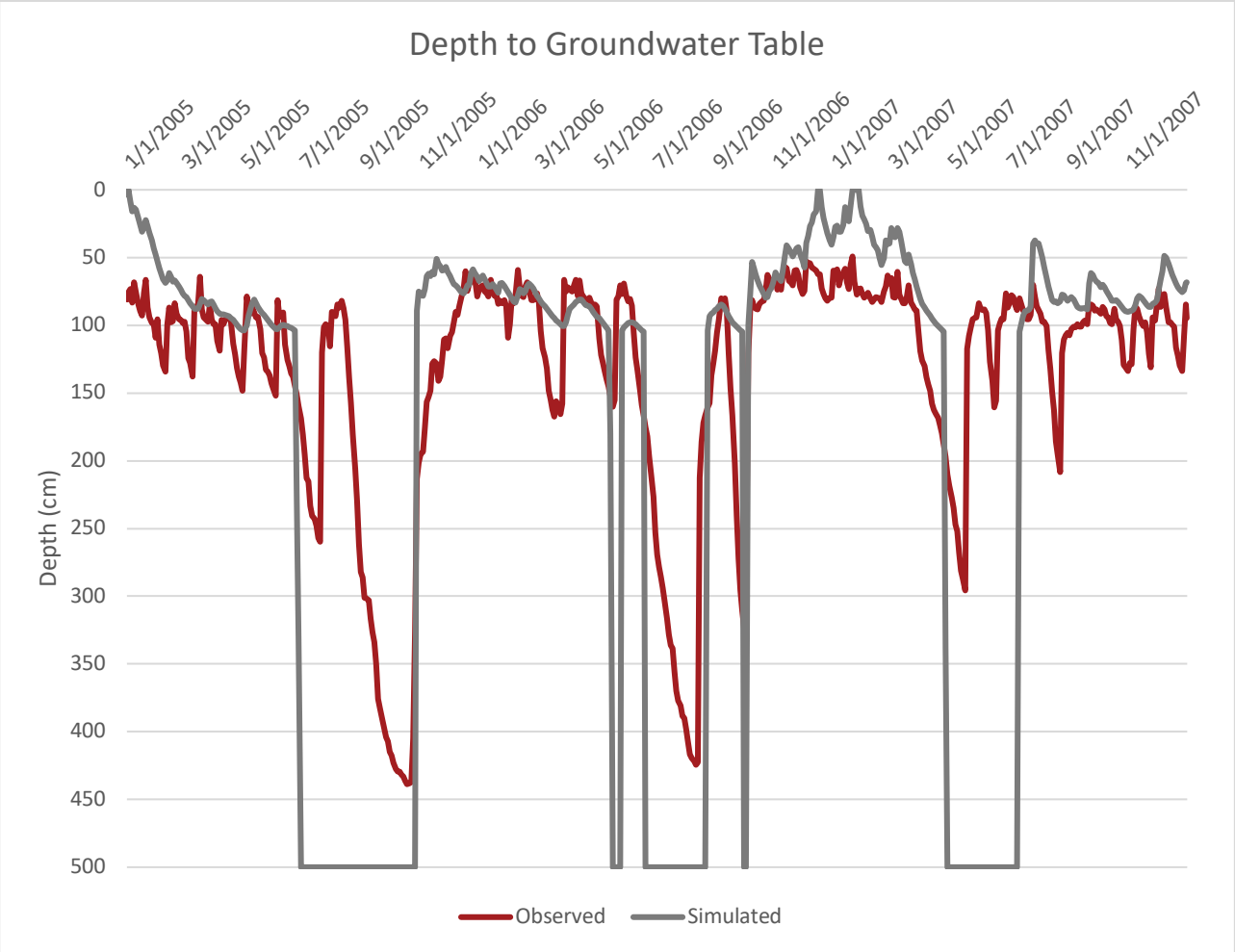

Figure 10: Figure showing the observed depth to the groundwater table (red line) and the simulated depth to groundwater table (grey line) in cm for Model A.

Data for saturation is part of the calibration as well. In Figure 11 the observed and simulated saturation are illustrated. The simulated data for saturation is too low compared to the observed saturation data.

The simulated saturation has the same dynamic behaviour, even though the values are lower. The extremes, where the observed saturation is either at its lowest or highest, the model duplicates these trends, especially from the 01-07-2006 to the 01-09-2006 (Figure 11).

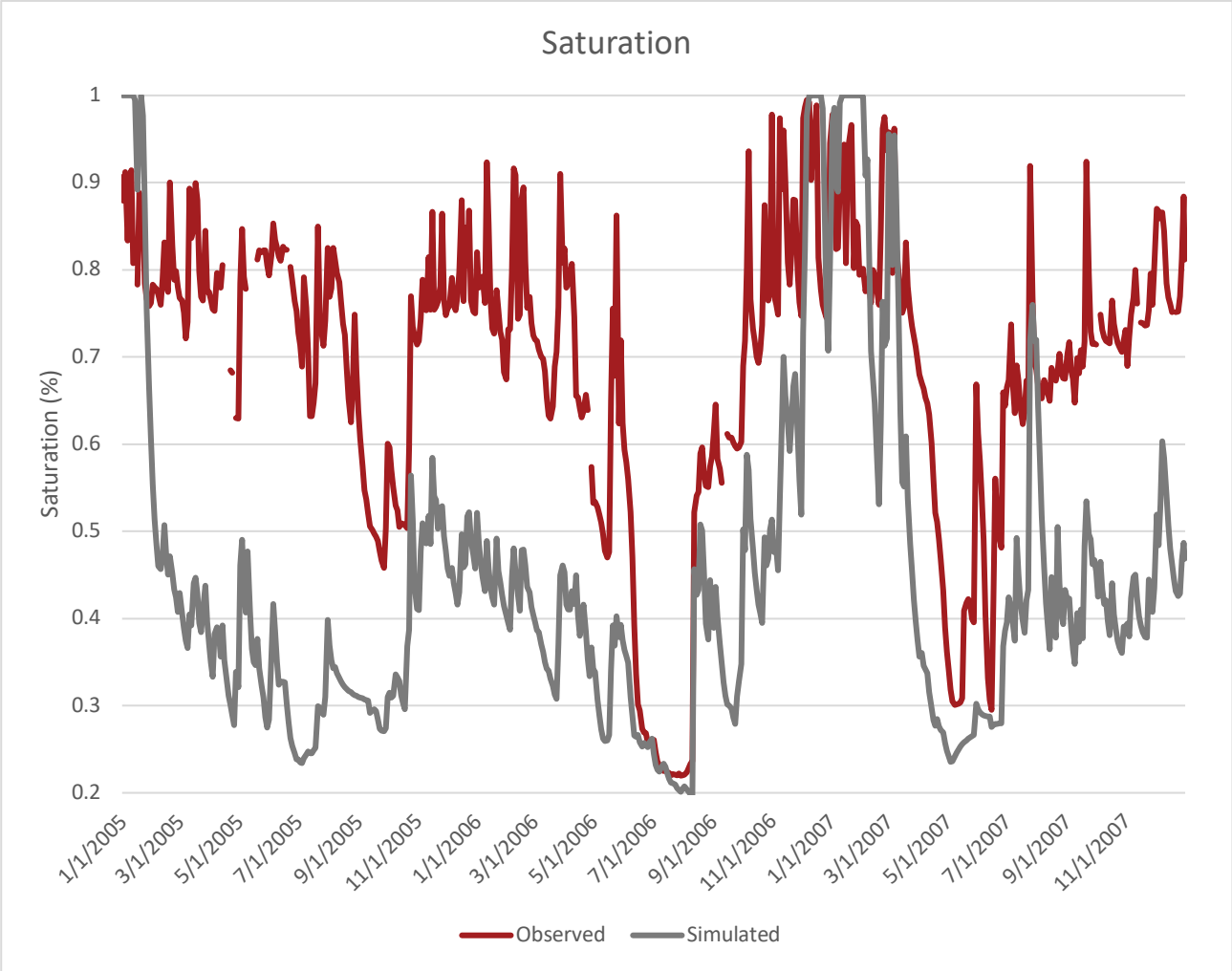

Figure 11: Figure showing the observed saturation (red line) and the simulated saturation (grey line) in % for Model A.

The model also simulates the drainage flow, and the simulated and observed drainage flow data are shown in Figure 12. The dynamic behaviour of the drainage is predicted by the model, but the model is not able to simulate the bigger peaks that are observed. The model also simulates a bigger average drainage, than the observed average drainage.

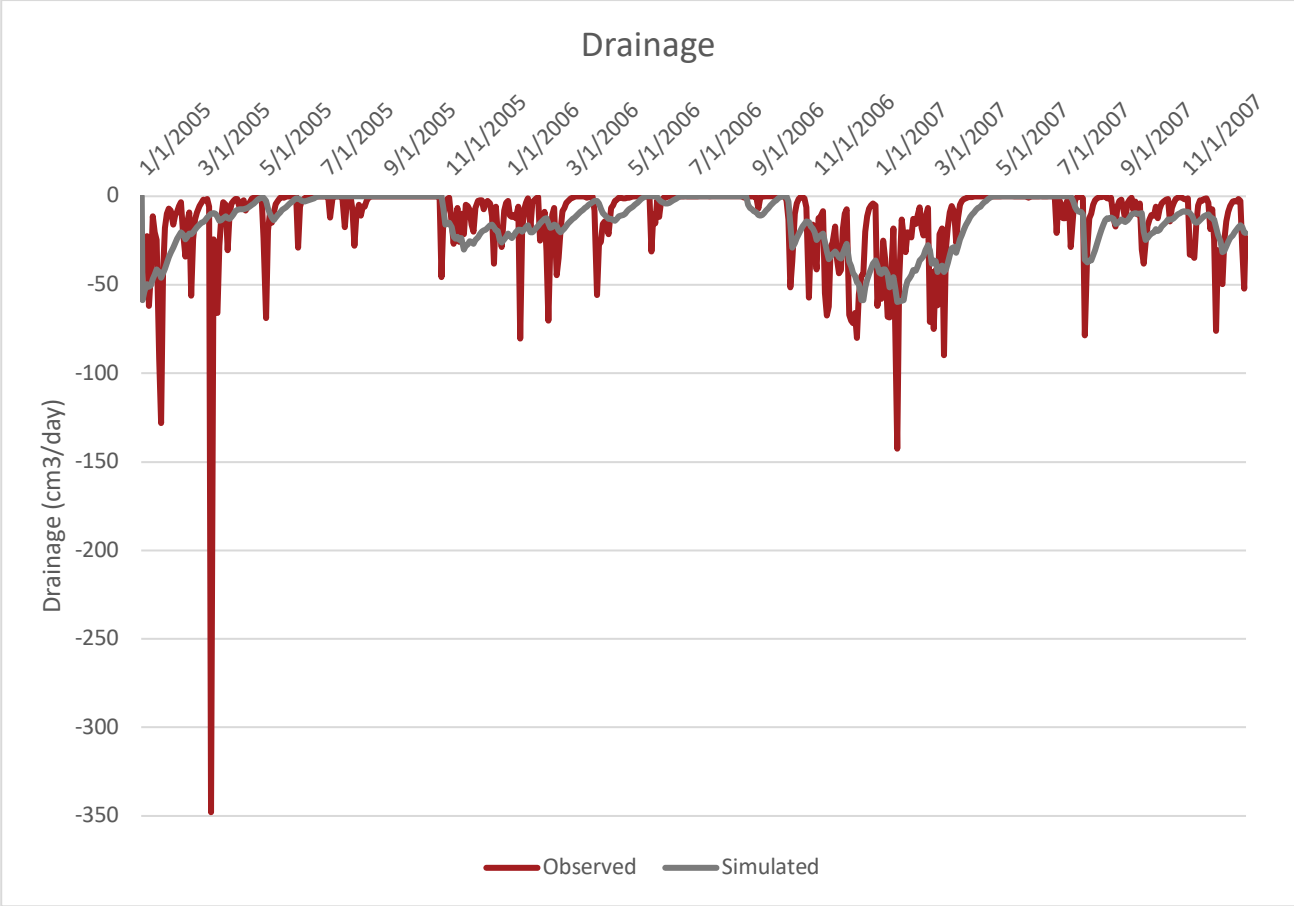

Figure 12: Figure showing the observed drainage (red line) and the simulated drainage (grey line) in cm^3/day for Model A.

The water balance for this model is presented in Table 8. And the only way water enters the model is by precipitation, where it is removed from the model by free drainage, which is the bottom boundary condition, evapotranspiration and by drain. The values of the amount of water enters and leaves the model is presented I Table 8, and a difference of 3.2% is calculated.

	In	Out
Precipitating	330.97	
Free drainage		-29.82
ET		-157.64
Simple drain		-154.25
Total	**330.97**	**-341.72**
difference number	-10.75	
difference percentage	3.20%	

Table 8: Table showing water balance for Model A, all values is in cm^3.

Model A with solute transport

When the model is calibrated (Model A) and the best values for the parameters are estimated, solute transport are added to the model. The simulated concentration of bromide is illustrated alongside the measured bromide concentration, see Figure 13 and Figure 14. Bromide is detected in different places on the field, and for this model (Model A) the simulated bromide is shown together with the measured data for the drain and suction cups in 1 m b.g.s. For the horizontal well which is located 3.5 m b.g.s. and the suction cups located 2 m b.g.s the concentration is close to 0, which indicates that the bromide has not reached these wells yet.

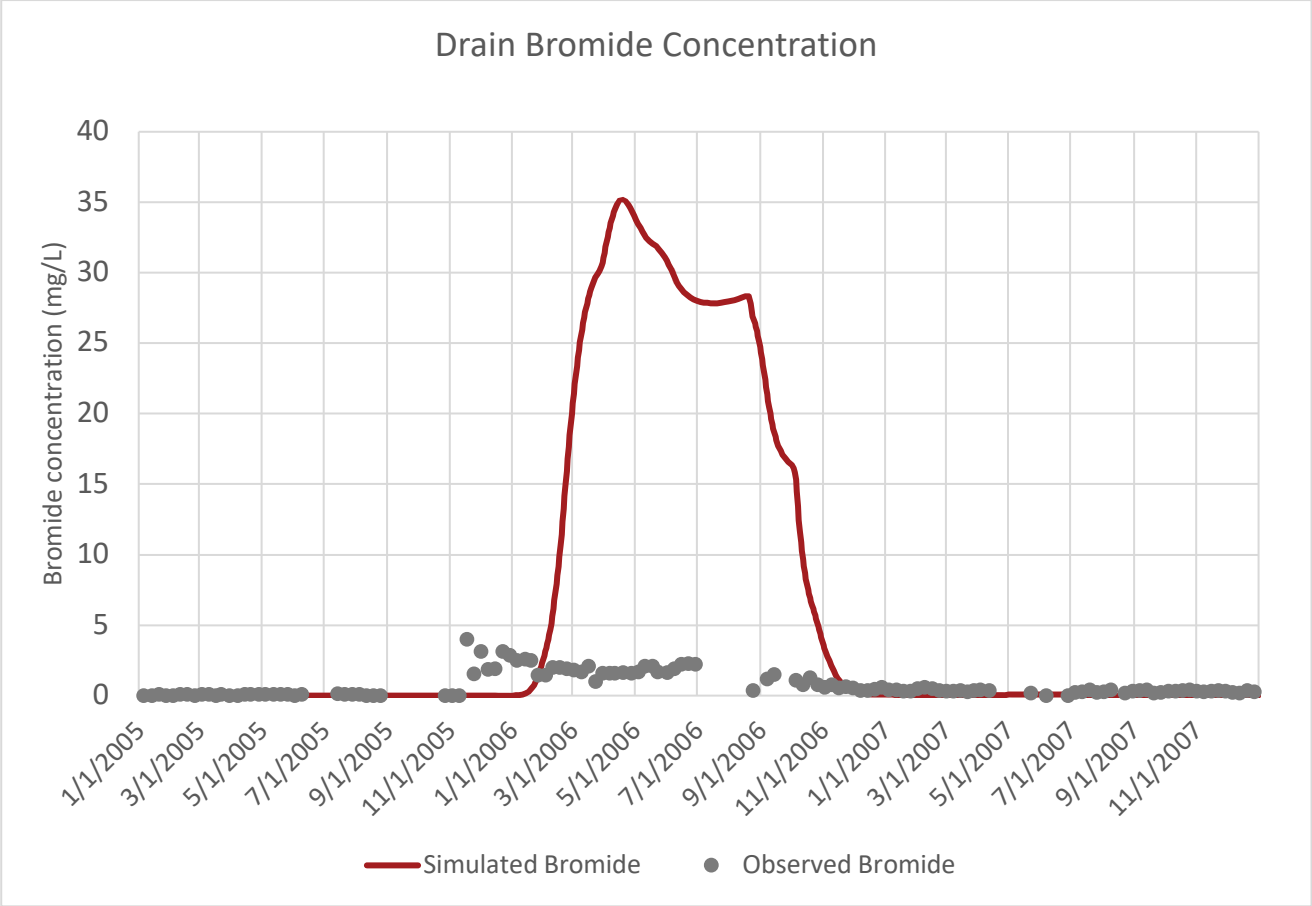

Figure 13: Plot showing the observed (measured) bromide concentration (red line) and the simulated bromide concentration (grey dots) for Model A.

The bromide concentration in the drain (Figure 13) shows a much higher concentration for the simulated bromide concentration (Figure 13) than there are measured. Otherwise, the shape of the simulated bromide concentration is quite similar to the measured bromide concentration. When the measured concentration increases the model simulates an increase of the bromide concentration as well. The pattern where the bromide concentration first increases, then decreases to increase a little again in the middle of 2006 is seen in both the measured and simulated concentrations. This similarity is hard to identify in Figure 13 because of the differences in the concentration.

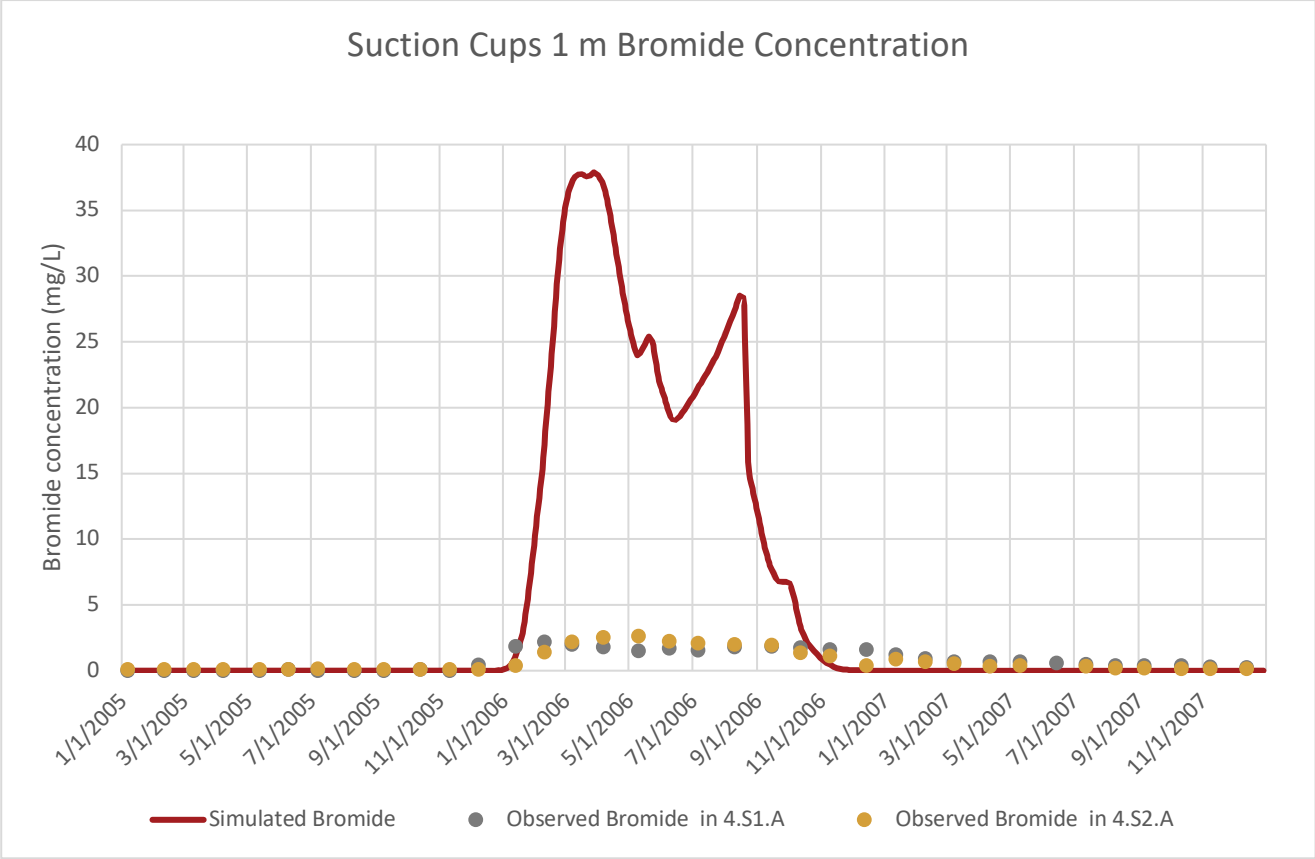

Figure 14: Plot showing the observed (measured) bromide concentration (S1 represented by grey dots and S2 represented by yellow dots) and the simulated bromide concentration (red line) for Model A.

The plot in Figure 14 is the same as Figure 13, where the measured and simulated bromide concentrations are plotted against each other. The measurements are taken from the suction cups in 1 m b.g.s. The concentration for bromide measured in the suction cups are measured two places (in S1 and S2, see Figure 2). The measured concentration in S1 is illustrated by the grey dots and the measured concentrations from S2 are illustrated by the yellow dots. Figure 14 shows a too high concentration of bromide. The measured and the simulated concentration also have the same tendency. In 2006, the concentration increases then decrease a little, where after it increase a little again, before it decreases definitively in the end of 2006. This tendency is present in the measured concentration as well (especially in S1) but is not as excessive as the simulated concentration. There are measurements from the suction cups in 2 m b.g.s. as well, but the bromide, even though it has a high concentration has not yet reached the 2 m observation point in the model.

Model A Calibrated with solute transport

Instead of just running the model with solute transport after calibration, Model A is calibrated with solute transport, to see if it has any impact.

A sensitivity analysis is also performed for this model, which gave the same results as the sensitivity analysis for Model A without solute transport included in the calibration (Figure 9). Where it is k3 and k4 there are most sensitive and b4 and drain there are less sensitive. In the correlation matrix it was also the same parameter there were correlated (Table 5), therefore were the four same correlated parameters (k2 and a4, a3 and b2) maintained under this simulation as well.

The calibration for this model gave the results presented in Table 9 where they are presented together with their 95% confidence interval. The objective function was reduced to 1.95. In this simulation the hydraulic conductivity for k1 was more than doublet compared to Model A.

Parameter	Parameter value	95 % confidence interval	
		Lower bound	Upper Bound
K1 (cm/day)	1915.92	1839.41	1995.60
K3 (cm/day)	16.52	14.66	18.62
K4 (cm/day)	0.034	0.031	0.037
A1 (cm^{-1})	0.037	0.034	0.041
A2 (cm^{-1})	0.039	0.036	0.042
b1	1.618	1.599	1.637
b3	1.552	1.428	1.686
b4	1.142	0.742	1.758
Drain (cm^2/day)	2.38	1.54	3.67

Table 9: Table showing the results of the parameter values from the calibration of Model A calibrated with solute transport, and their 95% confidence interval indication how good the value is.

Statistic for the observation groups for this calibration are calibrated and presented in Table 10. The RMSE value is 159.9 cm, when calculated with the values of 500 cm, and 37.7 when taking them out of the calculation, this is almost the same as in Model A. comparison of drainage is also quite similar,

in this model. RMSE for saturation is calculated to 0.17 and has a R^2 value of 0.5, saying that 50% of the simulated data can explain the observed data.

	Gwt (cm)	wsat	Drain (cm^3/day)
RMSE	159.9 or 37.7	0.17	
Fbal (%)			14.16

Table 10: Table with RMSE values for the depth to groundwater table and saturation and Fbal value for drain, for the results of Model A calibrated with solute transport.

The simulated and observed depth to groundwater table is illustrated in Figure 15. From this calibration the results are similar to the calibration for Model A (Figure 10).

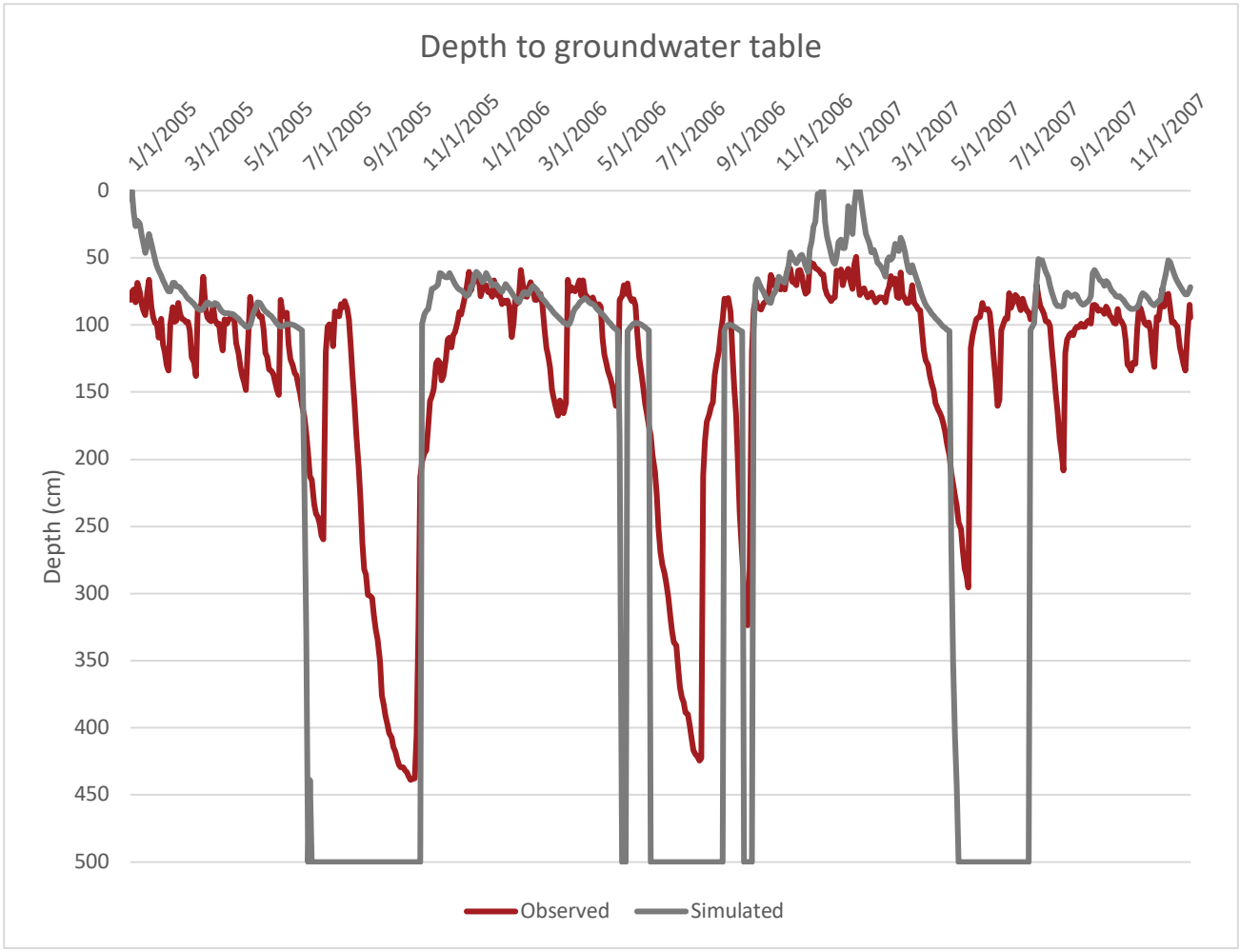

Figure 15: Figure showing the observed depth to the groundwater table (red line) and the simulated depth to groundwater table (grey line) in cm for Model A calibrated with solute transport.

In Figure 16 the observed and simulated data for saturation are illustrated. In this calibration the model has simulated saturation quiet well, it is still the case that the model simulates saturation better in the end of the period than in the start.

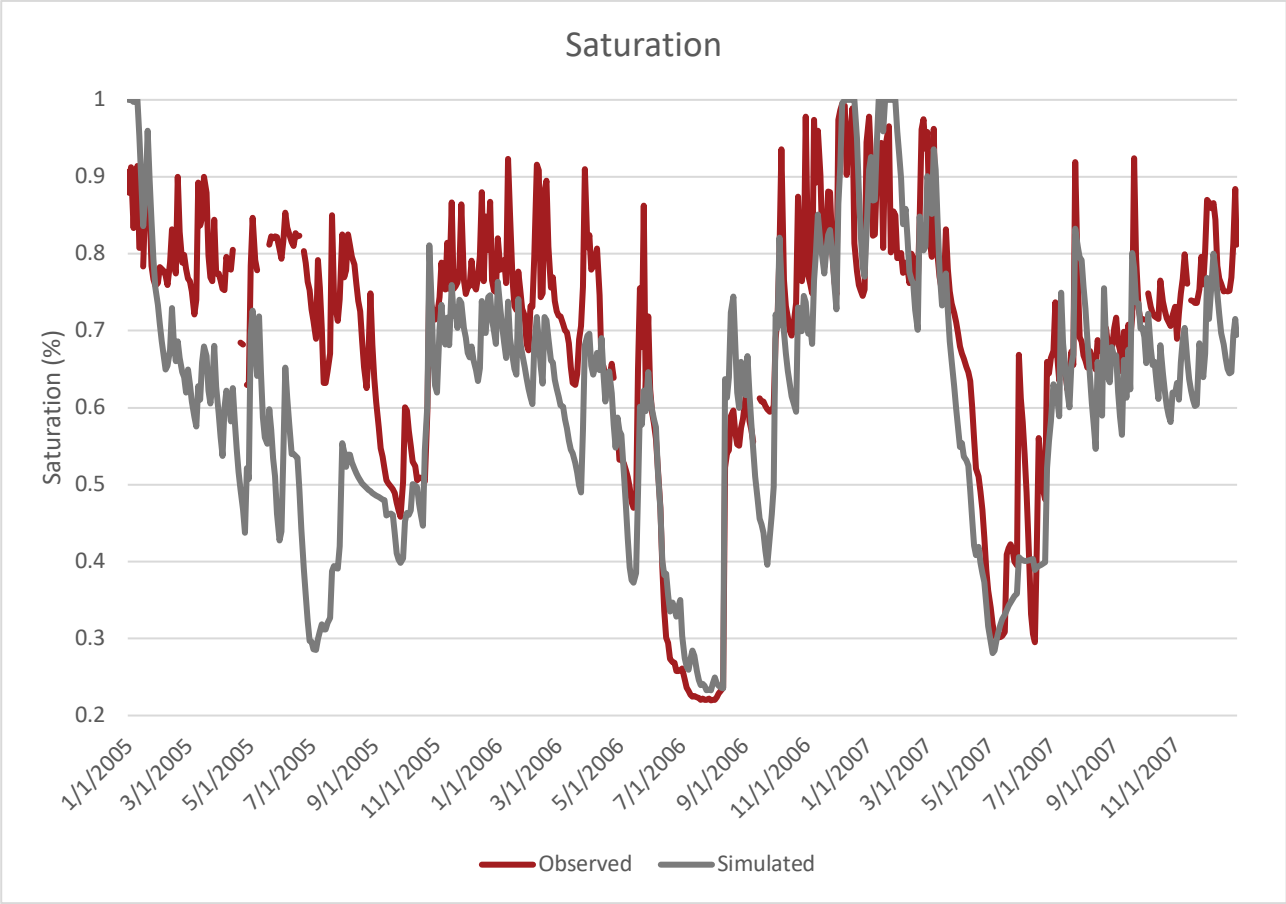

Figure 16: Figure showing the observed saturation (red line) and the simulated saturation (grey line) in % for Model A calibrated with solute transport.

Simulated and observed drainage is illustrated as well in Figure 17, the drainage in this calibration are like the depth to the groundwater table quite similar to that calibrated in Model A (Figure 12), where it not simulates the peaks very well.

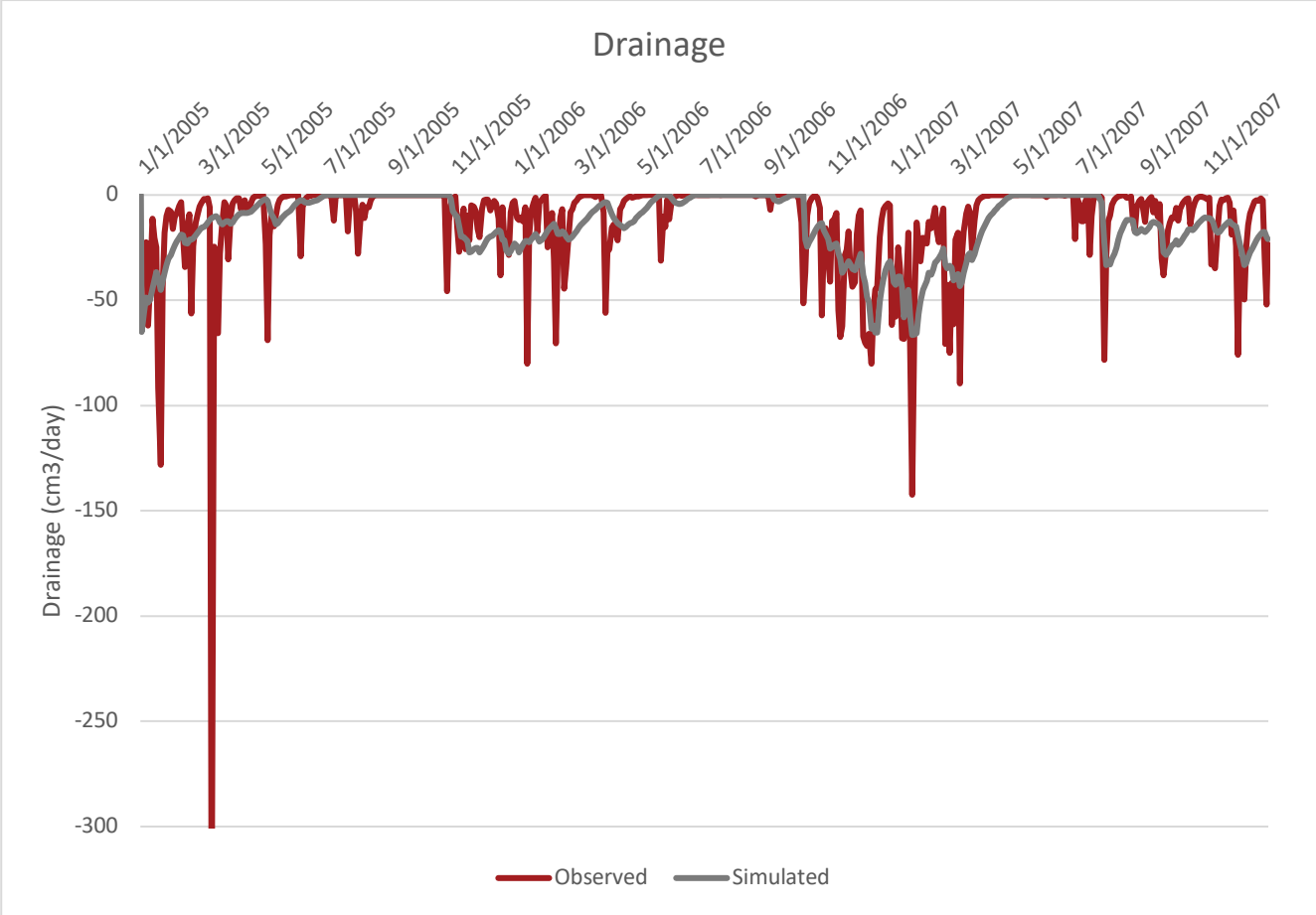

Figure 17: Figure showing the observed drainage (red line) and the simulated drainage (grey line) in cm^3/day for Model A calibrated with solute transport.

Solute transport was added to the model before this calibration. This resulted in a lower simulated concentration for bromide (Figure 18, 19 and 20), compared to when the solute is added to the model after the calibration which was the case in Figure 13 and 14 for Model A. It is easier to see in this calibration with solute transport that the dynamic of the simulated and measured concentration is similar. For this calibration a concentration was also present in the suction cup 2 m b.g.s. (Figure 20)

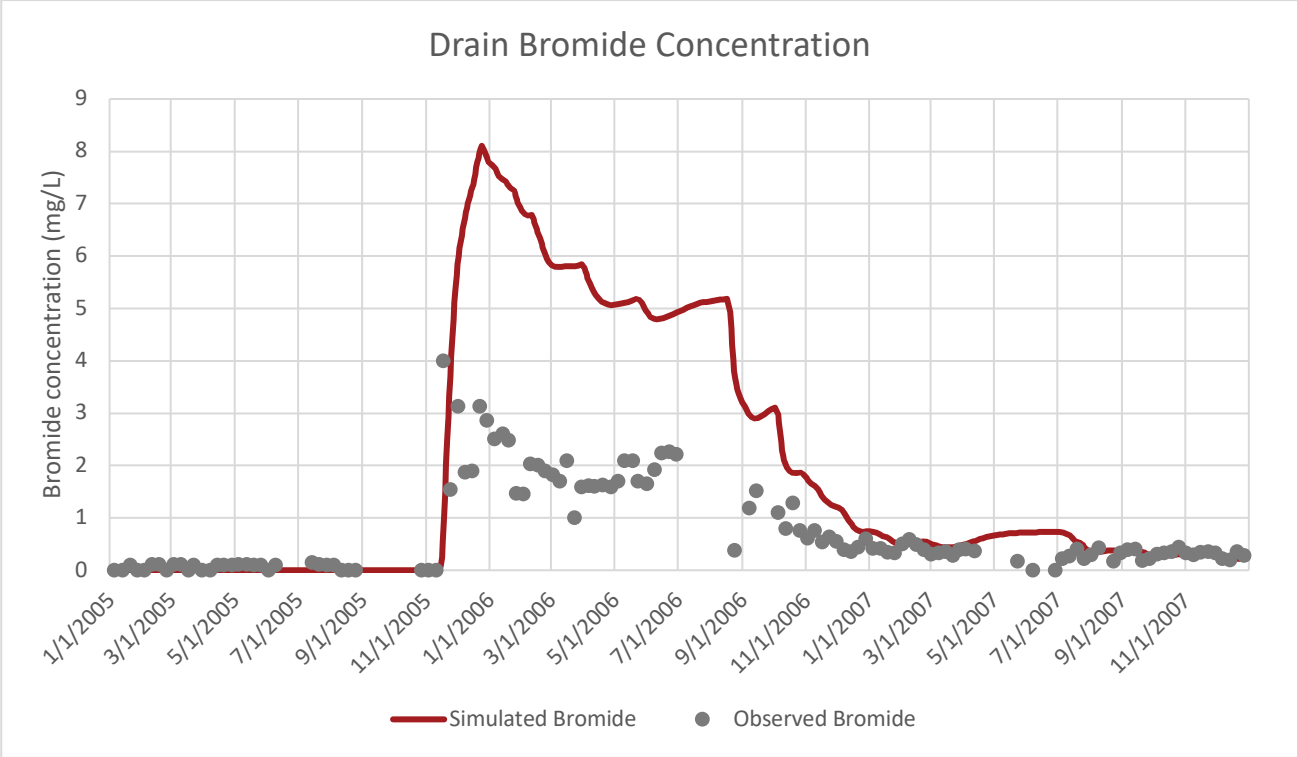

Figure 18: Plot showing the observed (measured) bromide concentration (red line) and the simulated bromide concentration (grey dots) for Model A calibrated with solute transport.

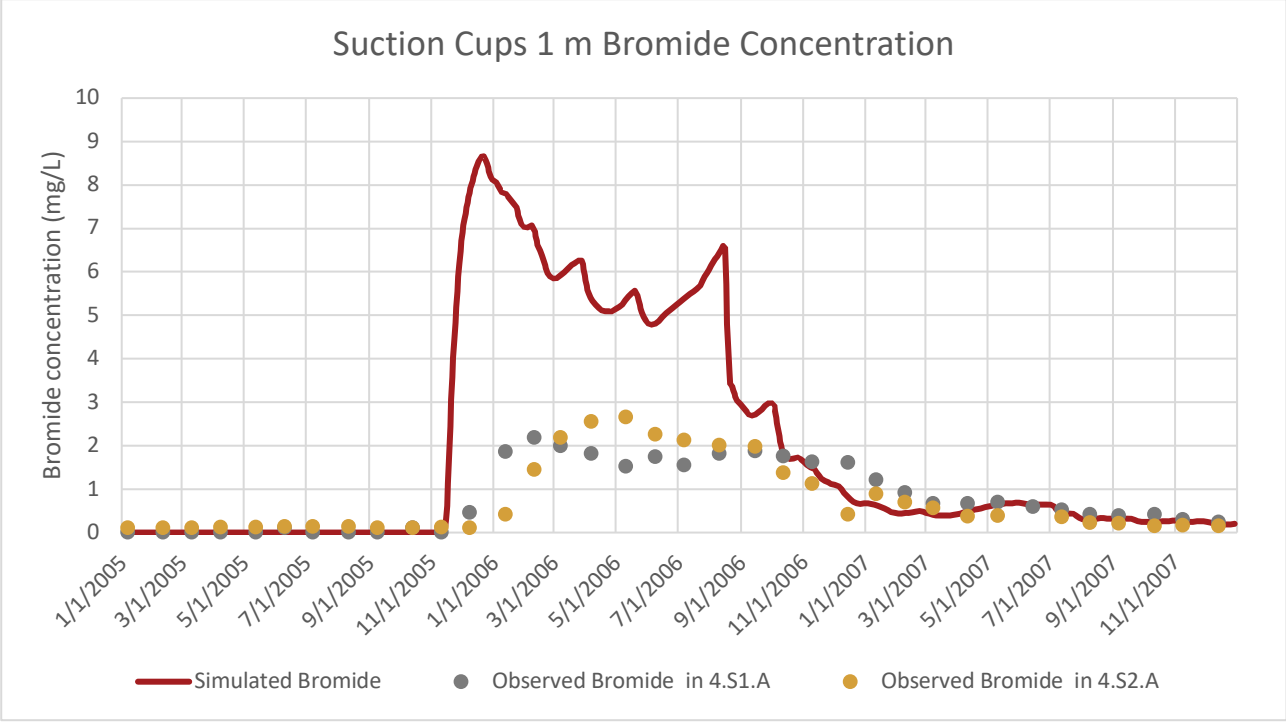

Figure 19: Plot showing the observed (measured) bromide concentration (S1 represented by grey dots and S2 represented by yellow dots) for the suction cup located 1 m b.g.s. and the simulated bromide concentration (red line) for Model A calibrated with solute transport.

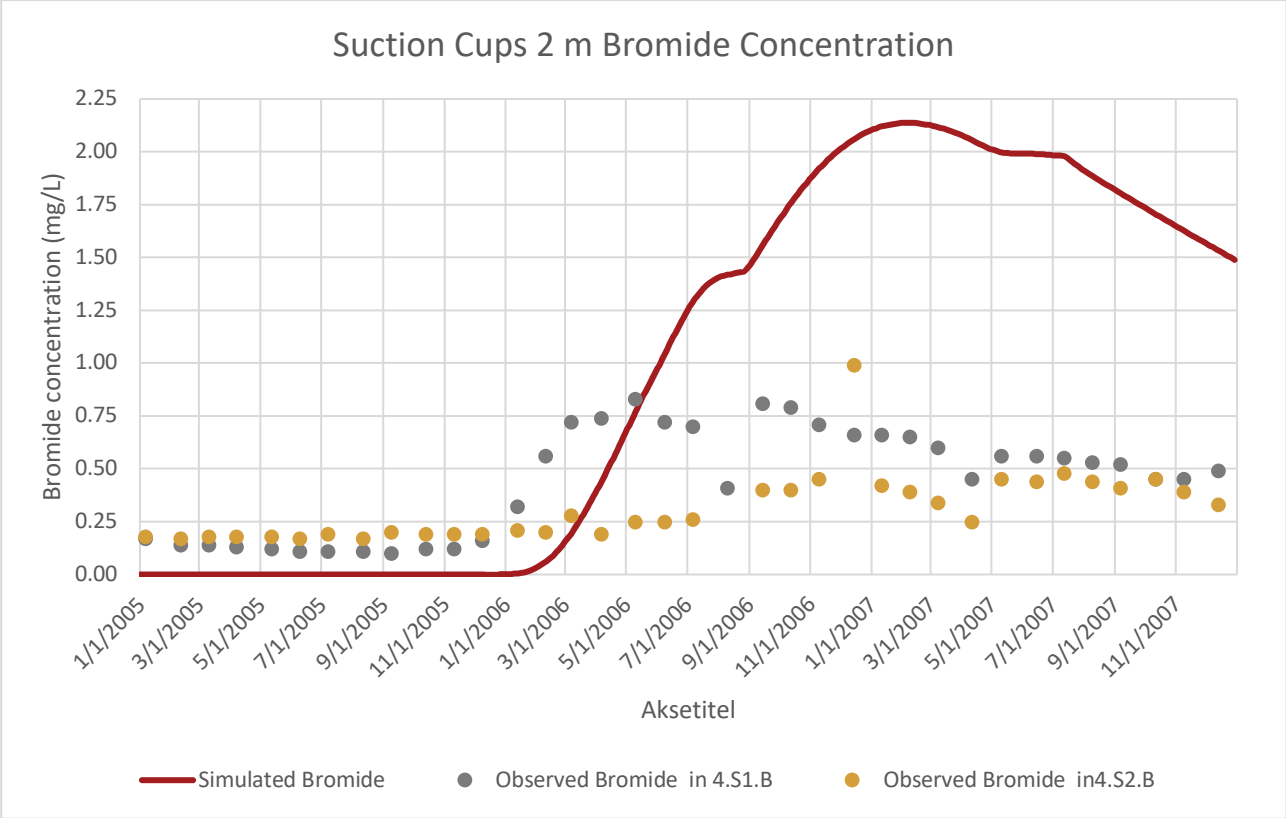

Figure 20: Plot showing the observed (measured) bromide concentration (S1 represented by grey dots and S2 represented by yellow dots) for the suction cup located 2 m b.g.s. and the simulated bromide concentration (red line) for Model A calibrated with solute transport.

Calibration results Model B

In this model the drain is moved up 10 cm, so it is located in zone 3 instead of zone 4. This is done to see if it has any impact on the calibration and if it is able to simulate the observed drain flow better than Model A.

A sensitivity analysis is made for this model as well. In this model, it is a2 and a3 that are the most sensitive, see Figure 21. The parameters that are least sensitive is the drain and the van Genuchten parameter β for zone 4 (b4). These parameters are the same as in Model A.

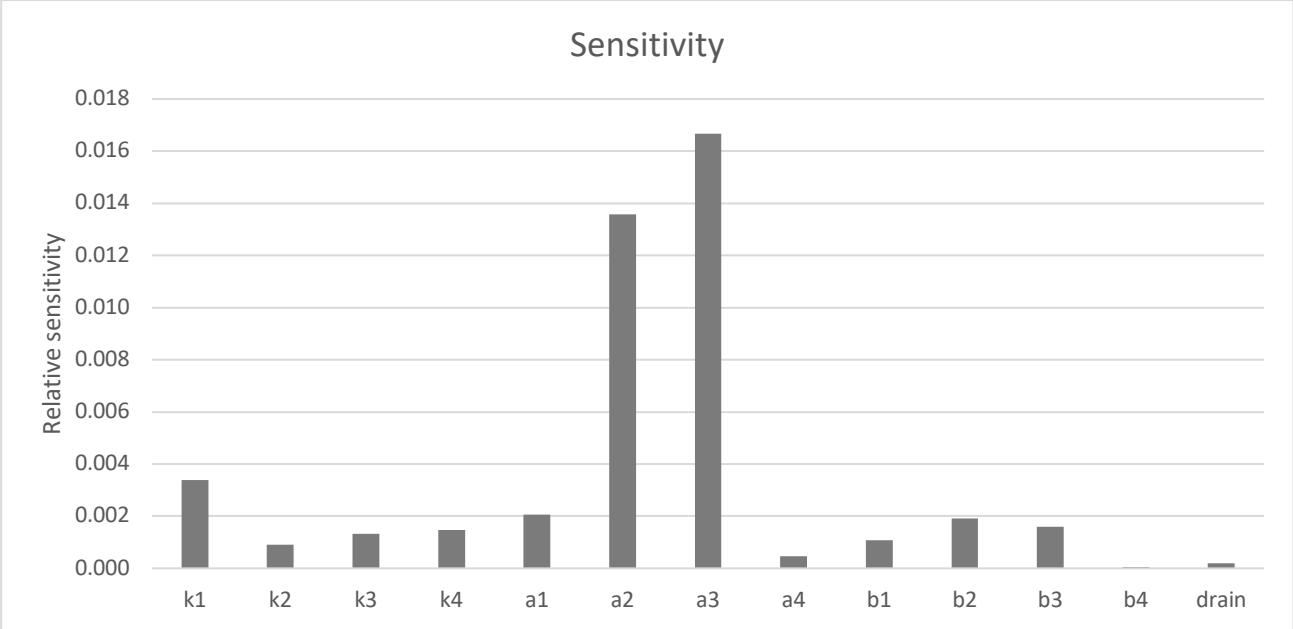

Figure 21: Graph of the parameter sensitivity for Model B.

In this sensitivity analysis, there are only two parameters that are correlated, which is the van Genuchten parameters in zone 3 (a3 and b3) (Table 11). These two parameters are maintained during the calibration.

Correlation matrix													
	k1	**k2**	**k3**	**k4**	**a1**	**a2**	**a3**	**a4**	**b1**	**b2**	**b3**	**b4**	**Drain**
k1	1	0.10	0.24	0.14	0.49	0.11	0.11	0.08	0.19	0.03	0.11	0.04	0.02
k2	0.10	1	0.27	0.02	0.10	0.06	0.05	0.00	0.10	0.04	0.06	0.28	0.19
k3	0.24	0.27	1	0.74	0.30	0.26	0.31	0.57	0.36	0.01	0.31	0.63	0.03
k4	0.14	0.02	0.74	1	0.11	0.05	0.10	0.67	0.13	0.06	0.11	0.49	0.14
a1	0.49	0.10	0.30	0.11	1	0.11	0.10	0.22	0.70	0.04	0.10	0.16	0.06
a2	0.11	0.06	0.26	0.05	0.11	1	0.88	0.14	0.10	0.57	0.87	0.17	0.49
a3	0.11	0.05	0.31	0.10	0.10	0.88	1	0.24	0.08	0.12	0.99	0.20	0.58
a4	0.08	0.00	0.57	0.67	0.22	0.14	0.24	1	0.16	0.12	0.24	0.37	0.00
b1	0.19	0.10	0.36	0.13	0.70	0.10	0.08	0.16	1	0.06	0.08	0.22	0.02
b2	0.03	0.04	0.01	0.06	0.04	0.57	0.12	0.12	0.06	1	0.12	0.02	0.03
b3	0.11	0.06	0.31	0.11	0.10	0.87	0.99	0.24	0.08	0.12	1	0.21	0.58
b4	0.04	0.28	0.63	0.49	0.16	0.17	0.20	0.37	0.22	0.02	0.21	1	0.24
Drain	0.02	0.19	0.03	0.14	0.06	0.49	0.58	0.00	0.02	0.03	0.58	0.24	1

Table 11: Table of the correlation matrix, with all the parameters in the optimization. The green colour illustrates the parameters which are highly correlated and are excluded in the calibration.

This calibration reduced the objective function to 1.71, which is a little less than in the calibration for Model A. The 95% confidence interval is presented together with the parameter values in Table 12. Like in Model A, all the parameters have a rather narrow interval, which indicates a good parameter certainty.

Parameter	Parameter value	95 % confidence interval	
		Lower bound	Upper Bound
K1 (cm/day)	613.2	556.6	675.6
K2 (cm/day)	40.6	34.8	47.3
K3 (cm/day)	28.7	23.9	34.4
K4 (cm/day)	0.030	0.029	0.032
A1 (cm^{-1})	0.066	0.062	0.070
A2 (cm^{-1})	0.073	0.070	0.077
A4 (cm^{-1})	0.006	0.005	0.007
b1	1.687	1.673	1.702
b2	1.135	1.129	1.140
b4	1.278	1.164	1.404
Drain (cm^2/day)	86.9	53.8	140.2

Table 12: Table showing the results of the parameter values from the calibration in Model B, and their 95% confidence interval, which indicates how precise the values are.

Different statistics are calculated for this model as well like in Model A (Table 13). A RMSE value is calculated for the groundwater table and the saturation. RMSE for the depth to the groundwater table are calculated to be 160.1. When accounting for the values which reach 500 cm, and excluding them, the RMSE becomes 37.7, which is a little higher than in Model A. RMSE for saturation is calculated as well to 0.21, which is lower than for Model A. The R^2 value for this calibration was not able to obtain for the depth to the groundwater table, because of the simulation was odd. For the saturation the R^2 value was calculated to be 0.08. The Fbal value is calculated for drain flow, and the simulated average value varies 12.59% from the observed average value, which is close to the Fbal value in Model A.

	Gwt (cm)	wsat	Drain (cm^3/day)
RMSE	160.1 or 37.7	0.21	
Fbal (%)			12.59

Table 13: Table with RMSE values for the depth to groundwater table and saturation, and the Fbal value for drain, for the results of Model B.

The calibrated values for the depth to the groundwater table are illustrated in Figure 22. In this calibration, the model was not able to simulate the dynamic behaviour of the groundwater table at all, not even when the groundwater table was closer to the surface like it could in Model A. The model simulating a squared groundwater table, where it was either stable at 100 cm b.g.s. or at 500 cm b.g.s. which is the model boundary.

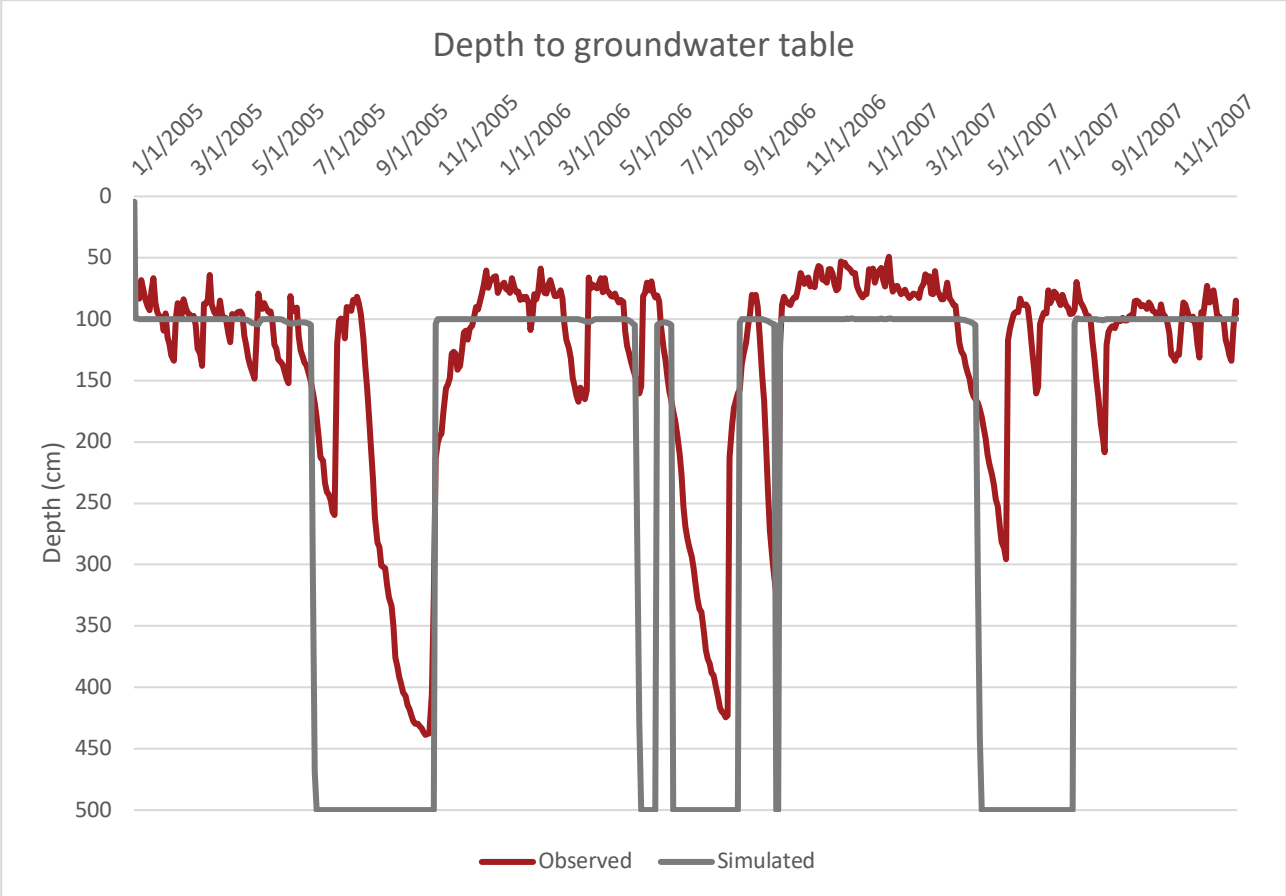

Figure 22: Figure showing the observed depth to the groundwater table (red line) and the simulated depth to groundwater table (grey line) in cm for Model B.

The simulated and observed data for saturation is illustrated in Figure 23. The model simulates the saturation dynamic oscillations well, though the model simulates a lower saturation in the start of the period. Until 01-11-2005 the model simulates a saturation that is less than observed, and from 01-11-2005 and forward the simulated fits the observed data for saturation well. There is a small variation in the graphs, for example around the 01-09-2006 where it has simulated higher saturation and around 01-05-2007 where it has simulated a lower saturation (Figure 23),

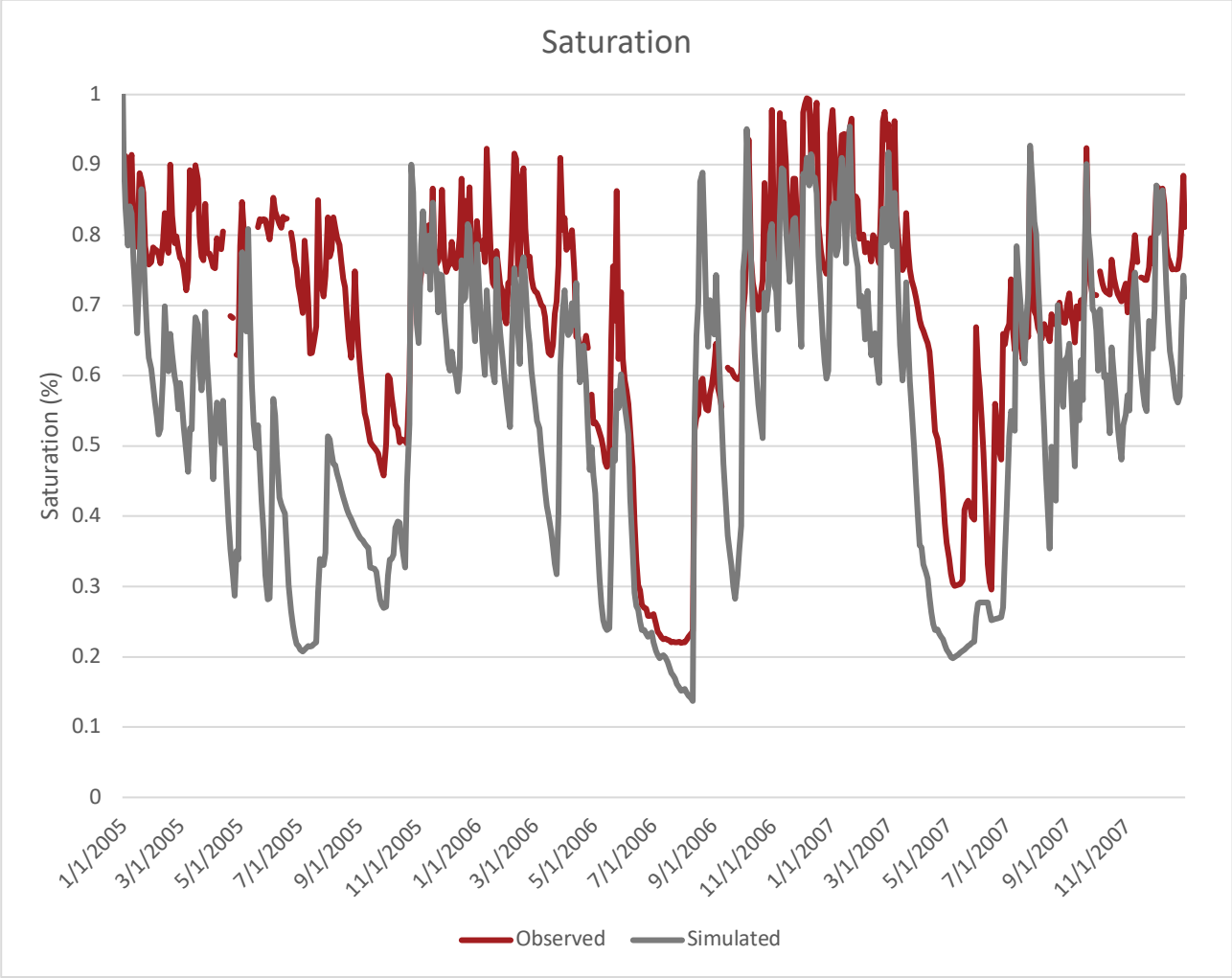

Figure 23: Figure showing the observed saturation (red line) and the simulated saturation (grey line) in % for Model B.

The simulated and observed drain flow is illustrated in Figure 24. The graph shows the impact on the drain flow when moving the drain 10 cm closer to the surface in the model. In this simulation, the drain is now able to simulate the bigger peaks which are observed in the Estrup field. The simulated

peak between 01-07-2007 and 01-09-2007 is also simulated bigger now than was observed. This was not the case in Model A, where the model did not reproduce any of the peaks.

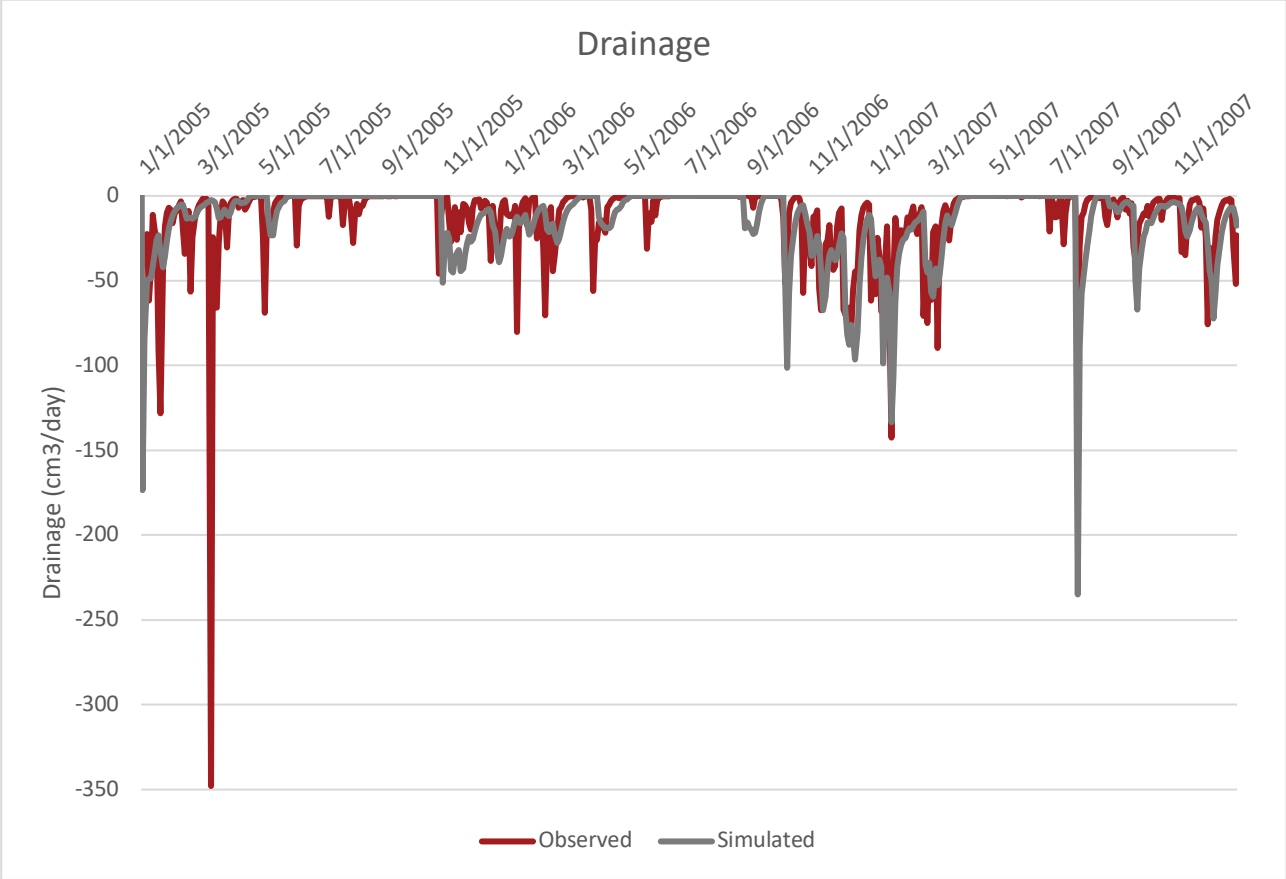

Figure 24: Figure showing the observed drainage (red line) and the simulated drainage (grey line) in cm^3/day for Model B.

The water balance for Model B is presented in Table 14. It is the same factors of which water enters and leaves the model as in Model A. The values of the amount of water enters and leaves the model is presented in Table 14, and a difference of 1.2% is calculated on what enters and leaves.

	In	Out
Precipitating	280.13	
Free drainage		-10.40
ET		-146.86
Simple drain		-126.26
Total	280.13	-283.52
difference number	-3.39	
difference percentage	1.20%	

Table 14: Table showing water balance for Model B, all values is in cm^3.

Model B with solute transport

Solute transport of bromide is applied in Model B after the calibration as well, to see if there are any differences now the model was calibrated with the drain moved.

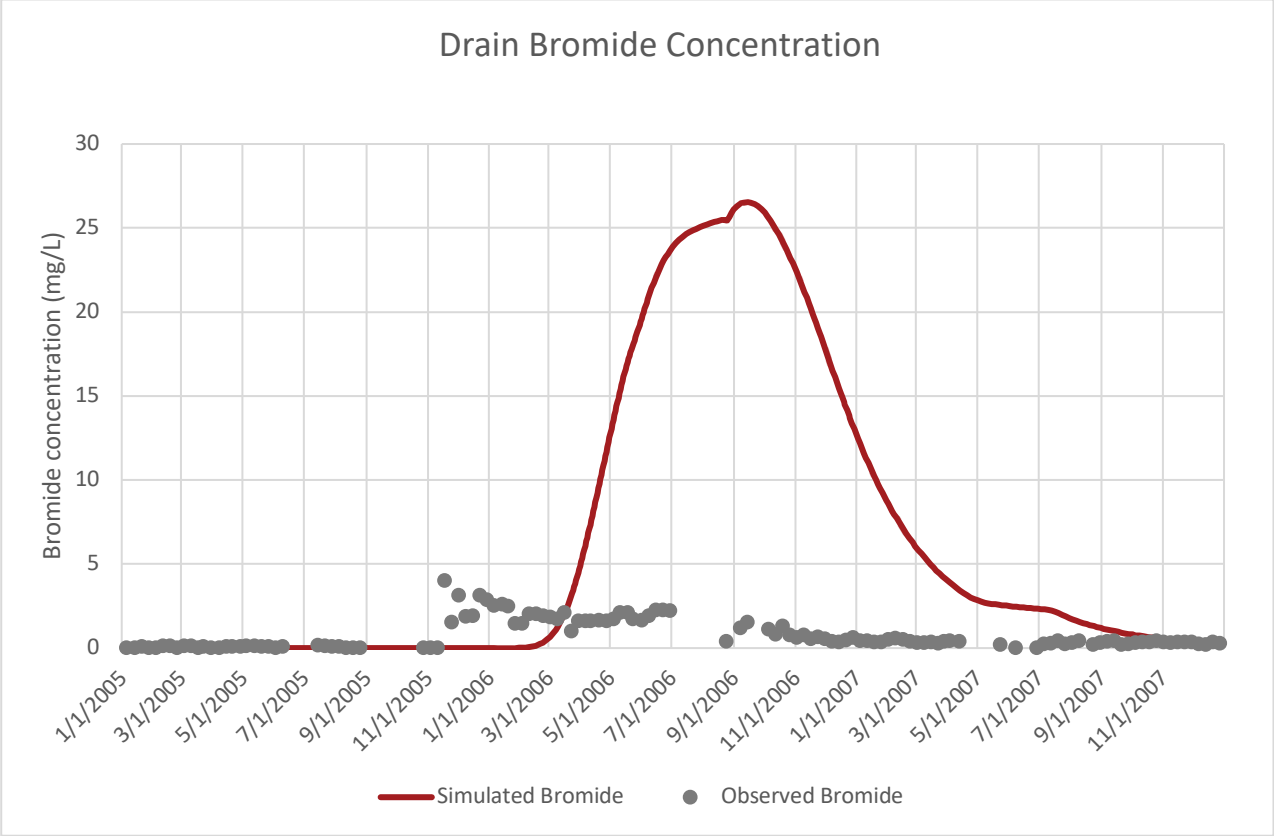

Figure 25: Plot showing the observed (measured) bromide concentration (grey dots) from the drain in 1.1 m b.g.s. and the simulated bromide concentration (red line) for Model B.

In Figure 25 the concentration for bromide is shown for the drain in this model. The drain is moved 10 cm up, so it is placed 1 m b.g.s. In Figure 25 the simulated bromide concentration is still from the observation point placed 1.1 m b.g.s., and the concentration for 1 m b.g.s is illustrated in Figure 26 for the suction cups. In Figure 25, the simulated concentration is shown by the red line and the measured concentration by the grey dots, like in Model A. Model B simulates the concentration of bromide to be higher than is measured. In Figure 25 it also shows that the simulated concentration peak is delayed, like in Model A (Figure 13). The simulated concentration for the model starts increasing later than when it is observed the bromide concentration should reach the drain.

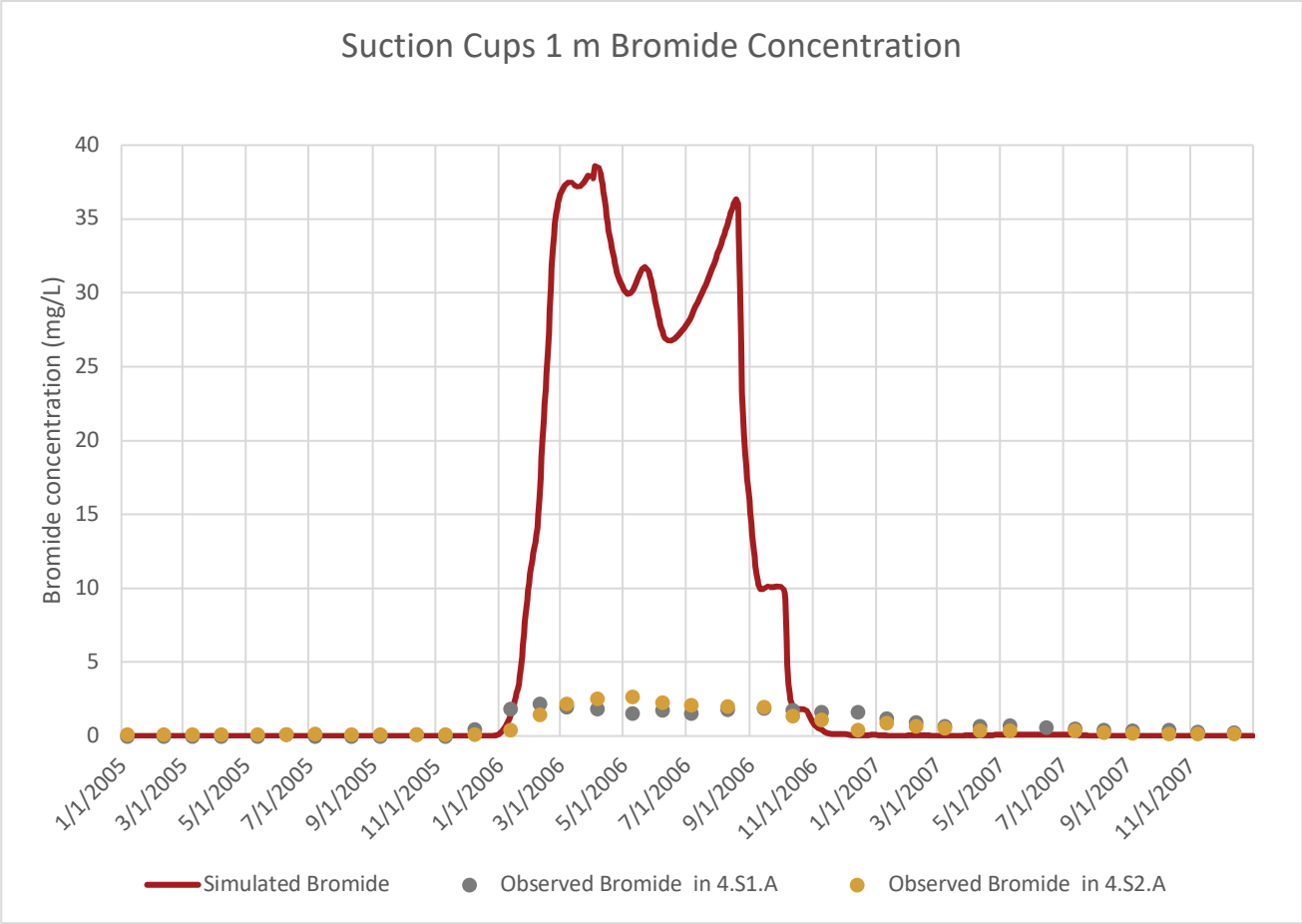

Figure 26: Plot showing the observed (measured) bromide concentration in the suction cups (S1 represented by grey dots and S2 represented by yellow dots) and the simulated bromide concentration (red line) for Model B.

In Figure 26, the concentration is presented for the suction cups placed in 1 m b.g.s. The simulated concentration is still too high, but here the concentration increases at the same time as the measured concentration of bromide. In the simulation of the concentration in the suction cups, the simulated concentration also show similarity to the trend of the observed bromide concentration, but due to the

magnitude differences in the simulated and measured bromide concentration, it is hard to see the shape of the measured concentration curve in the profile, see Figure 26.

Model B calibrated with solute transport

Model B is also calibrated with solute transport, to see if this has any impact to this model.
A sensitivity analysis is also performed before this calibration, which also gave the same results as the sensitivity analysis for Model B (Figure 21). Where it is a2 and a3 there are most sensitive and like all the other calibration b4 and drain are the less sensitive parameters. The correlation matrix was also the same as in Model B (Table 11). SO, the same parameters were maintained (a3 and b3).

For this calibration the objective function was reduced to 2.28 which is higher than in Model B. The 95% confidence interval is presented together with the parameter values in Table 15. The Drain is in this calibration the parameter which changed the most compared to Model B.

Parameter	Parameter value	95 % confidence interval	
		Lower bound	Upper Bound
K1 (cm/day)	556.37	528.62	585.57
K2 (cm/day)	42.18	37.96	46.87
K3 (cm/day)	31.92	29.82	34.17
K4 (cm/day)	0.052	0.050	0.053
A1 (cm^{-1})	0.099	0.094	0.104
A2 (cm^{-1})	0.038	0.035	0.041
A4 (cm^{-1})	0.011	0.010	0.014
b1	1.743	1.713	1.774
b2	1.566	1.458	1.681
b4	1.289	1.205	1.378
Drain (cm^2/day)	30.14	27.18	33.41

Table 15: Table showing the results of the parameter values from the calibration of Model B calibrated with solute transport, and their 95% confidence interval indication how good the value is.

RMSE for the depth to groundwater table is almost similar to RMSE calculated in Model B, where the RMSE for saturation is higher in this simulation compared to all the other calibrated models, which is also the case for the Fbal value for the average drainage. In this calibration the R^2 value was also not obtained for the depth to the groundwater table, because of the simulation was odd (Table 16).

	Gwt (cm)	wsat	Drain (cm^3/day)
RMSE	153.5 or 29.6	0.43	
Fbal (%)			18.6

Table 16: Table with RMSE values for the depth to groundwater table and saturation and Fbal value for drain, for the results of Model B calibrated with solute transport.

Like in Model B (Figure 22) the model is not able to simulate the depth to the groundwater table (Figure 27) which again is either 100 cm og 500 cm b.g.s.

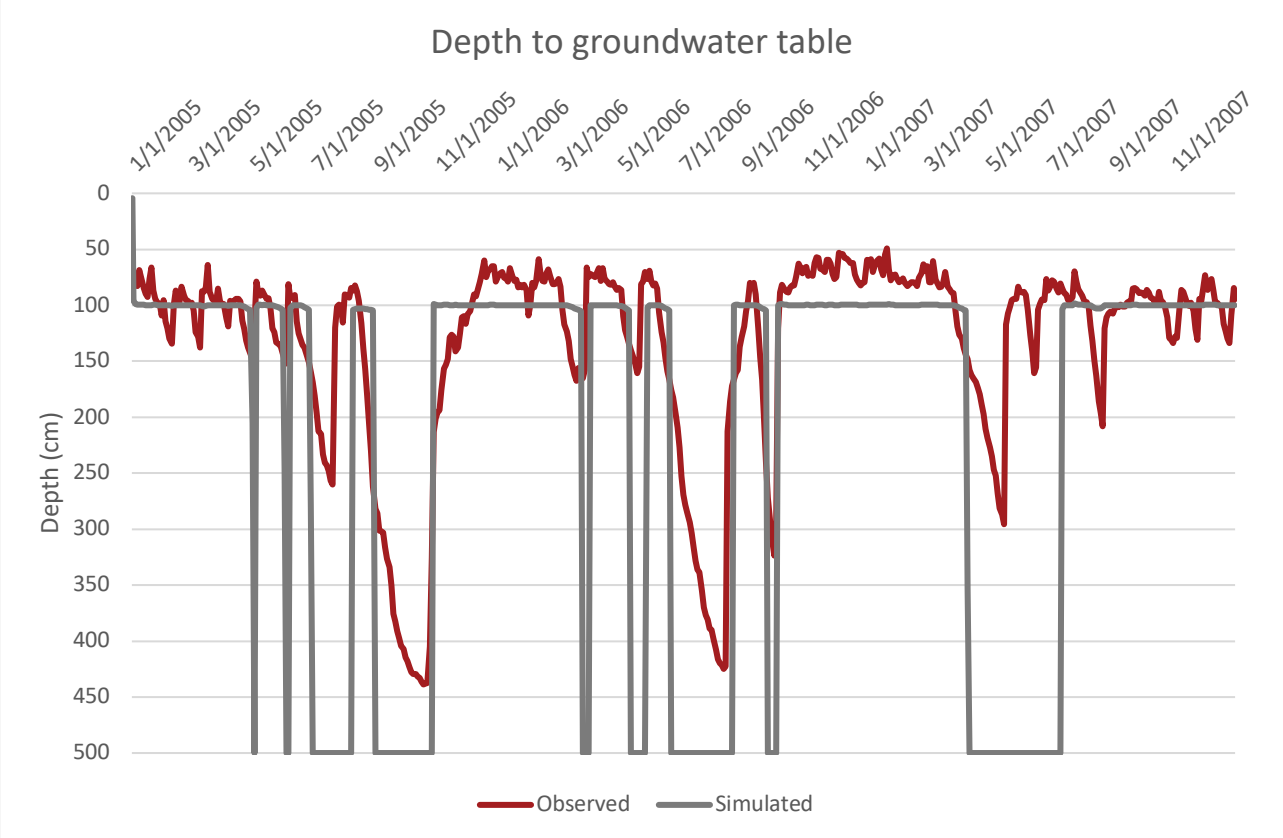

Figure 27: Figure showing the observed depth to the groundwater table (red line) and the simulated depth to groundwater table (grey line) in cm for Model B calibrated with solute transport.

The simulated and observed data for saturation is illustrated in Figure 28. In this calibration the model is not able to simulate the saturation very well, which the increased RMSE values also proves.

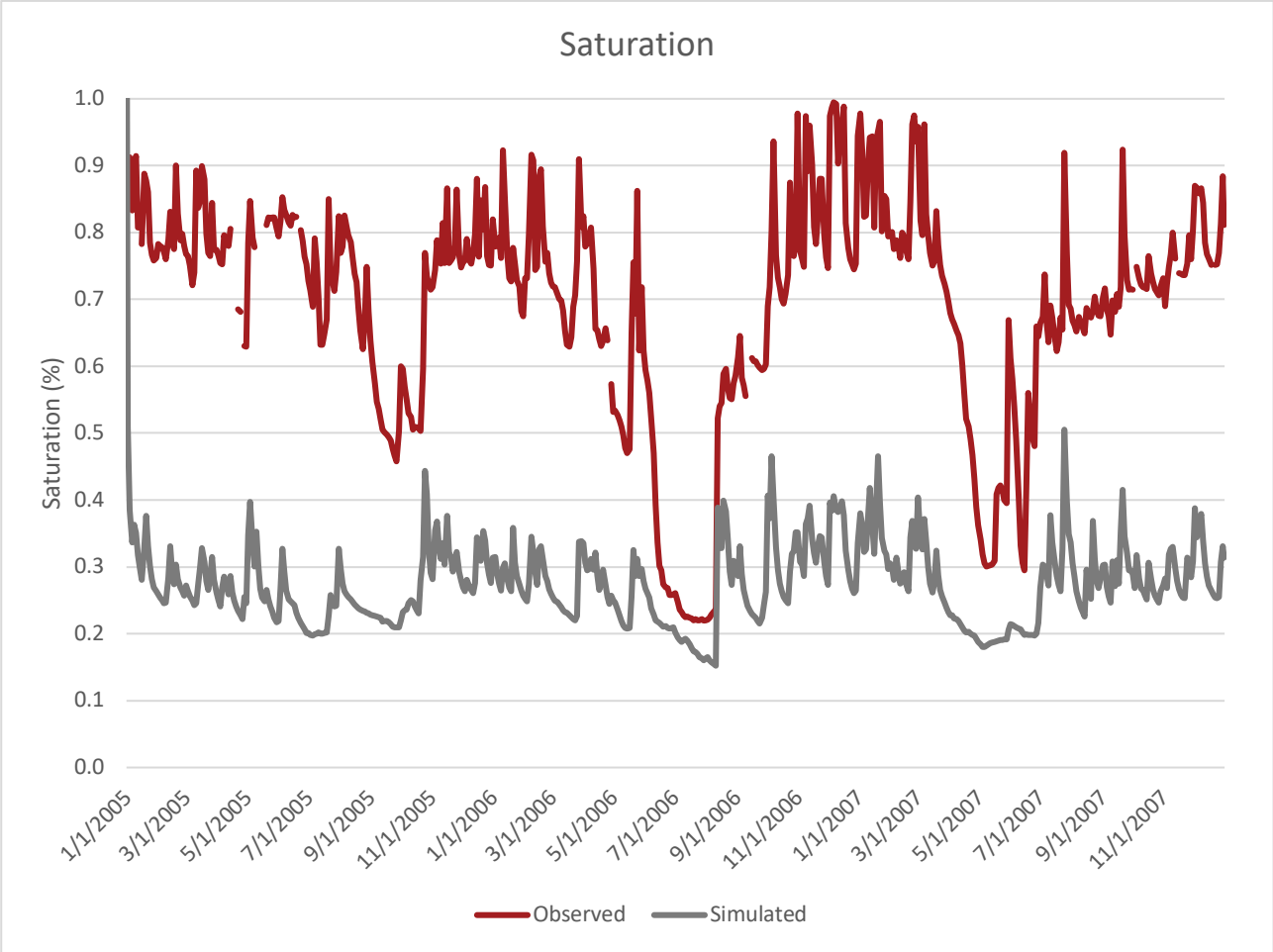

Figure 28: Figure showing the observed saturation (red line) and the simulated saturation (grey line) in % for Model B calibrated with solute transport.

In this calibration the model was able to simulate several of the peaks in the drain flow more accurately (Figure 29). Other than that, it simulates a very big peak in the beginning of the model which is a little earlier than the big peak in the observed values. This big peak in the simulated values is properly also the result of the increase in the Fbal values.

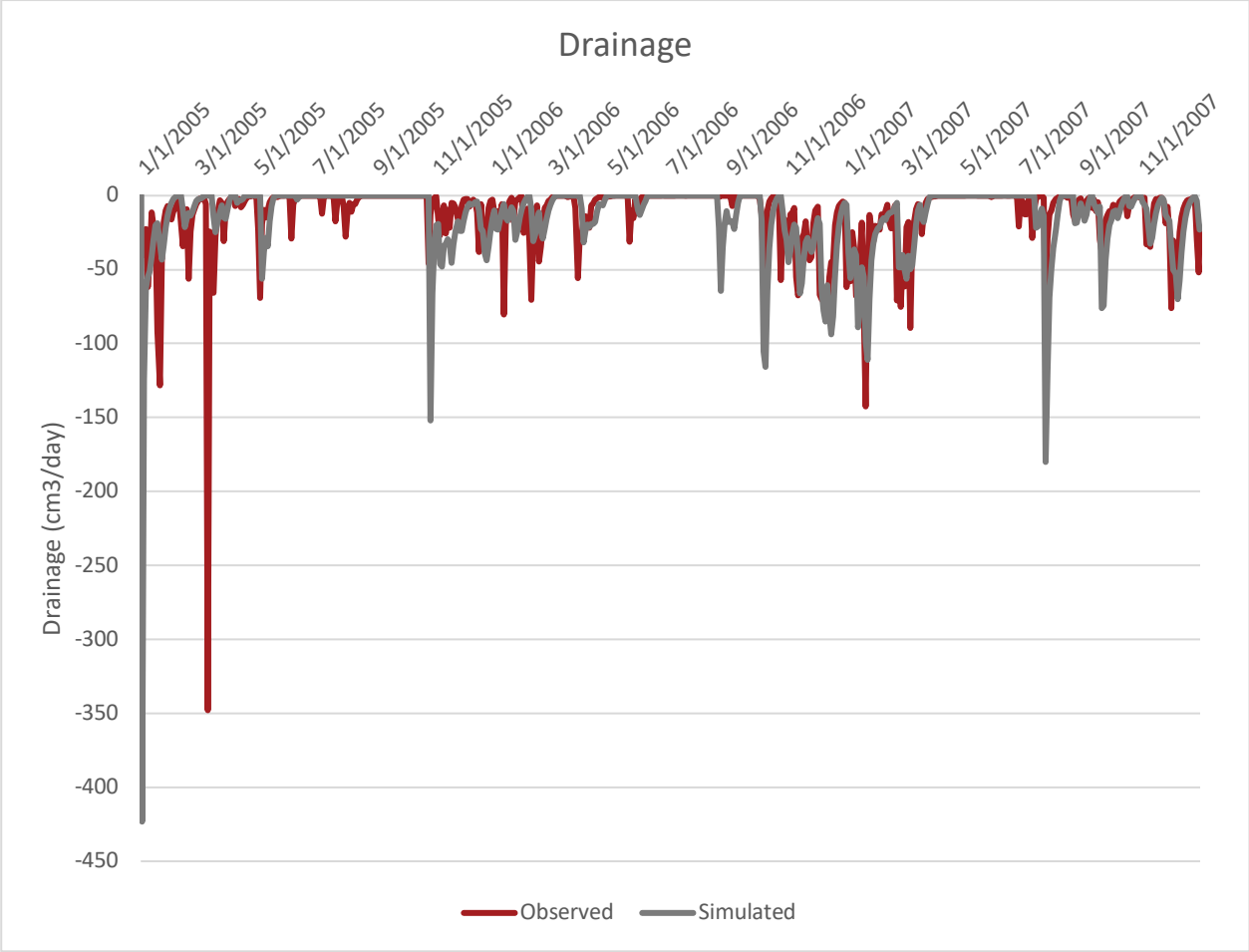

Figure 29: Figure showing the observed drainage (red line) and the simulated drainage (grey line) in $cm3/day$ for Model B calibrated with solute transport.

The comparison of simulated and measured concentration of bromide for this model is made (Figure 30, 31 and 32) where a lower concentration again is obtained like in Model A calibrated with solute transport (Figure 18, 19 and 20). This model simulated the dynamic in the concentration there are measured, much better than in Model B. Again, has it been possible to simulate a concentration of bromide in the suction cup located 2 m b.g.s. (Figure 32)

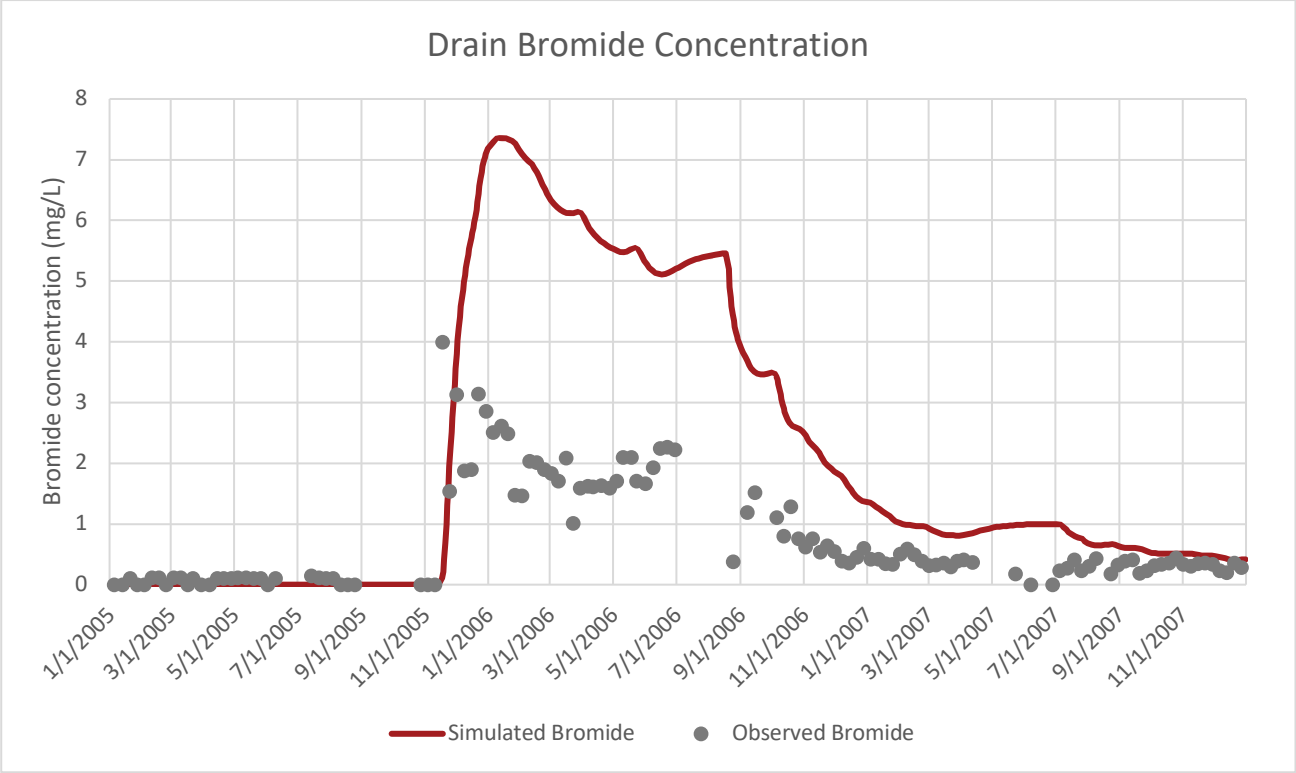

Figure 30: Plot showing the observed (measured) bromide concentration (red line) and the simulated bromide concentration (grey dots) for Model B calibrated with solute transport.

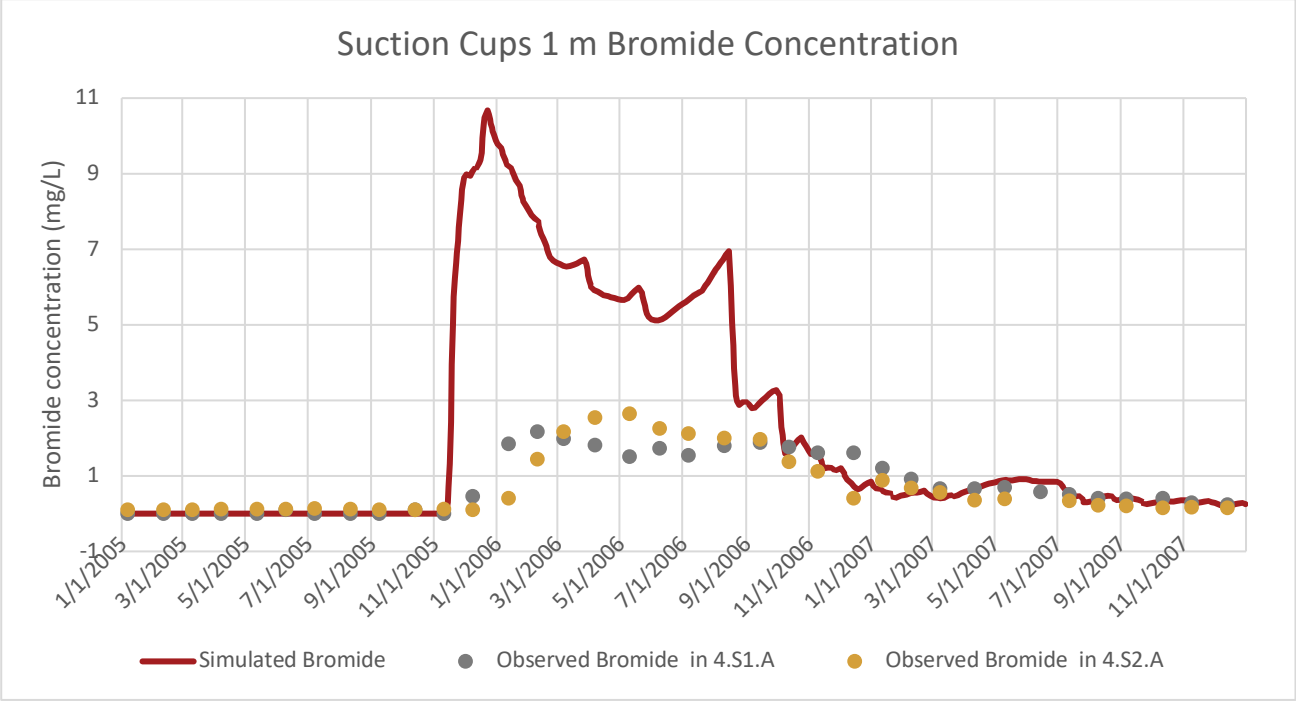

Figure 31: Plot showing the observed (measured) bromide concentration (S1 represented by grey dots and S2 represented by yellow dots) for the suction cup located 1 m b.g.s. and the simulated bromide concentration (red line) for Model B calibrated with solute transport.

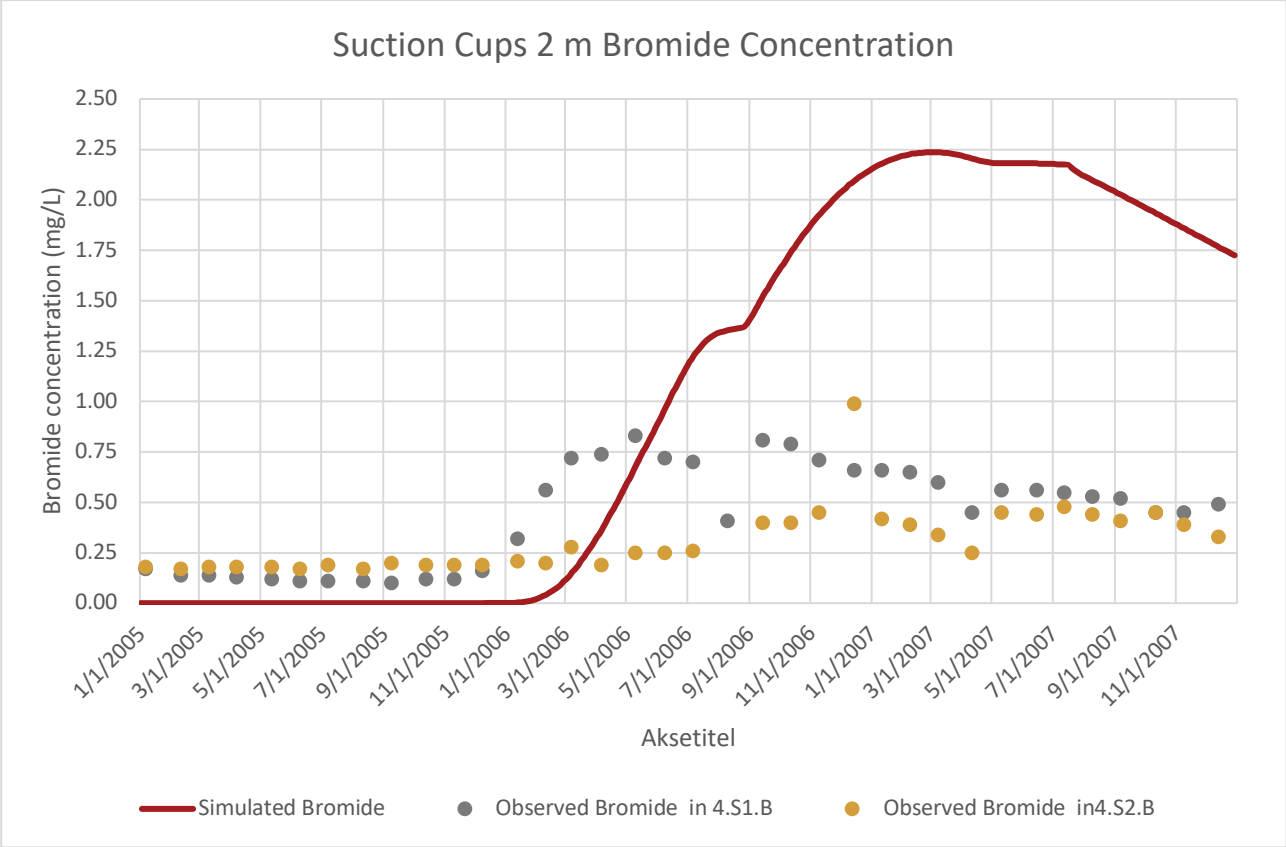

Figure 32: Plot showing the observed (measured) bromide concentration (S1 represented by grey dots and S2 represented by yellow dots) for the suction cup located 2 m b.g.s. and the simulated bromide concentration (red line) for Model B calibrated with solute transport.

Calibration results Model C

This model is established with a dual domain to represent macropores in the model. The model was established as described in methods, but due to complications getting the model to run and give results especially for the drainage, in time no results are presented for this model.

Discussion

Three different models are established, where two are calibrated and extended so they also include solute transport, where after they also are calibrated with solute transport. Model A is the simplest model and only parameters for water flow accounted for. Model B is the same model as Model A, but in Model A the drain is located in the upper part of zone 4. Zone 4 is the zone going from 105 cm b.g.s. to the bottom of the model (500 cm b.g.s.), so it is taking up most of the model domain and therefore dominates the model. Therefore, in Model B the drain was moved 10 cm up in the model so it was located in the lower part of zone 3 (100 cm b.g.s.) to determine if this could have an impact on the model performance, especially for the drain. The Models was afterwards calibrated with solute transport, to see if this could affect the simulated concentration. Model C is a further development of Model A, where macropores are also accounted for by adding a dual domain, which is important at field sites like Estrup, because of the clayey soil, which contains a lot of pores and fractures. Model C was established but did never get to run good enough to get a result from.

The values used as input for hydraulic conductivity are provided from the MACRO model of the Estrup field and consists of the result for the hydraulic conductivity for the zones from earlier calibration. As mentioned in the Method section, complication executing the model with the provided van Genuchten parameters α and β. Therefore, a HYDRUS model was developed to help solve this problem. HYDRUS has several standards incorporated, which are based on (Carsel & Parrish, 1988), for different soil types. These were instead used determine values for the van Genuchten parameters α and β which could be used in the model, while still being realistic. The estimated values from the calibration of the Models, were quite similar. The van Genuchten parameters α and β defined from the different models quite equal. Both α and β for zone 1 define the material as being loam, loamy sand or sandy loam. For zone 2 the material is loam, which also are the case for zone 3. These two zones are also quite similar. Zone 4 defined as silty clay loam or silty clay.

Parameters estimated for the hydraulic conductivity for all the models are also alike, excluding the values for k1 (hydraulic conductivity in zone 1) and the drain (drain conductance). In model A the k1 is estimated to 836.5 cm/day and the drain to 1.37 cm^2/day. In Model B is it 613.2 cm/day and the drain conductance to 86.9 cm^2/day. In Model A calibrated with solute transport k1 increased a

lot (1915 cm/day), in fact it was more than doubled in this calibration compared to the others. So, the drain conductance is one of the parameters, which varies much in the different models (Model A and B, and Model A and B calibrated with solute transport). The variation is expected, as the drain was also moved up 10 cm in Model B, so it is located in zone 3 instead of zone 4, which has different material properties, and different estimated parameters. This differences in the material properties could possibly have an impact, because the drain flow is dependent on the hydraulic conductivity of the material. In Model A, the drain was placed in the lowest permeable zone in the model (zone 4), which has an estimated hydraulic conductivity on 0.033 cm/day. In Model B the hydraulic conductivity for zone 3 was estimated to 28.7 cm/day. Even though the calculated Fbal values were similar (12.77% without solute transport in the calibration and 14.16% with in Model A and 12.59% without solute transport and 18.6% with in Model B) the graph for the drain for simulated and observed values were different. In Model A, the model was only able to simulate some of the dynamic patterns, and it was not able to simulate any of the measured peaks. Only when there were periods with larger amount of drainage, the model could register, that the drainage should increase and when this period ends, it should decrease again. In Model B, the model did not have the same issues modelling the peaks, which it did well. The reason for the model not being able to simulate drainage in Model A could again be the location, because zone 4 has low permeability and a large part of the model is zone 4. Perhaps the model not could react fast enough to simulate the observed peaks, and to fix this issue was to relocate the drain to zone 3, where the hydraulic conductivity was higher and then allowed the water to flow faster to the drain. The drain was also the parameter which was less sensitive in all the calibration so the variation in the value between the models may not have that great effect on the model. The model was not able to simulate the drainage, so the Fbal value became smaller than the accepted uncertainty of a variation on 10%. Both of the models came close to the accepted uncertainty and the models simulating solute transport had an even higher Fbal value than the models without. However, based on their graphs (Figure 12 and Figure 24) the performance of simulation of drainage was best in both Model B.

The calculated RMSE for the depth to groundwater table for Model A is calculated to 149.1 cm and 38.8 cm with and without the values reaching the model domain. For model B, RMSE is calculated to be 160 cm and 37.37 cm with and without the values reaching the model domain. The RMSE values are not far from each other and are almost the same for both Model A and B calibrated with solute transport (Table 10 and Table 16). When RMSE is calculated for the depth to groundwater

table, a RMSE is both calculated where the simulated values of 500 cm are included in the calculation and a RMSE where they not are included. Obviously, the RMSE value is much higher when they are included than if they were excluded. When excluding these values, the RMSE value for both Model A and B see Table 7 and 13 and Table 10 and 16 for the models calibrated with solute transport, become smaller than the accepted uncertainty for this data group on 50 cm. However, excluding these data in the calculation would result in a wrong result because some of the data in the calculation would result in a wrong result because some of the data is not accounted for. In Model A, around 130 days are excluded and in model B it is around 150 days, which is around 4.5 to 5 months that are excluded in three years. On the other hand, it would be just as much of a mistake to include this data in the calculation because it is not certain these data really are 500 cm. In fact, it would be unlikely they are presented as 500 cm because of the limitation of the model domain, which only is 500 cm in the z-direction. If the model domain was larger, the depth to the groundwater table the model would simulate would perhaps be even greater than 500 cm. By looking at the graphs of the depth to the groundwater table (Figure 10 and Figure 22) the model clearly has difficulties calculating values for the depth to the groundwater table for both Model A and B. In Model A (Figure 10), the model simulates the depth dynamic trends between the big peaks, which it does not do in Model B (Figure 22). In Model B, the model was not able to simulate any dynamic behaviour between the peaks, even though the RMSE value is a little bit less when excluding the depth of 500 cm for Model B than Model A, and even though both values are less than the decided uncertainty. The results for Model B do not look realistic and therefore Model A is clearly better at simulating the depth.

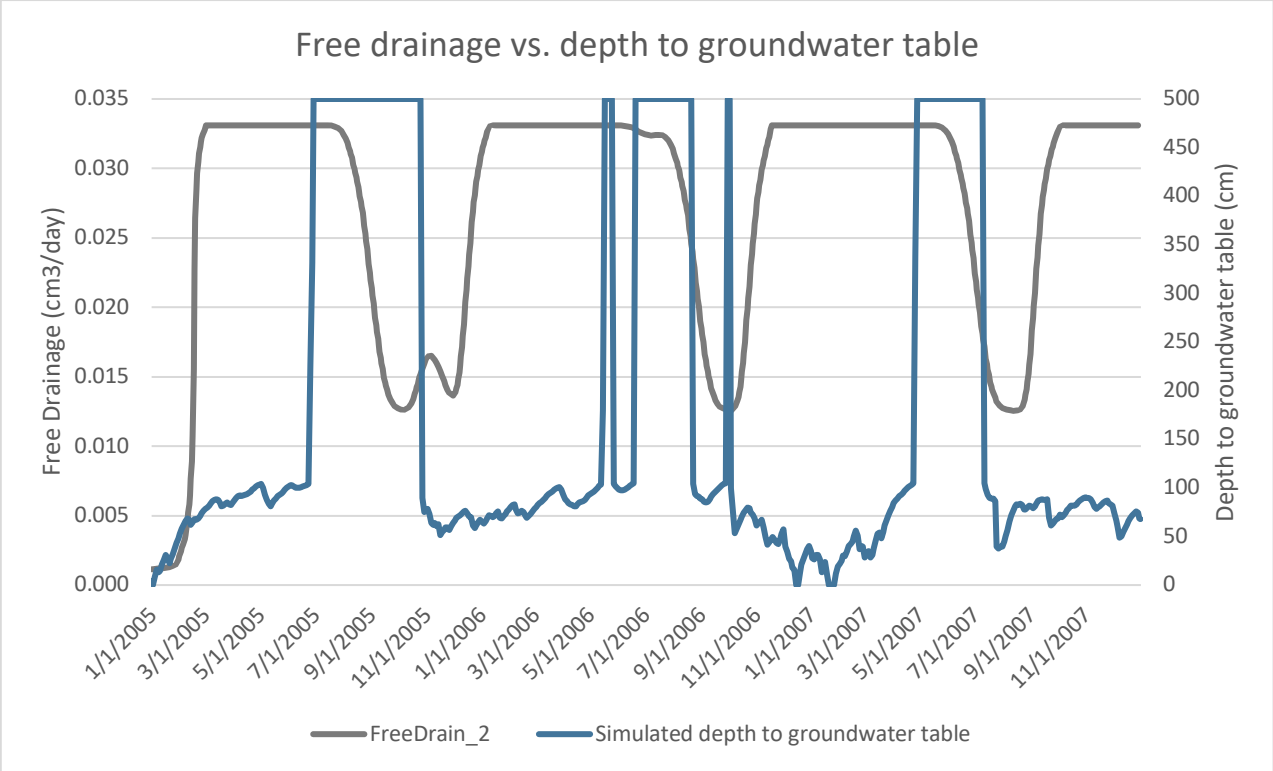

Figure 33: Figure showing the water leaving the model by free drainage in cm^3/day (red line) together with the graph for the depth to the groundwater table (grey line)

Figure 33 illustrates the amount of water removed by free drainage together with the depth to the groundwater table graph. This is done to determine if there is any connection between the boundary condition (free drainage) and why the model simulates a rapid decrease in the groundwater table. Every time the model simulates high values for free drainage, it results in an increase of the depth to the groundwater table. Whether it is just a coincidence, or the free drainage and groundwater level have a connection is hard to say. A way to have investigated this is to change the boundary condition in the bottom of the model to a specified head boundary condition instead of free drainage. This could have resulted in the model bottom boundary condition was more controlled. Even though, the bottom boundary condition is not the factor whereby most water leaves the model, in fact from the water balance presented in Table 8 for Model A and Table 14 for Model B it is from evapotranspiration and the drain most of the water leave.

A RMSE and R^2 values are calculated for the degree of saturation in both Model A and B, see Table 7 and Table 13. The RMSE vas calculated for Model A to be 0.29 and for Model B to be 0.21, and thus based on the RMSE value, Model B was better at simulating the saturation in the model. When

calibrating both Model A and B with solute transport, a RMSE value for Model A of 0.17 was achieved (Table 10). Model B calibrated with solute transport, a RMSE was calculated to 0.43, so this model was not able to calibrate the saturation very well. The accepted uncertainty decided for this group was 0.1, and neither of the models came within this value. This is also clear by looking at the plots (Figure 11, Figure 23 and Figure 28), where the observed and calculated values for saturation are illustrated. In Figure 11, Model A simulates values that are less than the observed values, but when Model A is calibrated with solute transport the simulation is more accurate (Figure 16). Model B (Figure 23) simulates the saturation much more accurately than Model A, but not as accurately as Model A with solute transport.

The R^2 value for Model A is 0.64 (Table 7), which means that the model can explain 64% of the observed data. This is not the case for Model B (Table 13) where the R^2 value claims that only 7% of the simulated data can explain the observed data. The low $R^2$of Model B is likely caused by the distribution of the residuals. In the beginning of Model B, the simulated saturation is less than the observed, and the residuals are bigger in the beginning as well. In the end, the simulated saturation is greater than observed, and these effects will result in a low R^2 value even though Model B clearly is the best to simulate saturation.

The objective function for Model B is reduced the most to a value of 1.71, but the Model did not perform very well simulating the depth to the groundwater table. Additionally, solute transport in Model B was very high, but was not in the model during the calibration. The objective function there were reduced the second most was for Model A calibrated with solute transport, here it ended on 1.95, This model was the one to simulate the saturation so, RMSE was closest to the accepted uncertainty. The depth to groundwater table did also have some dynamic between the big peaks, which not was the case for calibration of Model B. For simulation drainage the model was also able to simulate some of the dynamic but not the big peaks, and the Fbal value was calculated to 14.16% which is only 4% over the accepted uncertainty so still relatively good. The two last models were not able to get the objective function below 2, and Model A ended on an objective function of 2.03, but this model did not simulate the saturation very well, and like Model B when adding of solute transport afterwards the model simulated very large concentrations. Model B with solute transport in the calibration ended on an objective function of 2.28, which is also reflected in the performance simulation both depth to the groundwater table and saturation.

Solute transport was added to both models (Model A and B, Figure 13 and 14 for Model A and Figure 25 and 26 for Model B) after the calibration. In both simulations the models simulated considerable higher values for bromide concentration than are measured on the field for the drain 1.1 m b.g.s. and the suction cups 1 m b.g.s. The simulated concentration in the suction cups located 2 m b.g.s. was close to zero, thus the bromide had not yet reached this observation point, even though bromide was present in the measured data (see Appendix 1). Both Model A and B were also calibrated with solute transport, which gave a better solution for solute transport in both models (Figure 17, 18 and 19 for Model A calibrated with solute transport and Figure 30, 31 and 32 for Model B with), where the simulated concentration was not as high compared to the observed anymore. Results of solute transport is too high in all the models, but a reduction of 40% on the model A calibrated with solute transport (Figure 17, 18 and 19) could reduce the concentration to be more similar to the measured (Figure 34), so the model simulation of solute transport is not that far off. This would probably also be the case for Model B calibrated with solute transport (Figure 30, 31 and 32). In both Model A and B, where solute transport was added after the calibration, the concentration was very high (Figure 13 and 14 for Model A and Figure 25 and 26 for Model B) and even though the bromide concentration is reduced, the bromide concentration from the models is still higher than the bromide concentration measured on Estrup field. A reduction could possibly fix this issue, despite bromide being a conservative tracer.

A potential reason why the concentration was too high in the drain and in the suction cups placed 1 m b.g.s. could be the hydraulic conductivity. The suction cups placed in 2 m b.g.s. is in zone 4 and in the zone with lowest hydraulic conductivity. Therefore, the bromide could be delayed by the perhaps too low hydraulic conductivity and vise versa. The hydraulic conductivity could be too high in zone 1, 2 and 3 where the suction cups (1m b.g.s.) are located.

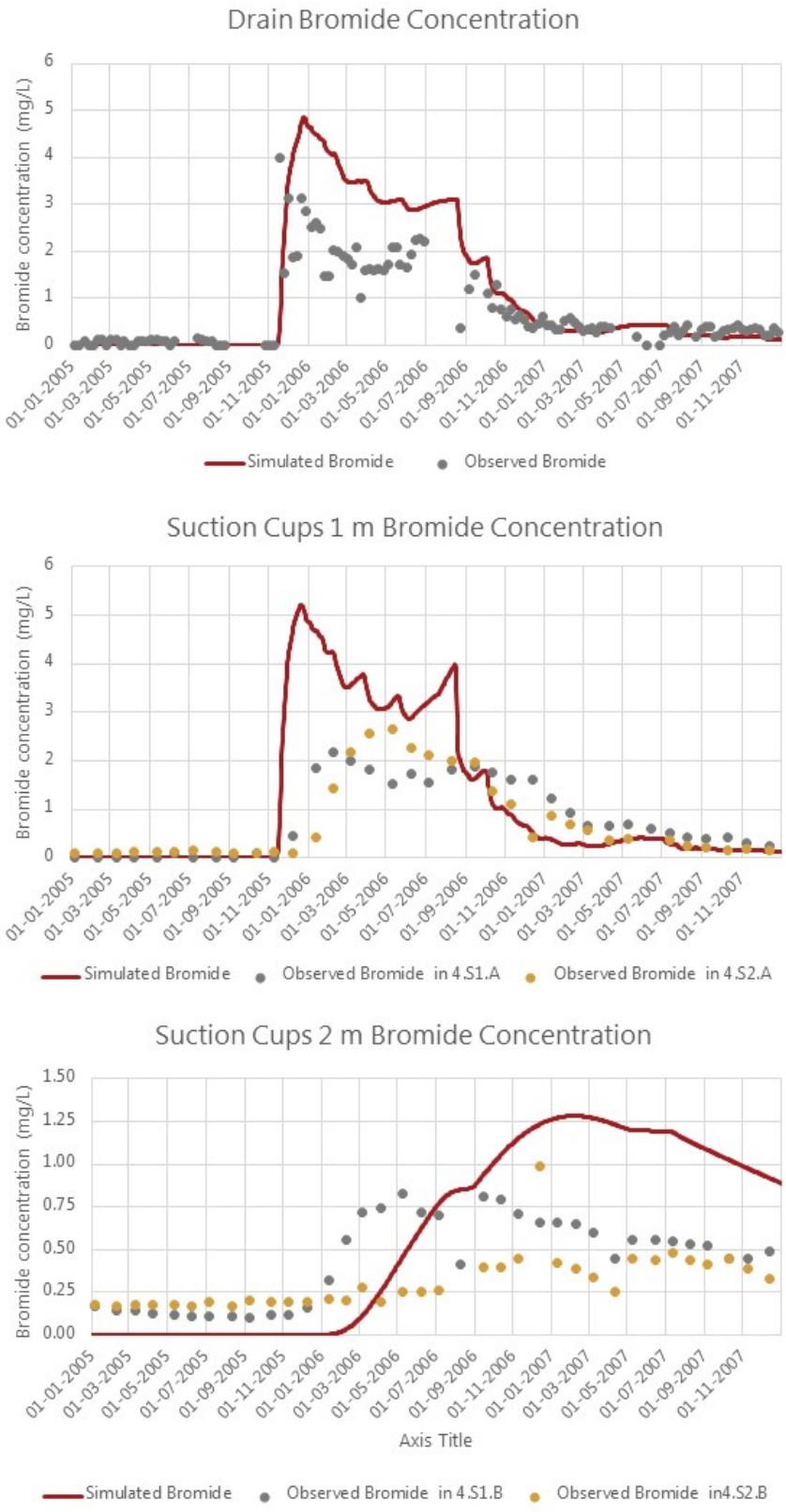

Figure 34: Same plots as in Figure 18, 19 and 20, where the simulated bromide concentration is reduced by 40%.

Field work was executed as preparation for this project, where the saturated hydraulic conductivity was measured at the field by a permeameter with ball-cock. The results (Table 17) for hydraulic conductivity are calculated by the given measurement tool, and the excel sheet with the results is presented in Appendix 3 for the three different depth. The hydraulic conductivities were of same magnitude, with values ranging between 5-11.8 cm/day. The calculated values are also not far from the calibrated values, for both Model A and B.

Depth (*cm*)	hydraulic conductivity K (*cm/day*)
20	11.8
40	6
60	5

Table 17: Table with results from the field investigation using the permeameter with ball-cock measurements in different depths.

Model uncertainties

A decision was taken when solute transport with bromide was added to the model, which could possibly cause differences in the results for the models. The decision was taken because the model was not able to simulate solute transport when all the bromide was put onto the field on one day, because if the day where the bromide not was applied anymore was not set as an output time, the model would not allow it and did not simulate any concentration at the different observation points. This issue could perhaps result in some errors in the simulated concentration and could be checked by adding another day to the model.

Another error for the model is that different results are calculated, when the same model is executed. Even when the same model is run twice the results differ. The files with the results for two identical model was compared and showed small differences in the calculated values for the observation groups, and this resulted in different values for the residuals, and could be due to rounding mistakes

in the model. It also resulted in different results for the estimated parameter values. The parameter, which has the greatest fluctuation was the drain, but the drain is also one of the parameters that is less sensitive and therefore, the estimated values may not have that big of an impact on the overall model performance.

The model was developed with an initial head, representing a day from a previous run, to give the model a better initial head, as a start condition. To improve the model, a varying pressure head for the column should perhaps have been used as an initial condition, where the model in the top should have a pressure head input to -100 cm and in the bottom should have a value of 400, such that the model would start with a groundwater table 1 m b.g.s., instead of starting with the same value for the initial head in the whole column.

Conclusion

- A model of the PLAP test field in Estrup has been built in HydroGeoSphere. The model was set up using field data and data from the already establish model in MACRO Model A. Further developing was performed, by changing the drain location (Model B) and inserting a dual domain, representing macropores (Model C).
- Model A was able to simulate a part of the depth to the groundwater table, and RMSE was accepted when it was below 50 cm, when excluding the values of 500 cm. Model A did not simulate saturation very well it simulated values less than was observed. A RMSE value 0.29 supports that the model performance could be improved. Drainage did only vary about 2% from the uncertainty and gave a fairly good result, even though it was not able to simulate the peaks.
- In Model B, where the drain was moved, the model could not simulate the depth to the groundwater table, as it only simulated values around 100 and 500 cm. The performance of saturation was better in this model, with a RMSE value at 0.2. The Fbal values for this model was the same as in Model A, but in this model, it was able to simulate the peaks of the drainage.
- Solute transport was performed for both models and in both models the concentration for bromide were considerable high in the drain (1.1 m b.g.s) and suction cups (1 m b.g.s.) than observed. Bromide was not present in the suction cups 2 m b.g.s., and even if bromide perhaps should be reduced by up to 40%, the result for the model simulation were still too high.
- Model A and B were also calibrated with solute transport, which gave better results for simulated concentration of bromide. The results were still a little too high, but if the simulated concentration was reduced by 40%, the results were almost the same as measured. So the model did not simulate the concentration too far off.
- Results for Model C was not possible to obtain in time due to complication running the model.
- Both models were calibrated with and without solute transport and evaluated to see how well the model could perform, by comparing the simulated values from the model with the observed values, measured at the field in Estrup. Several statistical parameters were able to give an estimate of how well the data fits and the model perform. The model performance was not as good as hoped, but also expected because macropores and fractures were not accounted for. When solute transport is included in the calibration, the model is able to simulate the bromide concentration much better, than if added after calibration.

Future work

There were several things I would have liked to further work on in this model, and some improvement that could have been done are:

- To further develop the model, more investigation of model parameter should be performed to ensure the model performance is the best possible.
- Adding fractures to the model to make it more true to reality.
- Adding a longer time series to the model. In this model a specific time period from 2005 to 2007 was chosen, but data for the field are available for about 20 years, so there is a possibility to continue the model for a longer time period.
- Making a setup for both a calibration and verification periods to evaluate how well the model performs, when no observation data is present to simulate against.
- To test other calibration scenarios, perhaps calibration against periods with extremes.
- Expand the solute transport model to simulate transport of pesticides instead of solute transport with bromide.

Acknowledgment

Throughout the writing of this master thesis, I have received a great deal of support and assistance. I would first like to thank my supervisors Karsten Høgh Jensen (IGN) and my co-supervisors Sachin Karan (GEUS) and Annette Rosenbom (GEUS), for their guidance throughout this project. I would also like to give a thanks to René Therrien, for providing assistance establishing the model. Finally, I would like to thank geochemical department at GEUS for providing a space for me to work on my master thesis.

References

Carsel, R. F., & Parrish, R. S. (1988). *Developing Joint Probability Distributions of Soil Water Retention Characteristics*. *24*(5), 755–769.

Danish meteorological institute. (1997). *TECHNICAL REPORT - Observed Precipitation in Denmark , 1961-90*. 40.

Doherty, J. (2016). PEST Model-Independent Parameter Estimation User Manual Part I: PEST, SENSAN and Global Optimisers. In *Watermark Numerical Computing*.

Fitts, C. R. (2002). *Groundwater Science*. Academic press.

Gelhar, L. W., Welty, C., & Rehfeldt, K. R. (1992). A critical review of data on field-scale dispersion in aquifers. *Water Resources Research*, *28*(7), 1955–1974. https://doi.org/10.1029/92WR00607

Hendriks, M. R. (2010). *Introduction to Physical Hydrlogy*. Oxford.

Kristensen, K. J., & Jensen, S. E. (1975). A Model for Estimating Apotential Evapotranspirationctual Evapotranspiration from. In *Nordic Hydrology 6* (pp. 170–188).

Larsbo, M., Roulier, S., Stenemo, F., Kasteel, R., & Jarvis, N. (2005). An improved dual-permeability model of water flow and solute transport in the vadose zone. *Vadose Zone Journal*, *4*(2), 398–406. https://doi.org/10.2136/vzj2004.0137

Lindhardt, B., Abildtrup, C., Vosgerau, H., Olsen, P., Torp, S., Iversen, B. v., … Graversen, P. (2001). *The Danish Pesticide Leaching Assessment Programme: Site Characterization and Monitoring Design*.

Mualem, Y. (1976). A new model to predict the hydraulic conductivity of unsaturated porous media. *Water Resources Research*, *12*(3), 1976.

Nimmo, J. R. (2009). Vadose Water. *Encyclopedia of Inland Waters*, 766–777. https://doi.org/10.1016/b978-012370626-3.00014-4

Rosenbom, A. E., Haarder, E. B., Badawi, N., Gudmundsson, L., von Platten-Hallermund, F., Hansen, C. H., … Olsen, P. (2017). *The Danish Pesticide Leaching Assessment Programme Monitoring results May 1999–June 2016*.

Rosenbom, A. E., Therrien, R., Refsgaard, J. C., Jensen, K. H., Ernstsen, V., & Klint, K. E. S. (2009). Numerical analysis of water and solute transport in variably-saturated fractured clayey till. *Journal of Contaminant Hydrology*, *104*(1–4), 137–152. https://doi.org/10.1016/j.jconhyd.2008.09.001

Šimůnek, J., Šejna, M., Saito, H., Sakai, M., & Th., van G. M. (2009). *The HYDRUS-1D Software Package for Simulating the One-Dimensional Movement of Water, Heat, and Multiple Solutes in Variably-Saturated Media*.

Šimůnek, Jiří, & van Genuchten, M. T. (2017). 8 Contaminant Transport in the Unsaturated Zone: Theory and Modeling. In *The Handbook Of Groundwater Engineering* (pp. 203–235).

Sonnenborg, T. O., & Henriksen, H. J. (2005). Håndbog i grundvandsmodellering. *Report ; 2005/80*, 320.

Therrien, R., McLaren, R. G., Sudicky, E. A., & Panday, S. M. (2010). HydroGeoSphere. A three-dimensional numerical model describing fully-integrated subsurface and surface flow and solute transport. *Groundwater Simulations Group*, 457. https://doi.org/10.5123/S1679-49742014000300002

Appendix

Appendix 1 Bromide breakthrough curves

Breakthrough curves for bromide concentration measured at Estrup field, at different location

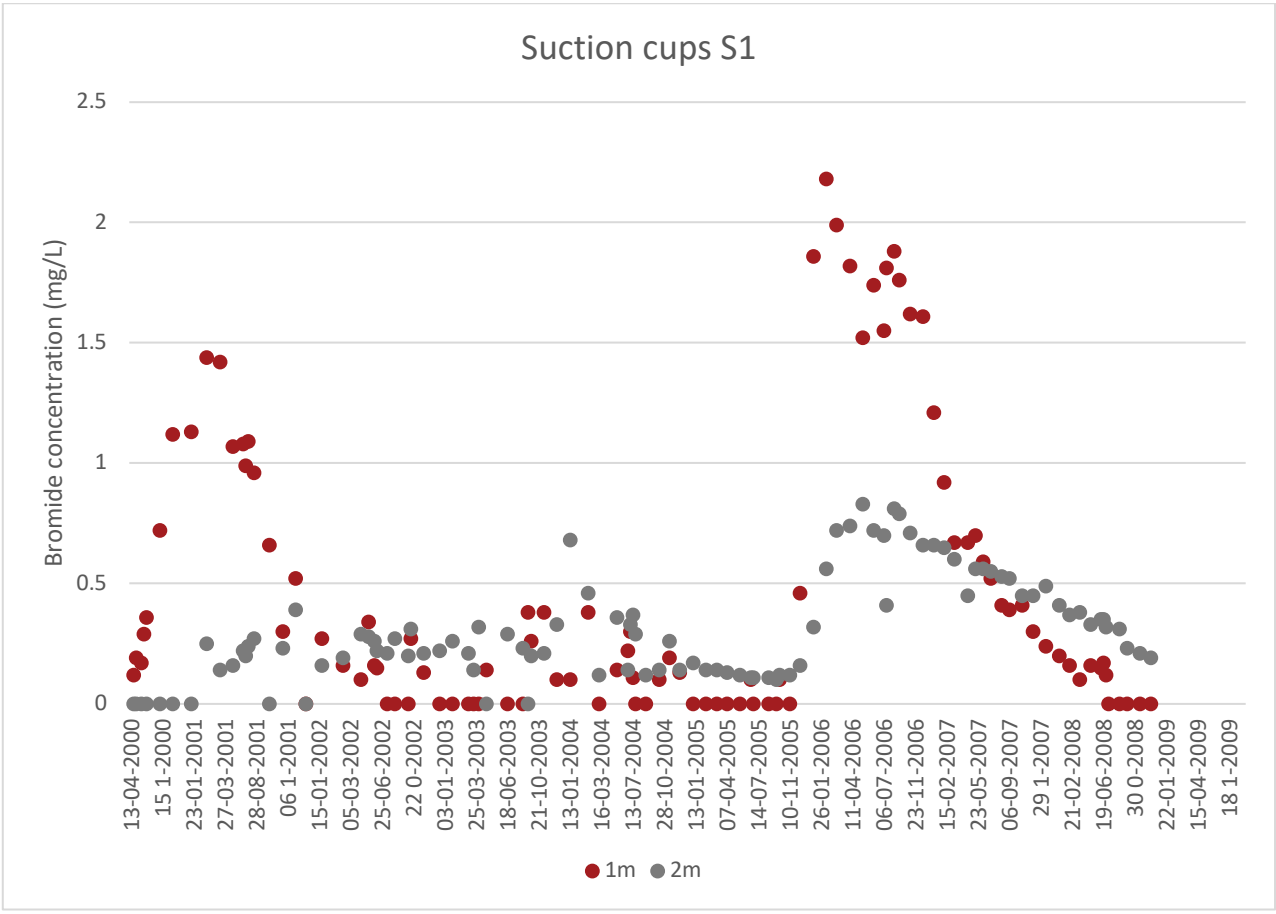

Figure 35: Figure of the measured bromide concentration in the suction cups located 1 m b.g.s.

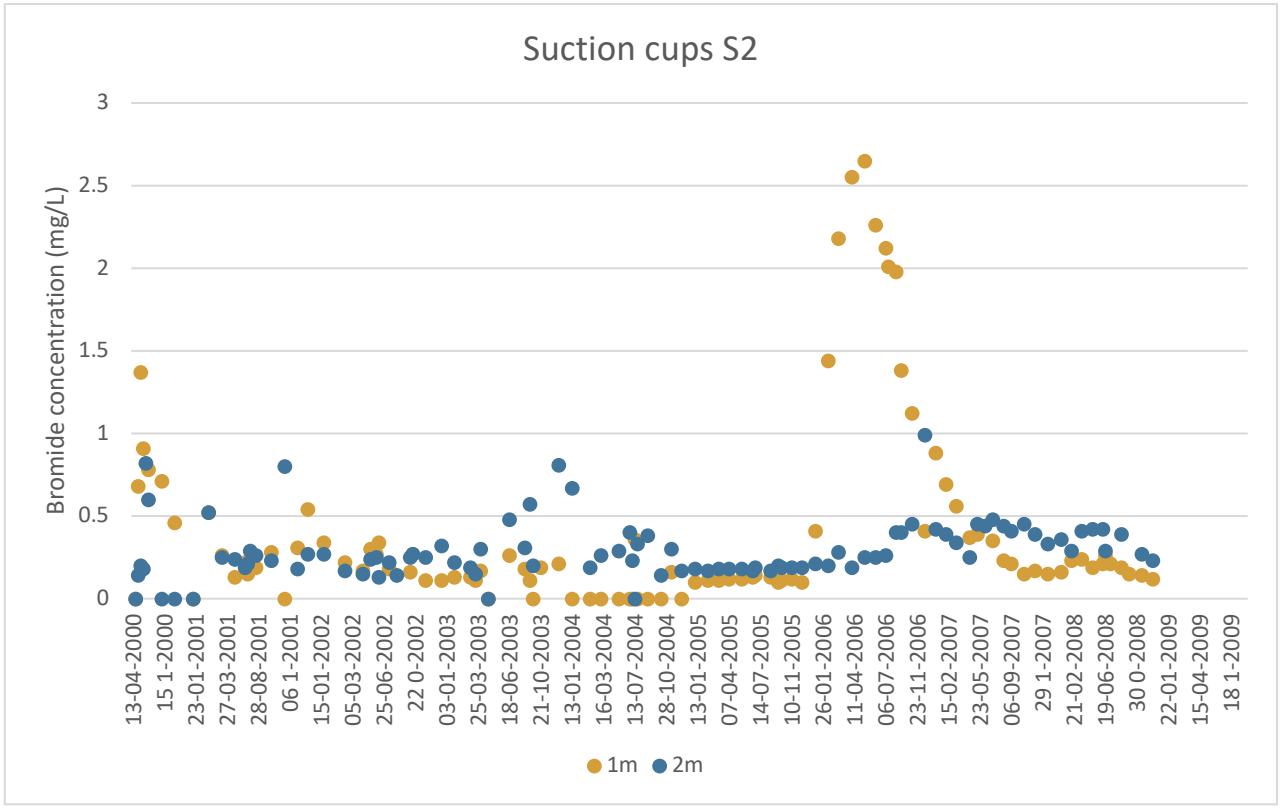

Figure 36: Figure of the measured bromide concentration in the suction cups located 2 m b.g.s.

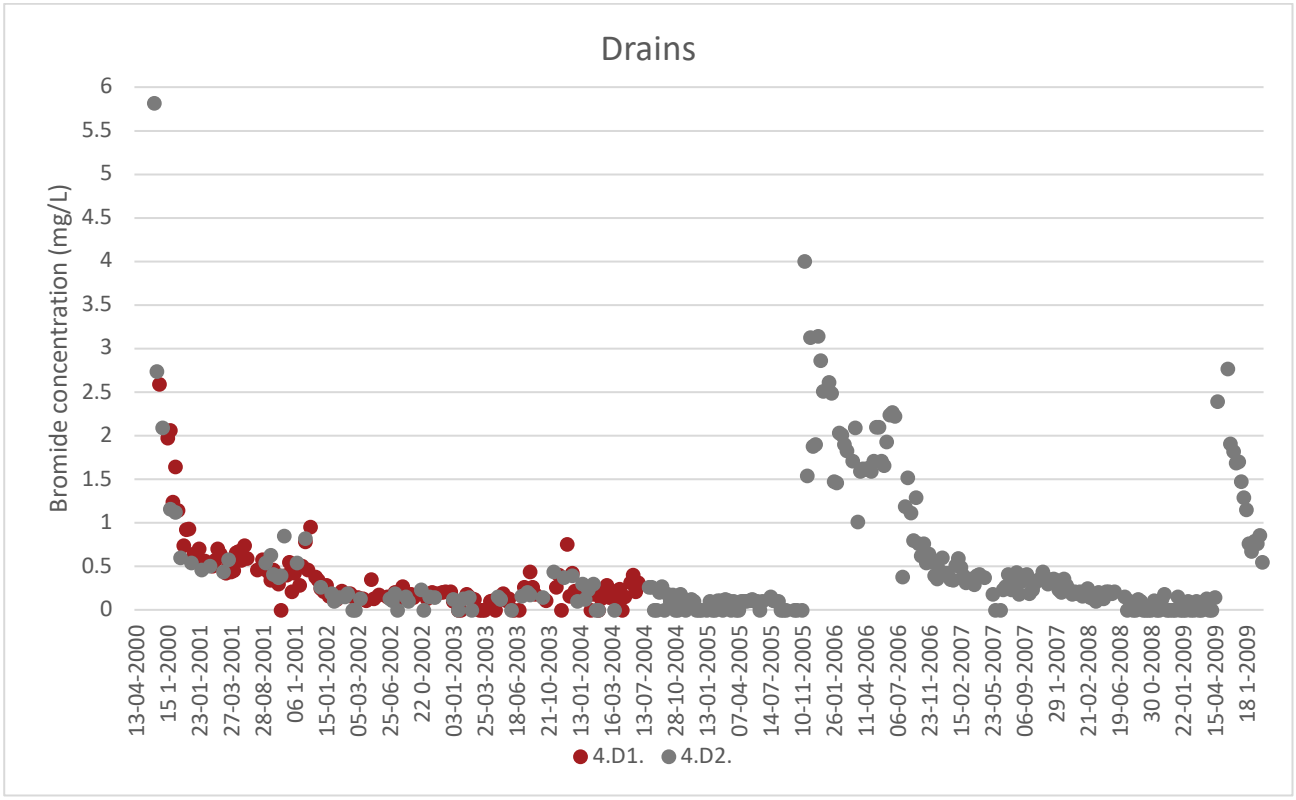

Figure 37: Figure of the measured bromide concentration in the drain located 1.1 m b.g.s.

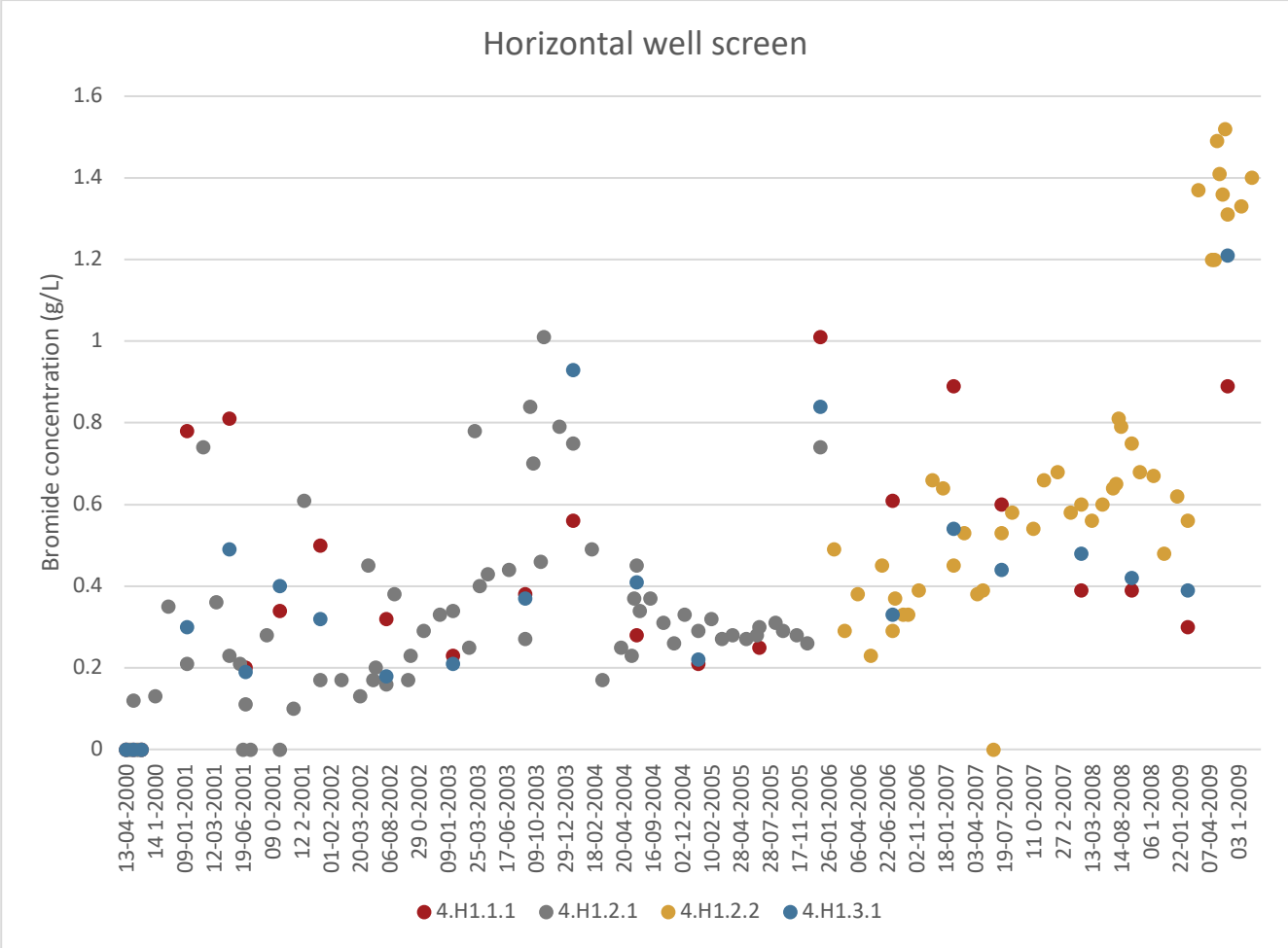

Figure 38: Figure of the measured bromide concentration in the horizontal wells located 3.5 m b.g.s.

Appendix 2 input files to HydroGeoSphere

For developing a model in HydroGeoSphere a model file (grok) and different material properties file are developed (mprops, etprops, oprops and dprops). The files are stored in a folder submitted as well. The folder contains:

- u_1d.grok
- u_1d.mprops
- u_1d.etprops
- u_1d.oprops
- u_1d_dual.grok
- u_1d.dprops

Appendix 3 field calculation sheets

Field investigation excel sheet for calculation of the saturated hydraulic conductivity in a depth of 20, 40 and 60 cm.

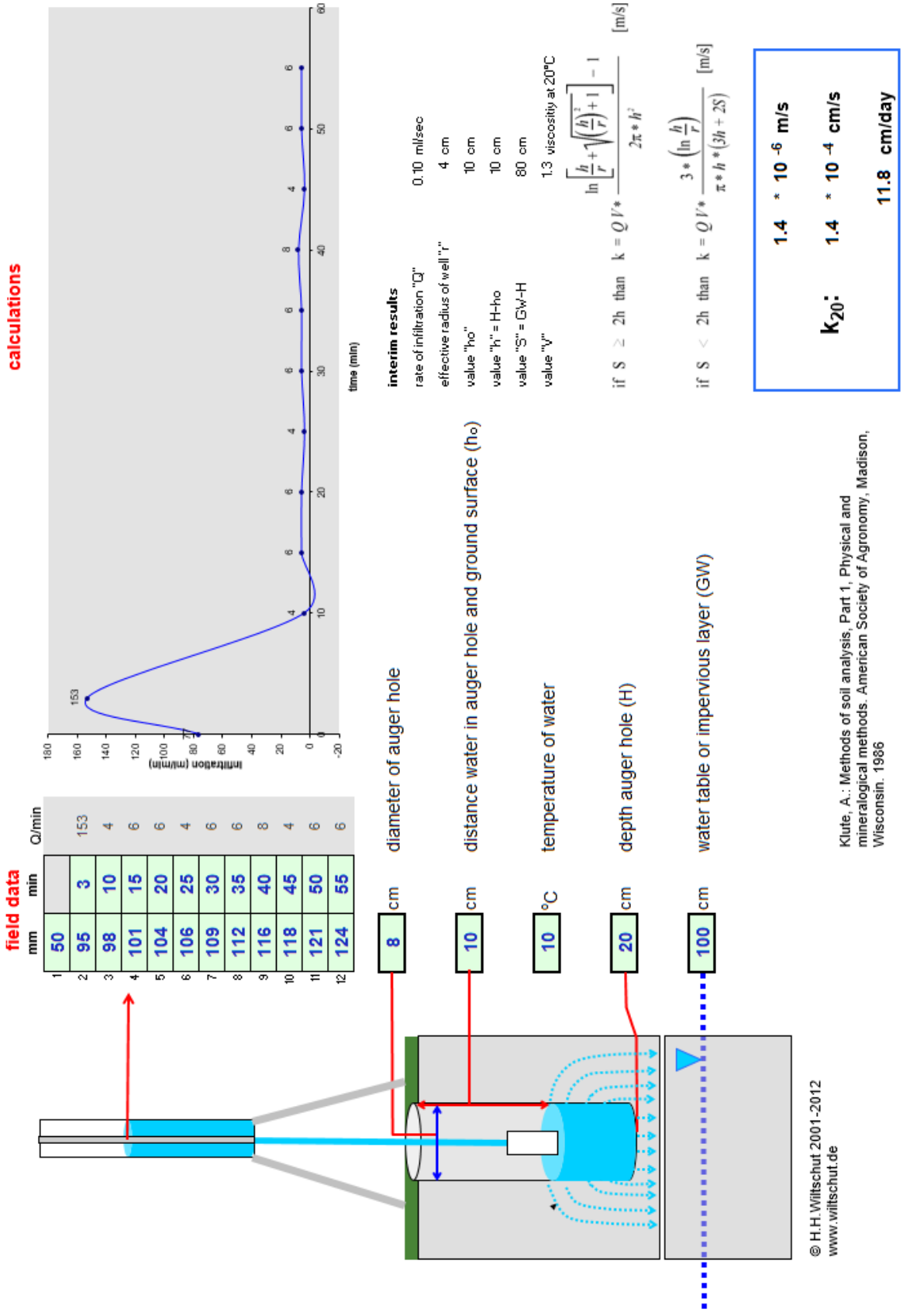

Figure 39: Calculation sheet for the permeameter with ball-cock, calculation for a depth of 20 cm.

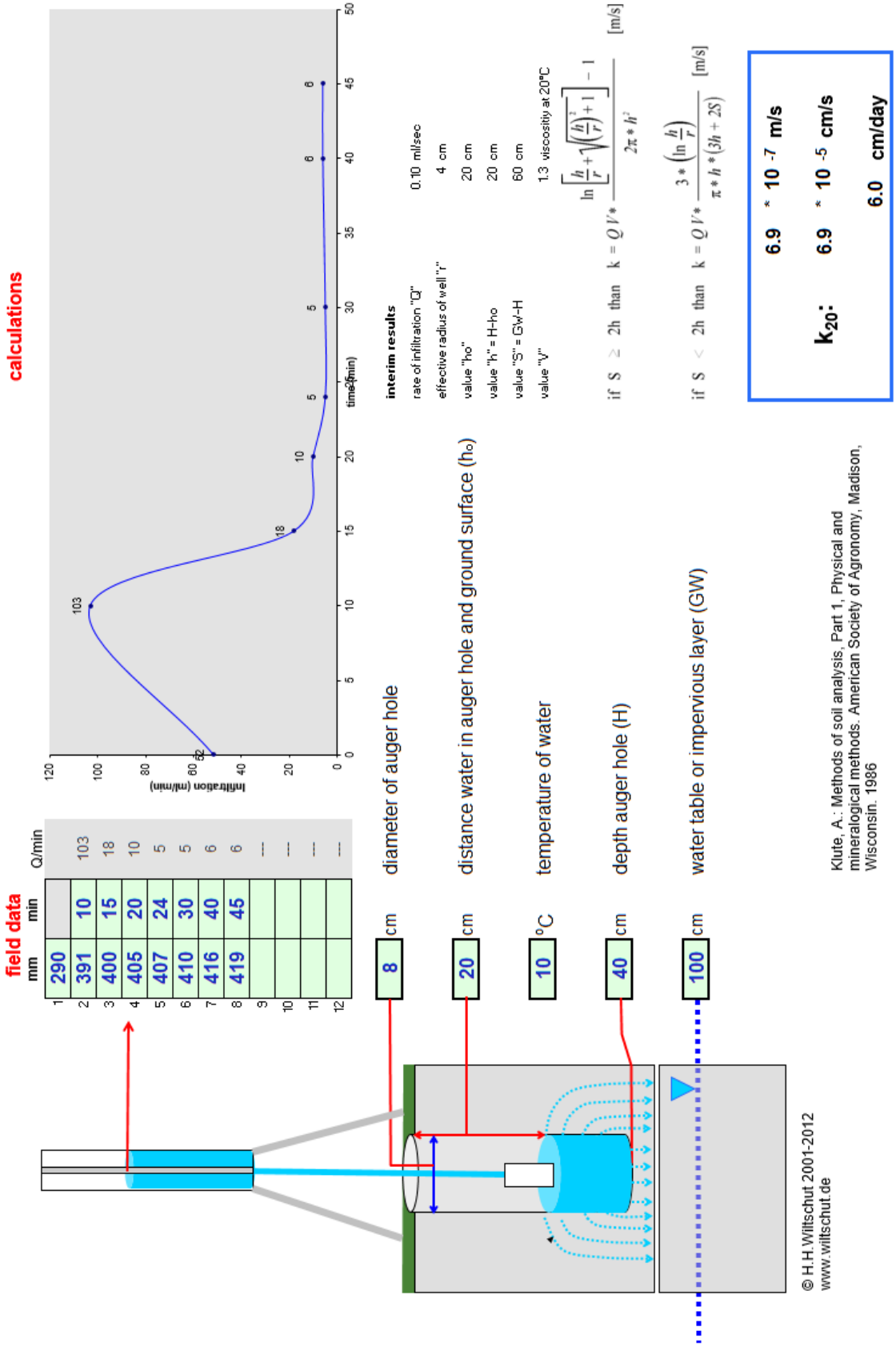

Figure 40: Calculation sheet for the permeameter with ball-cock, calculation for a depth of 40 cm.

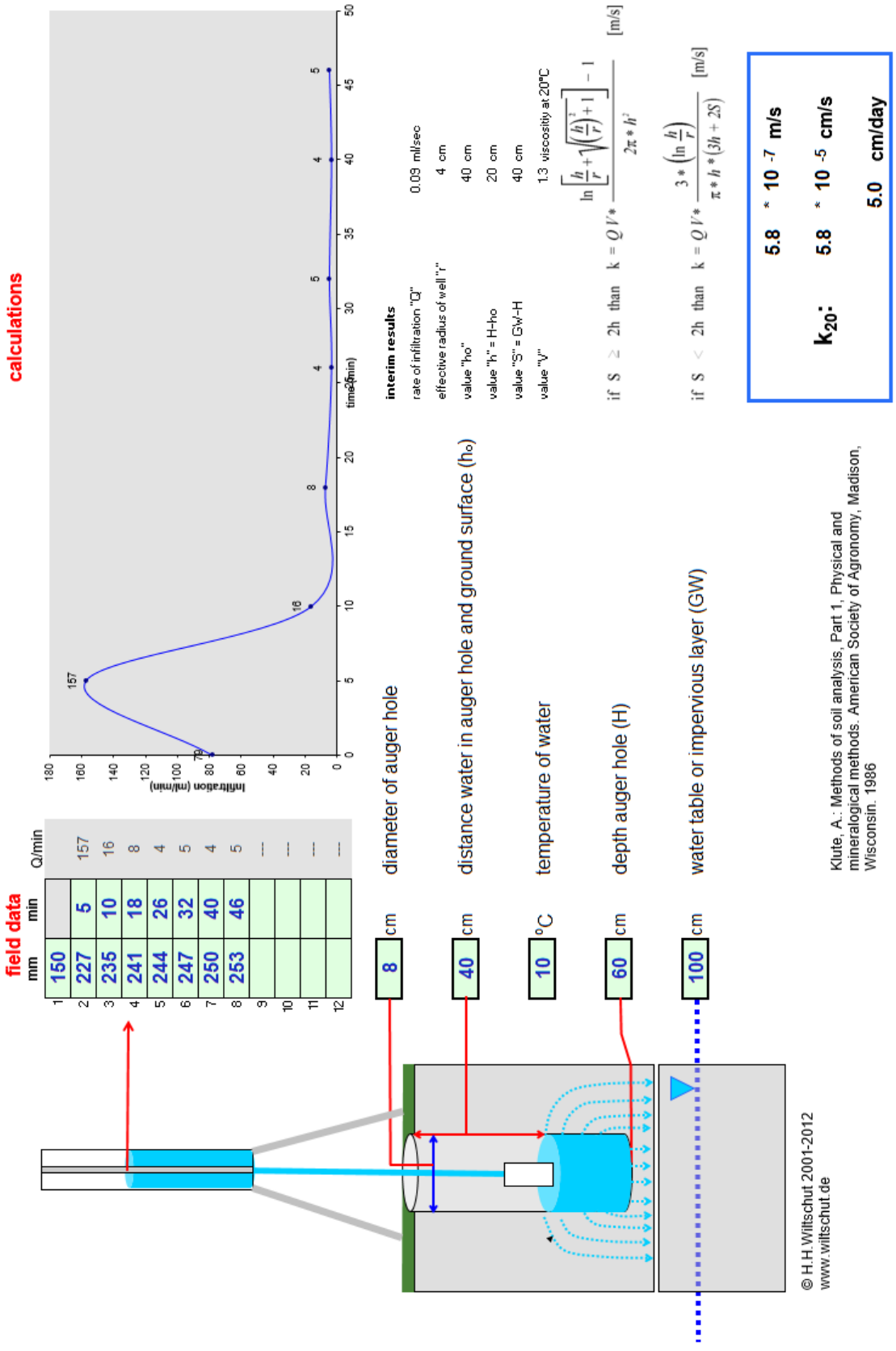

Figure 41: Calculation sheet for the permeameter with ball-cock, calculation for a depth of 60 cm.